The Impact of Cigarette Smoking on HDL Composition and Function

Katie Thomas

A dissertation

submitted in partial fulfillment of the

requirements for the degree of

Doctor of Philosophy

University of Washington

2014

Reading Committee:

Jay Heinecke, Chair

Karin Bornfeldt

Daniel Bowen-Pope

Program Authorized to Offer Degree:

Molecular and Cellular Biology

University of Washington

Abstract

The Impact of Cigarette Smoking on HDL Composition and Function

Katie Thomas

Chair of the Supervisory Committee:

Jay Heinecke, MD

Department of Medicine

It has been known for decades that cigarette smoking is associated with atherosclerosis; however, the specific mechanisms for this association remain unclear. High density lipoprotein (HDL) is known to play a key atheroprotective function by removing excess cellular cholesterol, thereby reversing atherosclerotic lesion formation. Here, we investigate whether smoking causes oxidation of HDL proteins, leading to loss of function. We utilized three separate study populations to interrogate HDL function, protein modification, particle size, and protein cargo—each of which provides distinct information about HDL and its potential roles in biological processes. We observed altered HDL function, particle subpopulations, and protein cargo in smokers. Notably, HDL levels of alpha-1 antitrypsin, an acute phase protein, were positively associated with smoking status. These observations have implications for a role of smoking in generating modified forms of HDL that promote atherosclerosis.

Table of Contents

List of Abbreviations:

A1AT – Alpha-1 Antitrypsin
ABCA1 – ATP Binding Cassette Transporter A1
ACS – Acute Coronary Syndrome
apoA-I – Apolipoprotein A1
BMI – Body Mass Index
CAD – Coronary Artery Disease
CCVD – Cerebro-Cardiovascular Disease
CETP – Cholesteryl Ester Transfer Protein
CPM – Counts Per Minute
HDL – High Density Lipoprotein
HDL-C – HDL cholesterol
HDLP – HDL Particle
IDL – Intermediate Density Lipoprotein
LCAT – Lecithin-Cholesterol Acyltransferase
LDL – Low Density Lipoprotein
LDL-R – LDL Receptor
MPO – Myeloperoxidase
PAH – Polycyclic Aromatic Hydrocarbon
PLTP – Phospholipid Transfer Protein
RCT – Reverse Cholesterol Transport
SFTPB – Pulmonary Surfactant Protein B
SR-B1 – Scavenger Receptor B1
VLDL – Very Low Density Lipoprotein

Chapter 1

Introduction

Cholesterol Homeostasis Under Physiological Conditions

Cholesterol plays an integral physiological role; it regulates cell membrane fluidity and is a synthetic precursor for bile acids and steroid hormones(1-3). It is obtained from the diet though consumption of animal products and is also synthesized endogenously through the mevalonate pathway(4; 5). Due to its lipophilic nature, it traverses the circulation associated with lipoproteins, macromolecular assemblies of lipid and protein.

There are several excellent reviews covering the topic of lipoprotein metabolism(6-8). **Figure 1.1** illustrates some of the key steps in this process. Briefly, dietary cholesterol taken up from the gut enters the circulation associated with chylomicrons, which are the largest lipoproteins, ranging from 50 to 200 nm in diameter. The primary function of the circulating chylomicron is to deliver dietary triglycerides to the periphery, while the cholesterol cargo of chylomicrons remains relatively fixed. The liver takes up triglyceride-depleted chylomicron remnants and breaks them down(9). The cholesterol component is processed and re-secreted as a very low density lipoprotein (VLDL) particle which contains cholesterol and triglycerides(10). Some of the VLDL particle cholesterol cargo is synthesized endogenously in the liver via the mevalonate pathway. Circulating VLDL particles undergo enzymatic hydrolysis of their triglyerides with the release of free fatty acids and glycerol; they also exchange their triglyceride cargo with tissues and other lipoproteins. Through loss of triglyceride cargo, the particles become increasingly denser, transforming first to intermediate density lipoproteins (IDL), then low density lipoproteins (LDL). LDL particles deliver some of their cholesterol cargo to peripheral cells before returning to the liver. LDL is taken up via receptor-mediated endocytosis

through the LDL-receptor (LDL-R)(11). LDL-R gene mutations that lead to reduced or absent LDL-R expression result in elevated circulating LDL particles. Persistent circulating LDL particles are eventually phagocytosed and/or endocytosed by macrophages, forming atherosclerotic lesions and skin lesions termed xanthomas. This condition is known as familial hypercholesterolemia and is associated with early-onset cardiovascular disease.(12) Although wild type mice are naturally resistant to developing atherosclerosis, LDL-R deficient mice are susceptible to lesion formation(13; 14).

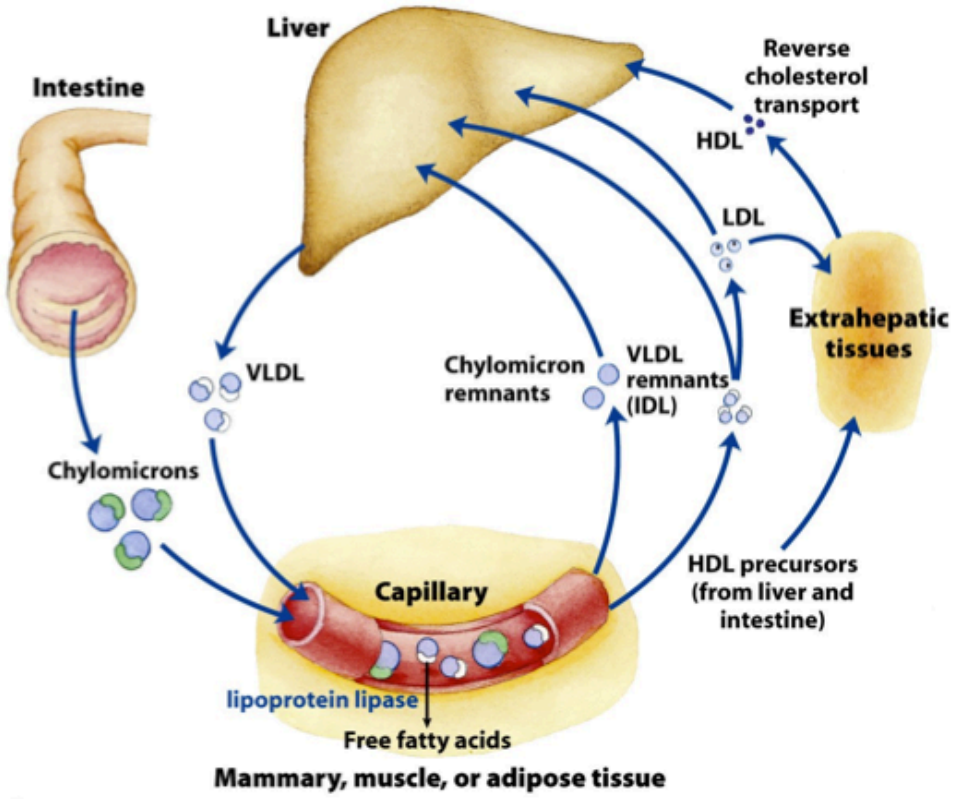

Figure 1.1: Basic lipoprotein metabolism. From (7).

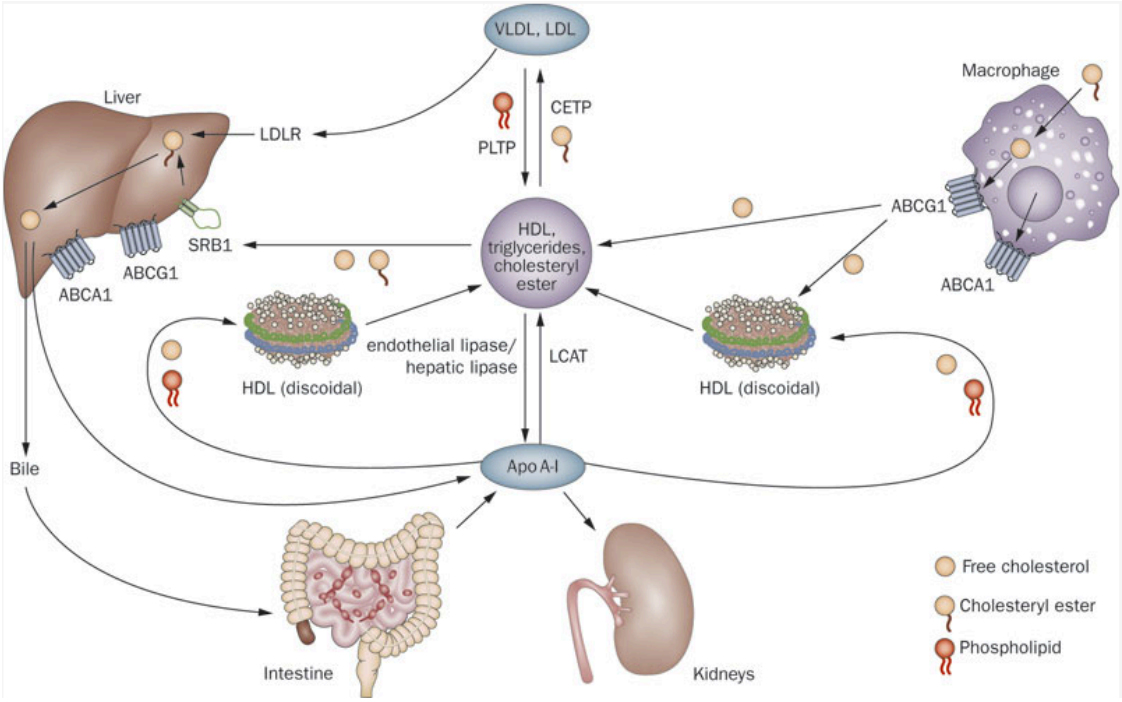

Figure 1.2: Reverse cholesterol transport. From (15)

While LDL particles transport cholesterol from the liver and gut to the periphery, high density lipoprotein (HDL) particles transport cholesterol from the periphery to the liver, where it is secreted as bile, in a pathway known as reverse cholesterol transport (RCT) (**Figure 1.2**)(16). Nascent HDL is secreted by the liver and enterocyte as lipid-free apolipoprotein A-1 (apoA-I). Upon entering the circulation it interacts with the membrane protein ATP-binding cassette A1 (ABCA1), thereby making the release and subsequent acquisition of membrane phospholipid and cholesterol energetically favorable(17). One study reports that this initial interaction prevents apoA-I from interacting with ABCA1 again, presumably due to a conformational shift.(18) This interaction alone generates a population of particles with a heterogeneous size distribution that then continue to take up more cholesterol through interaction with other lipid transporters such as ABCG1 and SR-B1(19; 20). Because free cholesterol and phospholipids are amphipathic molecules, initially these HDL particles take on a discoidal shape wherein apoA-I encircles the

sides and the two planar faces consist of phospholipid and cholesterol. The plasma protein Lecithin:Cholesterol Acyl Transferase (LCAT) associates with HDL to convert its amphipathic cholesterol molecules to hydrophobic cholesteryl esters, which then migrate to the core of the HDL particle, causing it to become spherical(21-24). As the HDL particle circulates it receives more cholesterol cargo from the periphery and grows larger in diameter. The HDL particle may also exchange its cargo with other lipoproteins; cholesteryl ester transfer protein (CETP) facilitates the exchange of triglycerides from LDL or VLDL particles for the cholesteryl esters from HDL particles. Some HDL-associated proteins are exchangeable as well. Finally, the HDL particle returns to the liver where it interacts with Scavenger Receptor B-1 (SRB1) in a process known as selective uptake, in which HDL cholesterol is selectively transferred to the liver for disposal.

Numerous detailed reviews of atherosclerosis exist(25-29). In summary, atherosclerosis is an inflammatory disease that results from the culmination of decades of damage to the artery wall. Sites of hemodynamic stress are most prone to lesion initiation, in which LDL permeates the artery wall and becomes trapped in the subendothelial space. LDL infiltration in turn stimulates nearby cells to secrete monocyte chemotactic protein-1 (MCP-1) and other chemokynes(30; 31). The buildup of LDL and chemokynes attract monocytes, which subsequently become macrophages and release pro-oxidative species that modify the LDL. These macrophages take up this LDL via the oxidized LDL receptor. In response to this inflammation, vascular smooth muscle cells undergo a transformation from a quiescent phenotype to one that is marked by proliferation, migration, and synthesis. There exists evidence that these cells are capable of transdifferentiation into macrophages, accounting for a portion of the macrophages present in lesions(32). Macrophages that are overloaded with oxidized LDL are

known as foam cells. In a self-perpetuating cycle, they release more inflammatory cytokines as they fill with an increasing amount of toxic oxidized LDL. Eventually foam cells die, which contributes to the necrotic core of an advanced lesion. As the lesion grows in size it expands toward the arterial lumen, protruding into the arterial channel. The narrowed space only exacerbates the hemodynamic stress at the site of the lesion, ultimately resulting in plaque rupture and thrombosis. HDL has the ability to remove cholesterol from foam cells, which reverses the progression of lesions in the artery wall(33). HDL can also slow foam cell formation through its anti-oxidative and anti-inflammatory properties.(34)

High Density Lipoprotein

The name "High Density" lipoprotein refers to the fact that HDL was historically defined as the fraction of ultracentrifugally separated human plasma floating in the density range of 1.063-1.21 g/ml, while other lipoproteins have lower densities(7; 35). The difference in density is a result of differing relative protein amounts; while HDL contains about 50% protein by weight, LDL contains only about 21% protein and IDL/VLDL contain even less. HDL particles themselves vary widely in terms of size and lipid content, so can thus be divided into subclasses. The majority of HDL subclasses have alpha electrophoretic mobility (same mobility as α-globulins), but some have pre-beta mobility (between α– and β- globulins)(36; 37). HDL2 particles are large and cholesterol rich, contributing to a large proportion of HDL cholesterol (HDL-C) levels in blood. HDL3 and pre-beta particles are smaller and denser, containing less cholesterol. In patients with acute coronary syndrome (ACS) or coronary artery disease (CAD), HDL2 levels are lower, while HDL3 levels are higher(38), which further supports the inverse relationship between HDL-C and cardiovascular risk. It is important to note that HDL subclasses are not static; a plasma sample should be seen a snapshot of the proportion of HDL particles at

specific points in the RCT pathway. Throughout this pathway, HDL particles exist in different phases of maturation, contain different levels of cholesterol, and therefore have different sizes and electrophoretic mobilities.

ApoA-I is the predominant HDL-associated protein, comprising approximately 70% of the protein cargo by weight(39). Every HDL particle contains at least one ApoA-I molecule. Mature ApoA-I is 243 amino acids long and has a molecular weight of 28 kDa. Its structure is moderately conserved across species(40). The double belt (**Figure 1.3**, top) and trefoil (**Figure 1.3**, bottom) structural models of apoA-I account for the HDL particle's dynamic ability to expand as it acquires more lipid cargo (41-44).

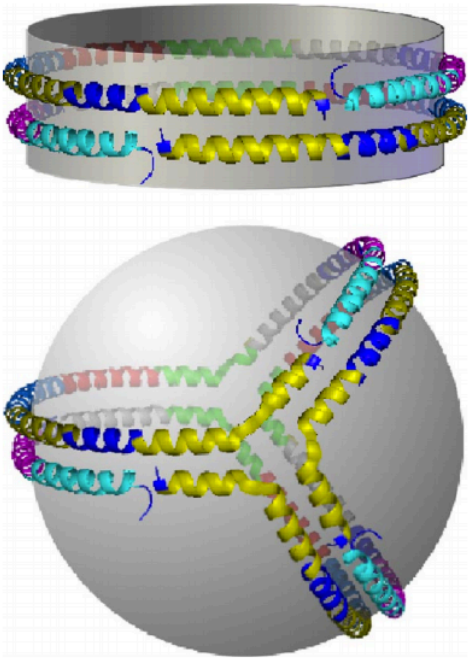

Figure 1.3: Double-belt (top) and trefoil (bottom) structural models of apoA-1 on HDL. From (41).

ApoA-II is the second-most abundant HDL protein, making up approximately 20% of the protein cargo. In spite of being positively associated with HDL-C levels, apoA-II is also associated with lesion progression.(45) The remaining 10% of the HDL protein mass consists of

a wide variety of proteins involved in distinct biological functions including lipid metabolism, protease inhibition, complement regulation, and acute-phase response(46). To date, over 80 proteins have been identified by more than one laboratory in HDL. The protein cargo across HDL particles is heterogeneous, indicating that HDL particles could have distinct functional subpopulations. The presence of specific proteins on HDL particles is strongly associated with the presence of other proteins; for example, clusterin and PLTP tend to be present on the same particles.(47) The HDL proteome can also reflect different disease states; for example, HDL from subjects with end-stage renal disease have elevated Serum Amyloid A, making this HDL more pro-inflammatory than that of a healthy control(48).

The Framingham Heart Study is an ongoing multi generational study aimed to identify genetic and behavioral risk factors for cardiovascular disease. Over 5,000 men and women living in Framingham, Massachusetts enrolled in the initial cohort in 1948. Later, many of the children and grandchildren of these subjects enrolled as well. This study was the first to establish that LDL-C levels are positively associated with an individual's risk for heart disease, while HDL-C levels are negatively associated with this risk(49-52). These findings have prompted decades of therapeutic efforts to lower LDL-C and raise HDL-C (consequently causing LDL-C to be known in layperson's terms as "bad cholesterol" and HDL-C as "good cholesterol").

Statins are a class of drugs that have been used since the 1980s to inhibit HMG-CoA reductase, the enzyme that catalyzes the rate-limiting step of cholesterol synthesis(53-55). By blocking the mevalonate pathway, these drugs heavily reduce endogenous cholesterol synthesis, which causes dietary absorption to be the predominant source of cholesterol. Thus, statins reduce the levels of circulating cholesterol in hypercholesterolemic individuals, reducing susceptibility to atherosclerotic plaque buildup. Furthermore, statins significantly reduce total mortality rates in

subjects with hypercholesterolemia(56). Statin treatment generally results in decreased LDL-cholesterol (LDL-C) and increased HDL-cholesterol (HDL-C). However, subjects that have undergone statin therapy still have a wide range of HDL-C levels. It is tempting to assume that statin therapy is less efficacious in subjects with lower HDL-C post-therapy, but differential HDL-C levels post-therapy may not account for the residual cardiovascular risk in these individuals(57; 58).

Recent clinical attempts to decrease CAD risk by way of pharmacologically increasing HDL-C levels have yielded only modest success, and only in subjects that were not treated with statins.(59-63). In the AIM-HIGH study, subjects undergoing statin therapy were randomly assigned to niacin or placebo. In spite of having significantly elevated HDL-C and significantly lowered LDL-C and triglycerides, the niacin group had no reduction in coronary events(59). Another strategy to increase HDL-cholesterol utilized a class of drugs that inhibited CETP. In spite of increasing HDL-C levels, the CETP inhibitor torcetrapib actually raised blood pressure and increased risk of cardiovascular events.(64-66) Another CETP inhibitor, dalcetapib, increased HDL-C, but failed to mitigate cardiovascular risk.(67) Although the failure of torcetrapib is now attributed to adverse off-target effects, these studies underline the fact that HDL-C is a limited lens through which to view HDL.

These studies support the notion that not all HDL particles are necessarily functionally equivalent. The functional differences could arise from differences in HDL protein cargo or from modification of the HDL itself. This “dysfunctional” HDL is associated with disorders such as diabetes, CAD, and renal disease. It is unclear whether dysfunctional HDL falls in the causal pathway or is the result of these disorders. Recent studies have sought novel ways to characterize HDL in order to compare healthy and diseased groups. For example, the Rader group developed

a cell-based cholesterol efflux assay that measures the capacity of HDL to remove labeled cholesterol from a macrophage cell line. They have thus demonstrated HDL macrophage cholesterol efflux capacity to be a better predictor of CAD status than HDL-C or LDL-C.(68) The cholesterol efflux capacity obtained via this assay is presumed to be proportional to the efficacy with which a subject's HDL removes cholesterol from a macrophage foam cell, reversing plaque formation in the artery wall.

Additionally, HDL particle number has been shown to be a predictor of residual vascular risk in subjects that have already undergone statin therapy. For every 1 standard deviation increase in HDL particle concentration, the hazard ratio for cardiovascular disease is 0.73(69). These results suggest that additional HDL metrics such as particle number and efflux capacity can account for residual cardiovascular risk across equivalent HDL-C levels, providing a more complete picture of cardiovascular health. It is possible that therapies that raise HDL-C levels have been ineffective at fully mitigating CAD risk because HDL-C is not the only clinically relevant characteristic of HDL.

Myeloperoxidase: A Mechanism for Loss of HDL Function?

The protein myeloperoxidase (MPO) is a heme enzyme that is predominantly produced by neutrophils, as well as monocytes and some populations of macrophages. It resides in the azurophilic granules, where it is a major component of the neutrophil, making up approximately 5% of its dry weight(70). When secreted into the pericellular environment it plays a role in innate immunity, as it generates reactive species that are toxic to microbial pathogens(71). However, these species are also capable of damaging host tissues. Like other proteins in the peroxidase family, MPO uses hydrogen peroxide as a substrate. MPO utilizes the hydrogen peroxide generated by neutrophil NADPH oxidase during the respiratory burst and *in vivo*

concentrations of chloride ion to produce hypochlorous acid (HOCl)(71). Hydrogen peroxide reacts with the ferric iron of the heme group to generate the catalytic form of MPO, which has an oxygen atom bound to the heme group. MPO then goes on to react with chloride in a two-electron reduction to generate HOCl(70).

HOCl reacts with tyrosine residues with a rate constant of 44/(M*s) to form the product 3-chlorotyrosine(72). Although HOCl reacts more readily with other amino acids, 3-chlorotyrosine is significant because it is stable and it is an MPO-specific product. For instance, MPO can oxidize methionine and tryptophan residues, but other pathways can generate these products. Thus, 3-chlorotyrosine is the only modified amino acid residue that specifically implies MPO-mediated damage.

The activated phagocytes in an atherosclerotic lesion express MPO. ApoA-I of HDL isolated from carotid lesions has elevated levels of 3-chlorotyrosine(73). Although the HDL is only transiently present at the lesion as it effluxes cholesterol, it can be damaged by MPO as well. Indeed, individuals with atherosclerosis have elevated apoA-I levels of 3-chlorotyrosine(74). Chlorinated tyrosine residues of apoA-I serve as more than a marker for MPO activity; this HDL has impaired ability to efflux cholesterol(75). Thus, the MPO pathway is one mechanism by which dysfunctional HDL is generated.

Human apoA-I has seven tyrosine residues, but site-specific modification studies using tandem mass spectrometry have demonstrated that not all are equally susceptible to modification by MPO. For example, Y192 is the most susceptible tyrosine residue in apoA-I to chlorination. Over 20% of Y192 residues are chlorinated after 1 hour at 37°C in the presence of 50 nM MPO and 0.1 M NaCl with 25M H_2O_2 /mol apoA-I(76). Y192 resides adjacent to K195 in an alpha helix, in a so-called YxxK motif, which could increase the propensity for generation of 3-

chlorotyrosine at this site(77). HOCl reacts with the amino group of lysine at a faster rate than it does with tyrosine; the rate constant for this reaction is 5000/(M*s)(72). However, this reaction generates lysine chloramine, an unstable intermediate that may facilitate the formation of the more stable 3-chlorotyrosine. Two of the other tyrosine residues of apoA1 are in YxxK motifs, but are less chlorinated, which could result from being shielded from the surface or by protection via adjacent methionine residues which react with HOCl more readily than any other amino acid side chains. In one study, a mutant with a methionine residue at position 189 (adjacent to Y192) was generated(78). The presence of this residue drastically reduced the susceptibility of Y192 to chlorination *in vitro* by MPO and HOCl. It is plausible that methionine residues could prevent chlorotyrosine formation in YxxK motifs that exist *in vivo*. ApoA-I mutants containing additional YxxK motifs were also generated. The tyrosine residues in the artificially created YxxK motifs of these mutants were more susceptible to chlorination than wild-type apoA-I. Mutation of K195 to arginine drastically reduced chlorination at Y192, indicating that the adjacent lysine residue promotes chlorination at this site. Therefore, it is plausible that the YxxK motif plays a role in promoting site-specific chlorination *in vivo*.

In a study aligning the sequences of apoA-I across 31 animal species, both Y192 and E191 are completely conserved, suggesting that this region is critical to the function of apoA-1(40). This was the only consecutive pair of amino acids in apoA-1 found to be completely conserved in this study. It is likely that chlorination of these conserved residues could affect HDL function. It has been proposed that this region acts as a hinge domain of apoA-I that is crucial for the protein's ability to change conformation in response to cholesterol loading. MPO could impair cholesterol efflux by impeding the ability of this region to act as a hinge (**Figure**

1.4). In total, five of the seven tyrosine residues in apoA-I are conserved, meaning that tyrosine residues are likely of functional importance to HDL(40).

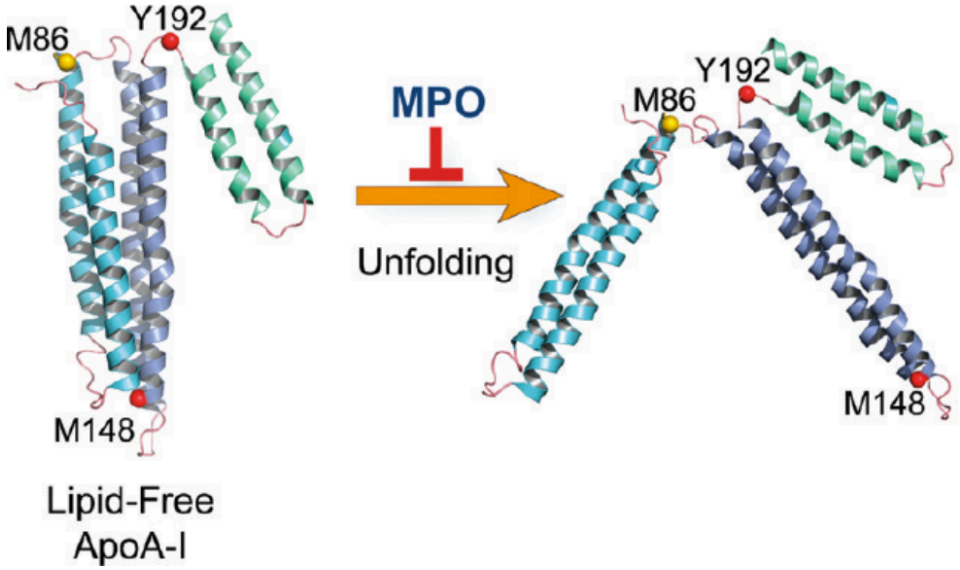

Figure 1.4: Y192 of human apoA-1 resides in a putative hinge domain, which may be necessary for the conformational shift that occurs upon ABCA1 association. Adapted from Shao, et al(75).

To determine the functional implications of the chlorination of Y192, one study compared wild type human apoA-I with a mutant that replaced Y192 with phenylalanine. Both forms of apoA-I were oxidized in vitro using a system of MPO + H2O2 + HOCl. There was no observed chlorination at the mutated site. Furthermore, mutation of Y192 to phenylalanine partially rescued the protein's cholesterol efflux capacity(78). Therefore, chlorination at this position likely results in reduced efflux capacity of apoA-I.

MPO activity can also result in the production of reactive nitrogen species, which react with tyrosine to form 3-nitrotyrosine, although unlike chlorotyrosine this product is not specific to MPO. Site-specific nitration is thought to occur independently of YxxK motifs, but may instead preferentially occur at solvent-accessible tyrosine residues(79).

MPO promotes oxidation of methionine residues as well, but like nitrotyrosine, methionine sulfoxide is not an MPO-specific product. Nevertheless, there is evidence that methionine oxidation is also deleterious to apoA-I function. ApoA-I that had been exposed to MPO or HOCL *in vitro* had markedly greater efflux capacity when methionine oxidation was subsequently reversed with PilB, a bacterial methionine sulfoxide reductase(78). Additionally, M148 is suspected to play a role in the ability of apoA-I to activate LCAT. Mutant apoA-I with a leucine residue replacing M148 had a greater capacity to activate LCAT than wild-type apoA-I after exposure to MPO or HOCl *in vitro*(80).However, mutating either of the other methionine residues to leucine failed to restore LCAT activation ability under these conditions. A decrease in LCAT activation ability would prevent esterification of surface cholesterol, thereby stunting HDL particle maturation and reverse cholesterol transport.

Smoking

Smoking is associated with an increased risk of many diseases including heart attack, stroke, chronic obstructive pulmonary disorder, and lung cancer. It is the single greatest cause of preventable deaths worldwide, responsible for over 5 million deaths per year(81). It is estimated that given current trends this number will increase to 8 million by the year 2030. In the United States, 25% of deaths between ages 35 and 69 are attributable to smoking(82). As many as half of all tobacco users worldwide will eventually die of a tobacco-related disease. Despite the advent of campaigns to increase awareness of the dangers of smoking, it is still prevalent. The developing world in particular has experienced an increase in the number of smokers, due to rapid population growth and aggressive tobacco advertising coupled with limited awareness of the dangers of smoking. These individuals are at an increased risk of mortality due to inadequate healthcare. In the developed world, less educated individuals are less likely to be aware of the

range of diseases caused by smoking(83). Smoking drastically reduces life expectancy; adjusting for educational level, alcohol consumption, and adiposity, smoking reduced life expectancy by 11 years for females and 12 years for males(82). In this model, while 70% of female and 61% of male never-smokers lived 80 years or more, only 38% of female and 26% of male current smokers lived this long. However, smokers can recover life expectancy by cessation. Cessation early in life recovers the most years, but even cessation in the 6th decade of life yielded a 4 year increase in life-expectancy compared to individuals who continued to smoke. Post-cessation circulating levels of inflammatory markers such as white cell count, C-reactive protein and fibrinogen remain persistently elevated, only approaching never-smoker levels by 20 years after cessation(84).

The mechanism by which smoking causes lung cancer is well established. Smoke itself contains a multitude of carcinogenic compounds including polycyclic aromatic hydrocarbons (PAH) and nitrosamines, which compromise genomic integrity by forming DNA adducts(85). Smoking also introduces reactive oxygen species into the airspace, both as a component of smoke, and endogenously produced by activating the body's innate immune system. Smoking promotes extensive neutrophil activation in the lung; upon smoking a cigarette, pulmonary retention of neutrophils increases(86; 87). There is also a dose-dependent relationship between number of cigarettes smoked and neutrophil levels(88). The influx of activated neutrophils to the lung causes significant damage to the host tissues by way of MPO. MPO activates smoke carcinogens such as the PAH benzo[a]pyrene(89). The significance of MPO in the development of lung cancer is evidenced by the fact that lower MPO expression is associated with decreased lung cancer risk. One study that included smokers and nonsmokers found that individuals

homozygous for a polymorphism in the MPO promoter resulting in reduced gene expression significantly decreases the odds of developing lung cancer(90).

In contrast, the mechanism by which smoking promotes CVD and stroke remains unclear. In a large prospective study of over 30,000 members of the German workforce, certain consequences of smoking, such an altered lipid profile and increased clotting factors accounted for some, but not all, of the increased risk(91). In a meta-analysis of 54 studies, smoking was demonstrated to significantly associate with increases in total cholesterol, VLDL-C, LDL-C, and triglycerides, and a decrease in HDL-C. Smokers have lower body mass indices (BMI) than nonsmokers, and former smokers have higher BMIs than never smokers. These observations are attributable to the role of nicotine as an appetite-suppressant. However, smoking results in an altered body fat composition; smokers have a higher waist to hip ratio than nonsmokers, indicating increased abdominal adiposity(92). This altered fat distribution has been attributed to the observation that smokers have elevated fasting cortisol levels, which could promote abdominal adiposity. Additionally, smokers have higher fasting glucose levels and an increased insulin response to an oral glucose load(93). These changes in lipid homeostasis could also manifest as altered lipid metabolism in the artery wall, potentially resulting in atherogenic consequences.

Protease-Antiprotease Imbalance

Neutrophil activation also damages the lung through the action of proteases secreted by the neutrophil. The proteases neutrophil elastase, proteinase 3, and cathepsin B are present in the azurophilic granules; their release coincides with the release of MPO(94; 95). Elastase degrades elastin in the lung, allowing the neutrophil to traverse the connective tissue(96). Under normal conditions, the serpin protease inhibitor alpha-1 antitrypsin (A1AT) regulates the proteolytic

activity of elastase. Like other serine protease inhibitors (SERPINs), A1AT forms a complex with its target protease and forces it to adopt an unstable conformation, inactivating it and resulting in its degradation(97). This in turn limits the location of elastin degradation; it is localized to the areas surrounding the neutrophil, which have superphysiological levels of elastase. However, prolonged neutrophil activation in the lungs leads to extensive elastin degradation, causing the tissue to lose its contractile ability over time(98; 99). The long-term presence of activated neutrophils in a smoker's lung is responsible for emphysema, a manifestation of chronic obstructive pulmonary disorder (COPD); approximately half of lifetime smokers develop this condition. Emphysema is caused by the irreversible degradation of lung elastin, trapping air in the lungs and resulting in shortness of breath. Ephysema progression is determined by measuring the amount of air that can be forced out of the lungs following a deep breath, known as the forced expiratory volume (FEV). As emphysema progresses, the lungs lose their elasticity, and the FEV is increasingly lower.

Thus, the proteases in the lung are tightly controlled by the lung's antiproteases. Protease-antiprotease imbalance occurs when this control is lost. Prolonged neutrophil activation triggers recruitment of pro-inflammatory cytokines, which in turn leads to an influx of additional leukocytes. This tips this balance toward the proteases, resulting in degradation of lung connective tissue. In addition to being pro-inflammatory, oxidative species are also capable of inactivating antiproteases(100; 101). Antiprotease deficient individuals are more susceptible to protease-antiprotease imbalance.

A1AT is a 394 amino acid protein encoded by the SerpinA1 gene. Although bronchial epithelial cells produce the A1AT that is found in the lung, hepatocytes produce the majority of A1AT in the body(102; 103). In addition to being present in the lung, it is the most abundant

protease inhibitor in the blood. As an acute-phase protein it becomes elevated within hours of an inflammatory stimulus and is a biomarker for acute coronary syndrome(104). The main function of circulating A1AT is thought to be to prevent excessive connective tissue damage at sites of inflammation. This in turn prevents a self-perpetuating cycle of inflammation that can arise when the immune system damages host tissues. A1AT has been identified as an HDL-associated protein by tandem mass spectrometry and 2-D SDS-PAGE(46; 105). Shotgun proteomics of HDL showed no significant difference in A1AT levels between healthy controls and smokers, although the CAD subjects showed a trend of having higher levels. In a study involving a mouse model of elastase-induced emphysema, a HDL-A1AT complex was more effective at mitigating elastin degradation than either HDL or A1AT alone(106). This suggests that HDL-associated A1AT is more bioavailable than free-circulating A1AT. A1AT has no reported function in lipid metabolism, highlighting the fact that HDL and its bound proteins are involved in other distinct physiological roles.

There are two well-characterized SerpinA1 mutations that result in reduced circulating A1AT: the Z allele and the S allele. The Z allele results in A1AT that is prone to polymerize within the hepatocyte, forming aggregates that are never secreted, and eventually result in cirrhosis(107). The S allele has reduced stability compared to wild-type A1AT, meaning that it has a reduced circulating half-life(108). Smokers with A1AT deficiency are at increased risk to develop emphysema, although this deficiency is rare, affecting only about 1 in every 2,000 individuals of European ancestry(107).

Alveoli and Pulmonary Surfactant

The pulmonary alveoli are the site of gas exchange, in which the carbon dioxide in venous blood is exchanged for oxygen. To facilitate gas diffusion, the alveolocapillary

membrane is extremely thin, consisting of only one layer of alveolar epithelium and one layer of capillary endothelium. Type I alveolar cells, which are branched squamous epithelial cells that are responsible for gas exchange, comprise the majority of the luminal alveolar surface area. Type II alveolar cells are columnar cells that are responsible for the secretion of pulmonary surfactant; and for the general maintenance of the alveolar space. They are also the progenitors for type I alveolar cells(109). Pulmonary surfactant forms a monolayer that lowers the surface tension in the alveoli, which prevents them from collapsing after expiration. Pulmonary surfactant is about 95% lipid and 5% protein, technically making it a lipoprotein. The majority of the lipid portion is phosphatidylcholine; other phospholipids such as phosphatidylglycerol and phosphatidylinositol are also present(110). The phospholipids are synthesized in the type II cell. Additionally, cholesterol plays an important role in maintaining the fluidity of the surfactant layer. Type II cells are capable of endogenous cholesterol synthesis but this is supplemented by cholesterol from circulating lipoprotiens(111). Type II cells store surfactant in lamellar bodies, specialized compartments which are derived from the Golgi apparatus(112). Lamellar bodies fuse with the luminal membrane when more surfactant is needed, generating a tubular myelin structure. Throughout life, surfactant components are re-absorbed into the type II cell and recycled(113).

Efflux of excess cholesterol from alveolar macrophages is primarily mediated by the ABCG1 transporter. ABCG1 deficient mice fed a normal diet experience progressive pulmonary lipidosis due to cholesterol accumulation in Type II cells and alveolar macrophages(114). They also consequently contain excess surfactant. Like the macrophage foam cells of the artery wall, these lipid loaded macrophages trigger a chronic inflammatory state(115). LDL-R deficient mice with ABCG1 deficient macrophages or total-body ABCG1 deficiency have increased

atherosclerotic lesion size(116). Furthermore, myeloid-specific ABCG1 deficiency is sufficient to trigger pulmonary inflammation, demonstrating the role of alveolar macrophages in pulmonary cholesterol efflux(117).

Type II cells also synthesize the four surfactant proteins, named A-D based upon the order in which they were discovered. Surfactant proteins A (SFTPA) and D (SFTPD) are hydrophilic while proteins B (SFTPB) and C (SFTPC) are hydrophobic. SFTPA and SFTPD are in the collectin family and play a role in innate immunity through acting as an opsonin for gram-negative bacteria(118). Only SFTPA is necessary for bacterial killing, but both proteins are necessary for modulation of cytokine production(119). SFTPA also facilitates the conversion of lamellar bodies to tubular myelin(120). SFTPB and SFTPC play a role in surfactant lipid dynamics by further lowering alveolar surface tension. SFTPB also plays a role in tubular myelin formation.

Pulmonary surfactant protein B is a hydrophobic 79 amino acid protein that exists as a homodimer(121). Like other saposin-like proteins, it contains seven cysteine residues, six of which form three intramolecular bridges, and one that forms an intermolecular bridge. It is necessary for proper lamellar body formation, a crucial step in the secretion of lung surfactant. Immature SFTPB is 381 amino acids long. SFTPB undergoes extensive proteolytic processing on its way from the Golgi apparatus to the lamellar bodies, and in turn is crucial for the fusion of multivesicular bodies and lamellar bodies(122). The N-terminal amphipathic alpha helix readily interacts with phospholipid head groups, disrupting phospholipid bilayers, resulting in membrane fusion(123). SFTPB is also necessary for appropriate post-translational processing of SFTPC(124). The processing steps and intermediate forms are currently not completely established, however Napsin A and Cathepsin H are known to play a role in this process(125).

SFTPB deficient humans and mice die postnatally due to a lack of functional surfactant, resulting in alveolar collapse(122). The type-II alveolar cells of SFTPB deficient mouse embryos have multivesicular inclusion bodies in contrast to the properly formed lamellar bodies present in their hemizygous littermates. Lethal mutations of SFTPB may prevent vesicle maturation entirely, thereby precluding the release of surfactant to the alveolar lumen.

Trace amounts of SFTPB are observable in the circulation, even in healthy individuals. The exact mechanism by which this protein enters the circulation is unknown, however these levels are higher in individuals with heart disease or lung inflammation, implicating increased alveolocapillary membrane permeability as a possible explanation(126). The concentration of SFTPB in the alveolus is 1500 times that in the plasma; permeable alveoli would enable SFTPB to diffuse down the concentration gradient(127). In a recent cross-sectional study of individuals aged 30-65 years, smokers were observed to have 5-fold higher circulating levels of SFTPB than nonsmokers, and these levels were proportional to lifetime smoking exposure(128). Additionally, circulating SFTPB levels were a significant predictor of aortic plaque levels and all-cause mortality in current smokers, adjusting for cardiovascular risk factors. These correlations have unclear implications; to date there is no known mechanistic relationship between the presence of circulating SFTPB and cardiovascular disease. SFTPB has been previously reported to associate with HDL; its levels are elevated in subjects with end-stage renal disease(48).

Numerous reactive species are inhaled on a regular basis. Another function of pulmonary surfactant is to shield pneumocytes from these damaging species. Vitamin E plays an important role in surfactant as an antioxidant; it protects surfactant lipids from oxidation(129). HDL delivers Vitamin E to the type II alveolar cells, which are reported to take up the HDL holoparticle via the cubilin and megalin receptors(130). Thus, in addition to removing excess

lipids, HDL also delivers Vitamin E to the lung, which further demonstrates that HDL has antioxidative and anti-inflammatory properties. Oxidative stress in the lung such as hyperoxia causes a higher vitamin E turnover rate(131). Provided that HDL is the sole source of Vitamin E to the lung, it follows that oxidative stress in the lung would lead to an increased uptake of HDL. ApoA-I levels were observed to be elevated in the bronchoalveolar lavage fluid of patients suffering from mustard gas exposure and acute respiratory distress syndrome(132; 133). ApoA-I is not expressed in pneumocytes, which means that circulating HDL is a likely source of apoA-I in BAL fluid. Currently the mechanism for this increase in apoA-I concentration is unknown, but it could be due to increased alveolar permeability or be due to increased HDL uptake by type II cells.

Cigarette Smoking as a Possible Mechanism for Generating Dysfunctional HDL

A recent *in vivo* study demonstrated that atherosclerosis is associated with increased oxidation of apoA-I(74). Subjects with stable coronary artery disease or acute coronary syndrome (ACS) had significantly higher chlorinated Y192 and oxidized M148 than healthy controls. Additionally, these two modifications were highly correlated, indicating that MPO was likely responsible for much of the oxidation at M148. Oxidation of apoA-I also correlated with ABCA1-mediated cholesterol efflux capacity in these subjects. Chlorination of Y192 was independent of the majority of traditional CAD risk factors; it had no association with age, sex, hypertension, total cholesterol, LDL-C, or triglycerides. It was negatively associated with HDL-C and positively associated with diabetes and smoking status. However, from this study, it was unclear whether there is a causal relationship between smoking and chlorination of Y192, as the majority of the control group was nonsmokers **(Figure 1.5)**; smokers with ACS and CAD drive

the trend of increased chlorination at Y-192. The four smokers from the control group do not appear to have increased chlorination at this site compared to nonsmokers.

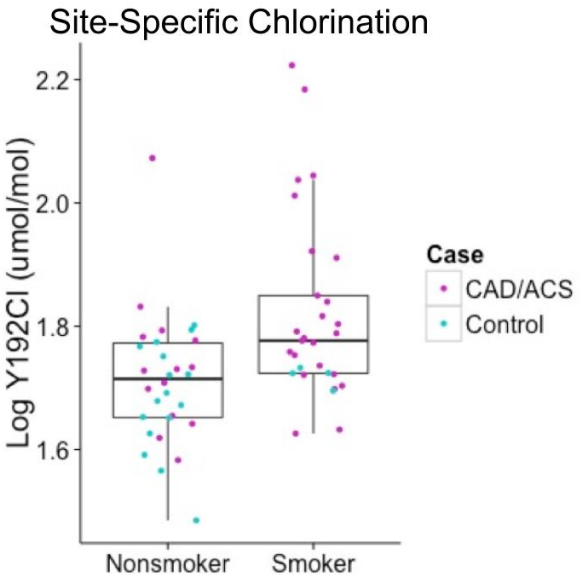

Figure 1.5: Smokers have significantly higher chlorination at Y192 than nonsmokers (two-tailed $P < 0.005$; nonsmoker n = 30; smoker n = 29). Adapted from Shao et al(74).

There is little information to date regarding the impact of smoking on HDL, other than the observed tendency for smokers to have lower HDL-C than nonsmokers(134; 135). The above study prompted interest in determining how (if at all) smoking status relates to HDL characteristics. This dissertation approaches this question by addressing several key aspects of HDL. It utilizes three different study populations with unique clinical characteristics in order to reduce the possibility of confounding. Due to the dearth of previous information regarding the ways in which smoking may affect HDL, we utilized the initial set of subjects to test the hypothesis that smoking is associated with increased apoA-I chlorination and decreased sterol efflux capacity, as well as to generate hypotheses regarding the effect of smoking on HDL particle subpopulations and protein cargo. The subsequent two analyses served to validate findings from the initial analysis.

Chapter 2

Materials and Methods

HDL Isolation

HDL was isolated from plasma in a two-step density gradient ultracentrifugation process. In the first centrifugation step, lipoproteins (d < 1.21 g/ml) were separated from other plasma components (d > 1.21 g/ml). 335 µl of EDTA plasma (assumed density 1.006 g/ml) was brought to a final density of 1.21 g/ml through the addition of 108.7 mg solid KBr. 150 µl of 1.21 g/ml KBr was added to a thick walled polycarbonate ultracentrifuge tube. 350 µl of the adjusted-density plasma was added below the KBr solution using a Hamilton syringe. To separate lipoproteins from denser plasma components, the samples were spun in a 120.1 rotor (Beckman Coulter) at 120K RPM (513,000 × *g*) at 5° C for 4.5 hours. The lipoprotein fractions were removed as the top 125 µl in the tube after the spin.

In the second centrifugation step, the HDL fraction (1.063 g/ml < d < 1.21 g/ml) was separated from the LDL/VLDL fraction (d < 1.063 g/ml). 120 µl of the lipoprotein fraction from the first step was transferred to a new centrifuge tube. 239.2 µl normal saline and 140.8 µl KBr (d=1.063 g/ml) was added. The samples were spun in a 120.1 rotor at 120K RPM (513,000 × *g*) at 5°C for 2 hours. The LDL/VLDL fraction was collected by removing the top 57.5 µl. The HDL fraction was collected by removing the bottom layer using a Hamilton syringe with a Chaney adaptor set for 125 µl.

The collected lipoprotein fractions were then dialyzed against a 300x volume of 20 mM potassium phosphate/100 µM DTPA and stored at -80˚C until ready for use.

Trypsin Digest of HDL

HDL proteins were digested with trypsin in order to generate peptides for mass spectrometric analysis. 10 μg of each UC-isolated HDL fraction was plated into 500 μl V-bottom 96-well plates (Axygen). The volume in each well was brought to 40 μl with 20 mM potassium phosphate, pH 7.4. 0.5 μg of 15-N labeled human apoA-I and 100 μg RapiGest surfactant (Waters) was added to each well. The remainder of the digest took place in the presence of 100 mM ammonium bicarbonate. Disulfide bonds were reduced with 5 mM dithiothreitol (DTT) (Bio-Rad) at 37°C for 1 hour. Cysteine thiol groups were alkylated in the presence of 15 mM iodoacetamide (Bio-Rad) for 30 minutes at room temperature in the dark. Unreacted iodoacetamide was scavenged with 2.5 mM DTT for 15 minutes at room temperature. 0.5 μg trypsin (0.1 μg/μl in 1 mM HCl) was added to each well. pH was verified to be >7.5 and plates were incubated at 37°C. After 2 hours, 0.5 μg additional trypsin was added to each well. pH was once again verified to be >7.5 and samples remained at 37°C overnight. Rapigest was cleaved by adding 9 μl 10% trifluoroacetic acid in water. pH was confirmed to be <2 and plates were incubated at 37°C for 45 minutes. Digests were dried down in a vacuum concentrator and stored frozen at -80˚C prior to reconstitution for mass spectrometric analysis. Samples were reconstituted in 0.1% formic acid one day prior to analysis.

Liquid Chromatography-Mass Spectrometry

The coupling of liquid chromatography and mass spectrometry (LC-MS) allows for detection and quantification of specific compounds in complex mixtures. Like other chromatographic methods, liquid chromatography separates a mixture of samples based upon their affinity to the stationary phase. However, the liquid chromatography in all of the following

experiments was reverse-phased, so called due to the use of a hydrophobic stationary phase (historically, stationary phases were made of a hydrophilic material such as silica). For the following experiments, peptides were loaded onto a column containing C18-bonded silica packing material. In the presence of a polar mobile phase, peptides readily bind the packing material. However, acetonitrile (which is nonpolar) was then added to the mobile phase in increasing concentrations, causing peptides to elute off the column once they were surpassed in nonpolarity by the mobile phase. Thus, the most polar peptides elute off the column first.

The peptides enter the mass spectrometer through the electrospray ionization source. The tip of the capillary column is highly charged, transforming the eluting peptides into a spray of charged droplets consisting of peptide ions solvated in the mobile phase. Some of the solvent evaporates, resulting in smaller droplets. Eventually, the droplet ions are forced into close enough proximity to result in columbic repulsion, which prompts droplet fission. Ions at the surface of the droplets are ejected into the gas phase, into the sampling skimmer cone of the instrument.

A quadrupole mass analyzer is a set of four parallel metal rods. Each pair of opposing rods is electrically connected, and an RF voltage superimposed with a DC current is applied to each pair in an alternating fashion. The ion will oscillate within the quadrupole; the amplitude of its oscillation depends on its mass to charge ratio (m/z). If an ion oscillates with an amplitude exceeding the width of the interior of the quadrupole, it will strike the rods. If its amplitude of oscillation does not exceed this size, it will pass through the quadrupole. The applied voltages can be changed such that amplitudes will also change, making it possible to select which ions pass through the quadrupole at a given time.

A quadrupole can also be used as a collision cell, used to generate product ions by fragmenting precursor ions for tandem mass spectrometry (MS/MS). In this instance, only an RF voltage is applied, but the chamber contains an inert gas such as argon. As the ions migrate across the quadrupole, they collide into these atoms, which results in their fragmentation.

Ion traps are another type of mass analyzer. They are electrode chambers in which ions oscillate with a stable trajectory, preventing them from hitting the sides. The oscillation of each ion once again depends on its m/z and changes with the voltage applied. Ions of specific m/z can be ejected from the trap by changing the electrode system potential. This generates unstable ion trajectories, causing them to be ejected from the trap. Ion traps exist in several configurations, but all are essentially chambers that store ions and eject them according to their mass. For example, an orbitrap is an ion trap that consists of a hollow electrode encasing a spindle-like inner electrode. As reviewed by Scigelova(136), it uses an electrostatic field to trap ions in a complex orbit-like motion about the inner electrode. Due to the complexity of the motion, a Fourier transform must be performed to de-convolute the m/z. These analyzers have extremely high mass accuracy, often less than 2 ppm, even in complex mixtures. They also have high resolving power, which is advantageous when working with complex mixtures.

Once the ions have been separated by the mass analyzer, they are sent to the detector. Detectors typically employ an electron multiplier in order to magnify the ion signal. Essentially, a single ion bombards a material that facilitates secondary emissions, or the emission of additional electrons. The electron multiplier is configured such that these emitted electrons subsequently encounter another emissive surface, prompting further electron emission. This emission cascade continues for several cycles until the voltage generated is large enough to be read as total ion current and interpreted by a computer.

The basic mass spectrometry workflow consists of three steps: ionization, separation by mass analyzer, and detection of the ion signal. MS/MS features a fragmentation step after the initial mass analysis, followed by a second round of mass analysis of the products of fragmentation. In this way, it is possible to discern structural information about the analyte by comparing the m/z of a precursor ion to those of the product ions generated.

Tandem Mass Spectrometry Applied to Proteins

The field of proteomics utilizes tandem mass spectrometry to identify specific peptides and detect modifications of amino acid side chains. Fragmentation of peptides occurs at distinct places along the backbone to generate characteristic product ions(137). These different fragmentation products are specified by a letter, which designates the cleaved bond in the backbone and the side of the cleavage where the charge is retained. A, B, and C ions result from charge retention in the amino terminal fragment and X, Y, and Z ions result from charge retention in the carboxy terminal fragment. A and X ions result from the cleavage of the bond between the α-carbon and the carbonyl carbon, B and Y ions from the cleavage of the peptide bond, and C and Z ions from the cleavage of the bond between the nitrogen and the α-carbon. The ions are also numbered based upon the position of fragmentation; the ion number is equivalent to the number of side chains present in the ion. For example, a b-5 ion would be fragmented 5 amino acids away from the N-terminus of the peptide.

B ions and Y ions are the most commonly used peptide fragment ions in proteomics and result from lower-energy collision techniques. Fragmentation does not occur evenly throughout the peptide bond; for instance, peptide bonds located N-terminally to proline residues are particularly prone to y-ion formation(138). The relative abundance of specific peptide product ions can be predicted based on these rules or base upon previously observed data. Peptide Atlas

is an example of a database of peptide MS/MS data that can be used to predict future fragmentation patterns(139). Peptide fragmentation can be used to map the presence of side chain modification. In **Figure 2.1**, the upper spectrum shows an unmodified peptide of apoA-I, while the lower spectrum shows a peptide with a nitrated tyrosine residue. All of the fragments that contain tyrosine in the lower spectrum have masses that differ from those in the upper spectrum by 45.

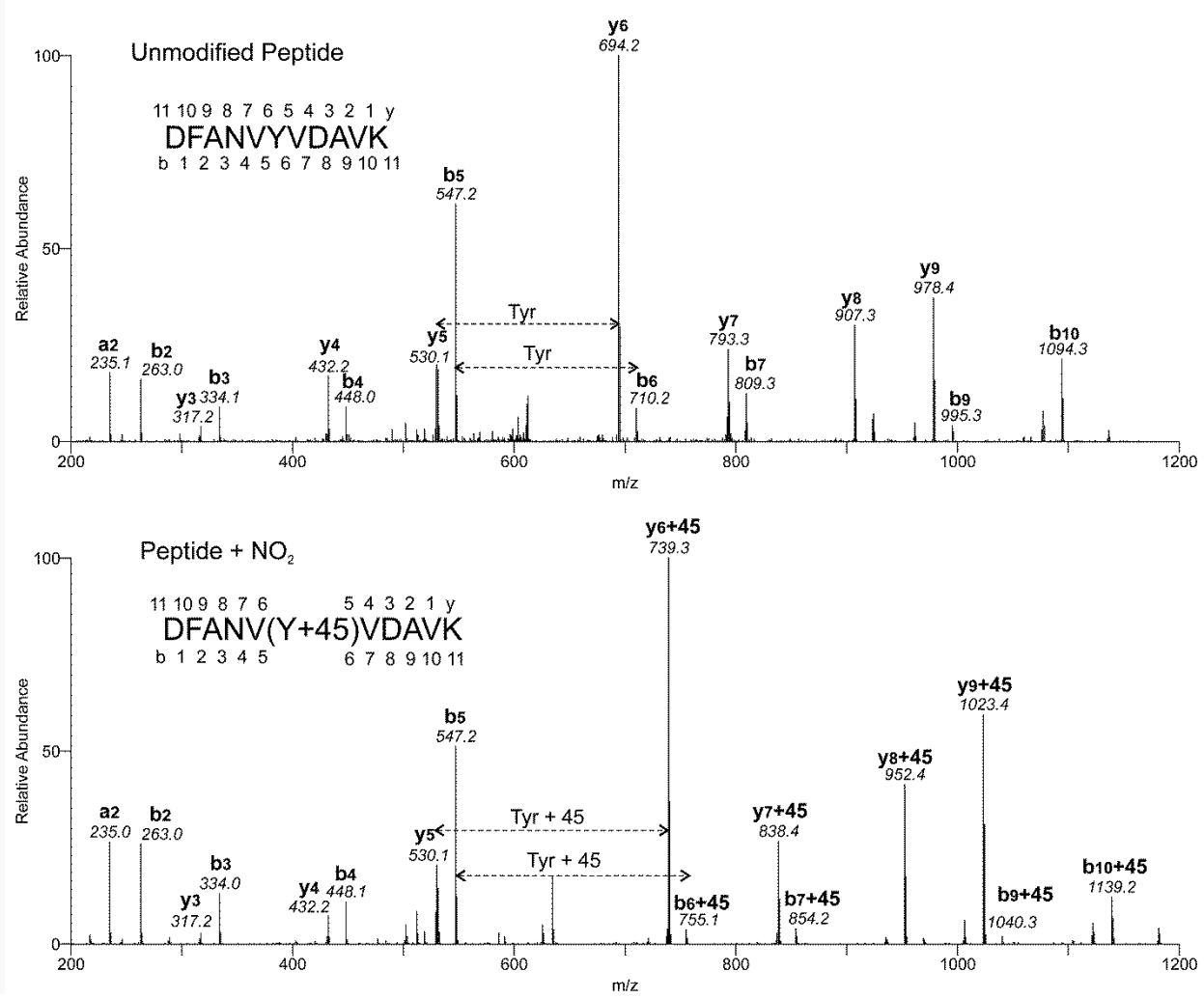

Figure 2.1: Tandem mass spectra of unmodified peptide (upper) and nitrated peptide (lower).

Shotgun proteomics

Shotgun proteomics was used in order to generate candidate proteins for quantitative analysis. This technique uses data-dependent scanning of the most abundant peptides, and is therefore a semi-quantitative technique. It has been used to determine relative differences in protein levels among groups(140), but with the advent of more advanced technologies it should be viewed as a hypothesis generating method.

Samples were set into the rack of a Michrom Paradigm AS1 HPLC system coupled to a Thermo Finnigan LTQ 2d linear ion trap mass spectrometer. The mass range was set to 300-2000 m/z. The instrument was in data-dependent scanning mode, meaning that the instrument selected ions to scan based on relative ion abundance. It made one full MS scan followed by nine MS/MS scans. In between every sample run, angiotensin/neurotensin was injected. This served two purposes: to monitor instrument performance over time, and to reduce carry-over from sample to sample.

The system was set up without a trap column; the de-salted samples were loaded directly onto the analytical column. The stationary phase was a Magic C18 AQ column (150 x 0.15 mm, 5 μm 200Å, Michrom BioResources, Inc). The flow rate was 1 μl/min. Mobile phase A was 0.1% formic acid; mobile phase B was 0.1% formic acid in 90% acetonitrile,

Each sample run yielded a RAW file, which was converted to mzXML format, then searched against the UniProt human database using SEQUEST(141). Search results were processed using the Trans-Proteomic Pipeline(142), then uploaded to CPAS, wherein comparisons in peptide abundance across samples could be addressed(143). In order for a protein to be considered present in a sample, two unique valid peptides had to be observed. Peptide

validity was determined using the statistical algorithm Peptideprophet(144); its cutoff value was set to ≥ 0.9.

Targeted Proteomics

10 μg HDL digests were injected into a nanoACQUITY UPLC system (Waters) coupled with a TSQ-Vantage mass spectrometer (Thermo). The stationary phase was a 5 μm, 100 Å Magic C18 column (Michrom) packed in-house to 15 cm in a 75 μm fused silica capillary tube (Polymicro); mobile phase A was 0.1% formic acid and mobile phase B was 0.1% formic acid in 90% acetonitrile. The flow rate was 0.6 μl/min, the run time was 2.5 hours. The instrument operated in SRM mode. For a complete list of transitions used, see **Appendix**. Data was analyzed using Skyline(145).

Total Modified Tyrosine Analysis

Because MPO is capable of modifying tyrosine residues on any protein, the overall amount of modified tyrosine residues on HDL was also measured.

UC-isolated HDL samples underwent an initial delipidation process adapted from that of Wessel and Flügge(146). 15 μg HDL protein (as measured by Bradford protein assay) was brought to a final volume of 185 μl in H_2O with 27% methanol and 30% chloroform in a borosilicate glass autosampler vial insert (Microliter). Samples were vortexed until completely opaque, then centrifuged at 3,000 x g at 4ºC for 15 min. The chloroform layer was removed and 400 pmol of [$^{15}N_1$, $^{13}C_9$]-tyrosine, 10 fmol [$^{13}C_6$]-3-Cl-Y, and 10 fmol [$^{13}C_6$]-3-NO_2-Y, were added to the delipidated samples. Samples were dried in a vacuum concentrator.

For acid hydrolysis, 20 μl of 0.1% phenol (w/v) in 6 M HBr was added to each sample. Oxygen was purged from samples with three iterations of flushing with argon, freezing with liquid nitrogen, and thawing under vacuum. Samples were hydrolyzed at 100 ºC for 17 hours,

then dried in a vacuum concentrator. For modified tyrosine quantification, samples were resuspended in 30 μl 0.1% formic acid. For tyrosine analysis, resuspended samples were subsequently diluted 1:100 in 0.1% formic acid.

Hydrolyzed HDL was submitted to HPLC/MS/MS analysis on a Xevo-TS-Q mass spectrometer (Waters). The stationary phase was a 2.6 μm, 100 Å C18 column (Kinetex); mobile phase A was 0.1% formic acid and mobile phase B was 0.1% formic acid in methanol. The flow rate was 0.3 ml/min. The run time was 15 minutes for 3-Cl-Y and 3-NO_2-Y and 2.5 minutes for unmodified Y. The mass spectrometer operated in SRM mode, monitoring the following transitions: 216→170, 222→163, and 226→179 for Cl-Y; 227→18, 233→216, and 233→216 for NO_2-Y; and 181→136 and 192→145 for tyrosine.

PEG Precipitation of plasma

Plasma samples were PEG-precipitated in order to generate serum for cholesterol efflux assays. This process removes the majority of apoB containing lipoproteins(147). Plasma was rapidly thawed in a 37°C water bath. 100 μl was added to a 0.6 ml microcentrifuge tube. 1 μl 2.5 M $CaCl_2$ was added to each plasma sample and dispersed by inversion. Tubes were incubated at room temperature for one hour. Any formed clots were pushed to the bottom of the tube with a pipet tip. To each tube, 40 ul 20% PEG (8 kDa) in 200 mM glycine, pH 7.4, was added and immediately mixed with a pipet tip. Samples were incubated at room temperature for 20 minutes. Then, samples were spun for 30 min at 10,000 x g and 4 °C. 100 μl was transferred from the supernatant to a 1.7 ml microcentrifuge tube.

Cholesterol Efflux Assays

These assays provide a surrogate measure for HDL atheroprotective function by measuring the ability of apoB-depleted serum to remove cholesterol from cells. Cholesterol

efflux was measured using two different cell lines: J774 murine macrophages (ATCC) and BHK cells expressing ABCA1 under a mifepristone-inducible promoter(148) (kindly provided by Chongren Tang, University of Washington). The purpose of using two different cell lines was to differentiate ABCA1 mediated efflux from other efflux mechanisms. As a macrophage cell line, the J774 cells efflux cholesterol to HDL through a variety of mechanisms: ABCA-1, ABCG-1, SR-B1, and passive diffusion. Both cell types were cultured in DMEM high glucose medium + 10% FBS + 1% Penn-Strep. BHK cells were split 1:5 three times a week; J774 cells were split 1:2 three times a week. Cells were incubated at 37°C, 5% CO_2, 90% humidity.

J774 cells were plated in 48-well plates at 200,000 cells per well in 0.25 ml culture medium. BHK cells were plated at 150,000 cells per well in the same volume of culture medium. After 24 hours, medium was removed and replaced with fresh DMEM containing 10% fatty acid-free albumin (FAFA) + 0.5 μCi/ml [1,2-^{3}H(N)]-cholesterol (Sigma). J774 cell medium additionally contained 0.1% Sandoz 58-035 (Sigma), which prevents internal esterification of labeled cholesterol by inhibiting Acyl-CoA Cholesterol Acyltransfrase (ACAT). After another 24 hours, the medium was replaced with fresh DMEM + FAFA. J774 cells once again received Sandoz 58-035 and also 1% 8-(4-Chlorophenylthio)adenosine 3′,5′-cyclic monophosphate (Sigma). BHK cells received 1% mifepristone. Each of these treatments stimulated the expression of cholesterol transport proteins in their respective cell types. After 24 hours, medium was replaced once more, this time with 7.5 μl PEG-precipitated serum in 45 μl of medium. To control for baseline cholesterol efflux in the absence of stimulation, cells that had not been stimulated to express transport proteins were also treated with serum. To control for the amount of cholesterol loaded in the cells at the time of serum treatment, some cells were treated with plain medium that lacked serum. Medium was collected after 4 hours and passed through Acro-

Prep™ Advance 96 Filter Plates (Pall). Cholesterol that remained in the cells (non-effluxed) was extracted using hexane-isopropanol. Filtered medium and cell-lipid extracts were then transferred to scintillation vials containing 4 ml Ecolume liquid scintillation cocktail (MP Biomedicals). ^{3}H-cholesterol was measured using scintillation counting.

These assays were performed in duplicate and the total counts per minute (CPM) in the effluxed medium was given as the sum of these two values. Baseline corrected efflux values were determined by subtracting CPM values from non-stimulated cells from the CPM values in stimulated cells. Percent efflux was given as the baseline corrected efflux value divided by the non-serum-treated cell CPMs.

LCAT activation assay

LCAT activation is another function of apoA-I, and there is evidence that site-specific oxidation of M148 is associated with impairment of this function(80). This assay measures HDL LCAT activation through the conversion of radiolabeled cholesterol to cholesteryl ester as previously described(149). 2 μg UC-isolated HDL was equilibrated with 0.08 μCi [1,2-^{3}H(N)]-cholesterol (Sigma) in 12.5 mM Tris-HCl, 175 mM NaCl, 1.25 mM EDTA, pH 7.4 at 37°C. After one hour, 2-mercaptoethanol and BSA were added for final concentrations of 4 mM and 5 mg/ml, respectively. Samples were incubated for another hour at 37°C before adding 100 ng recombinant human LCAT (kindly provided by John Parks, Wake Forest University). After 2 hours at 37°C, the reaction was stopped with 800 μl absolute ethanol.

Cholesterol and cholesteryl esters were separated by thin layer chromatography. First, lipids were extracted into 12 x 75 mm borosilicate glass culture tubes (Fisher) with two applications of 1.7 ml hexane. To facilitate visualization of bands, 50 μg unlabeled cholesterol and 25 μg unlabeled cholesteryl oleate were spiked into each sample. The solvents were removed

under airstream. The sidewall of the tube was washed with 500 μl choloroform, then dried under airstream. Finally 110 μl chloroform was added and gently vortexed. Samples were loaded onto a TLC silica plate (Whatman) using a Thin-Layer Chromatography Multi-Spotter (Analytical Instrument Specialties). The plates were developed in a TLC tank containing Hexane:Ethyl Ether:Acetic Acid (108:30:1.2) for 30 minutes. Plates were dried for 10 minutes under airstream. Bands were visualized in a TLC tank containing iodine, then cut from the plate and placed in scintillation vials containing 4 ml Ecolume liquid scintillation cocktail (MP Biomedicals).

LCAT activation was expressed as percent cholesterol esterified, which was calculated by dividing the CPM for cholesteryl ester by the sum of the CPM for cholesterol and cholesteryl ester.

HDL/LDL particle analysis

Lipoprotein particle populations were analyzed to determine the relative abundance of the different size subspecies, described in detail by Hutchins, *et al*(150). Briefly, 57 μl of the plasma lipoprotein fraction (d < 1.21 g/ml) was dialyzed against 5 mM NH_4OAc, pH 7.2 in a constant flow dialysis apparatus. The dialysis occurred at a flow rate of 5 ml/min at 4°C for 4 hours. After dialysis samples were diluted 500x initial plasma concentration in 5 mM NH_4OAc, pH 9.2. 150 μl from this final dilution was transferred to an autosampler plate. Purified glucose oxidase was diluted to 10, 5, 2.5, and 1.25 μg/μl in 5 mM NH_4OAc, pH 9.2 to generate a standard curve.

The IMA device utilizes three steps that are akin to those of a mass spectrometer: ionization, separation, and detection. While a mass spectrometer separates on the basis of m/z, the IMA separates based upon particle size. Samples were injected into an HPLC system set to a flow rate of 100 nl/min. The HPLC was coupled to an electrospray apparatus, which ionized the lipoprotein particles. The particles then entered an ion mobility chamber with a current set to 400

nanoamps and voltage set to 2.3 kV. Particles were detected by laser light scattering and enumerated. Raw data was imported to Fityk curve-fitting software and curves were generated for the 3 distinct HDL particle populations: small HDLP, medium HDLP, and large HDLP; and LDLP (8.1, 8.9, 10.5, and 20.8 nm diameters, respectively)(151). Particle concentrations were determined by integrating each of the curves.

Protein Assay

BSA (Pierce) was serially diluted from 1 mg/ml to 15.6 µg/ml in 20 mM potassium phosphate/100 µM DTPA to be used as a standard. 5 µl of each sample or standard was added in duplicate to 96-well plates. Then 150 µl of Coomassie reagent (Pierce) was added to each well. Plates were mixed for 30 seconds, and then incubated at room temperature for 10 minutes. Absorbance was measured spectrophotometrically at 595 nm using a microplate reader (Molecular Devices).

SDS-PAGE

The constituent proteins of lipoprotein fractions were separated via SDS-PAGE. 5 µl NuPage LDS Sample Buffer (Novex) and 2 µl NuPage Sample Reducing Agent (Novex) were added to 3 µg (as measured by Bradford) of each sample and were brought to a final volume of 20 µl. Samples were reduced at 75°C for 10 minutes, then loaded into a 4-12% Bis-Tris Protein gel (Novex). Gels were run at 130V in MES buffer for 1 hour in an XCell SureLock Mini Cell Electrophoresis System (Life Technologies).

Immunoblotting

Immunoblotting was used to validate the proteomics results, and to determine which specific processing intermediates were present. Transfer buffer was made by adding 20% methanol to 1x Novex Transfer Buffer. The gels were soaked in transfer buffer for 20 minutes

prior to transfer. Polyvinylidene fluoride membrane was cut to the dimensions of the gel, wetted in methanol and soaked in transfer buffer. Filter paper sheets (BioRad) were soaked in transfer buffer prior to transfer. Proteins were transferred in an OWL-Hep1 Semidry Electroblotting System (Thermo) at 100 mA. Membranes were blocked for 2 hours in blocking buffer (1x PBS + 0.1% Tween + 5% milk powder). They were then incubated overnight with 3.3 μg Rabbit-Anti-SFTPB (Abcam) diluted into 10 ml blocking buffer. Membranes were washed for 1 hour in PBS/Tween. Membranes were incubated for 1 hour with HRP-conjugated Donkey anti-Rabbit diluted 1:10,000 (1 μl antibody in 10 ml blocking buffer). Membranes were once again washed for 1 hour in PBS/Tween. 1 ml ECL Western Blotting Substrate (Pierce) was then pipetted evenly over the membrane. Bands were visualized after 30 min using a BioRad imager in chemiluminescence mode.

CLEAR subjects

Plasma samples were kindly provided by Dr. Gail Jarvik at the University of Washington. Subjects were selected from participants in the Carotid Lesion Epidemiology and Risk (CLEAR) study, an ongoing case-control study aimed to identify predictors of coronary artery disease and atherosclerotic plaque instability(152; 153). Inclusion criteria were HDL-C< 90 mg/dl, TG < 225 mg/dl, LDL-C < 200 mg/dl, and age 50-90. No subject was diabetic or had abnormal coagulation. Subjects were defined as cases if they had >15% angiographically confirmed carotid stenosis and controls if they had <15% carotid stenosis. The discovery analysis compared 30 smokers and 30 nonsmokers in the control (non-stenotic) group; one of the validation analyses compared 67 smokers and 58 nonsmokers in the case (stenotic) group.

The unit of measure for lifetime cigarette exposure is the “pack year,” which is equivalent to the cigarette exposure from 20 cigarettes (one pack) per day for a year. To avoid

potential confounding by residual effects of smoking in former smokers(154), subjects were only classified as nonsmokers if they had never smoked and only classified as smokers if they currently smoked at time of sample collection. One weakness in using this classification for these subjects was that there was a large variance in lifetime cigarette exposure among smokers, ranging from 0.75 to 110 pack years; lifetime exposure was therefore included in the analysis as a covariate.

Although the exclusion and inclusion criteria yielded no significant differences in initial characteristics between smokers and nonsmokers in the absence of CCVD, there were marked differences in several of the variables in the presence of CCVD. Between smokers and nonsmokers with CCVD, smokers were significantly younger, had lower apoA-I and HDL-C, higher LDL-C, and lower BMI. It is also possible that the smaller sample sizes in the CCVD absent set precluded the ability to detect differences between groups; LDL in particular had a trend to be lower in this group. **Table 2.1** outlines the subject characteristics for the two studies:

	CCVD Absent			**CCVD Present**		
	Nonsmoker	**Smoker**	***P***	**Nonsmoker**	**Smoker**	***P***
n	30	30		58	67	
n female	18 (30%)	18 (30%)		14 (24%)	9 (13%)	
n Statin User	0 (0%)	0 (0%)		45 (78%)	45 (67%)	
Age (years)	67 (4.5)	66 (4.2)	0.23	76 (8.0)	67 (7.9)	<0.001
ApoA-1 (mg/dl)	150 (28)	150 (25)	0.52	150 (21)	140 (29)	<0.01
HDL-C (mg/dl)	56 (14)	53 (15)	0.37	53 (11)	48 (14)	0.05
VLDL (mg/dl)	20 (8.4)	23 (8.7)	0.24	22 (8.6)	24 (8.9)	0.29
LDL-C (mg/dl)	130 (28)	120 (35)	0.30	89 (30)	99 (25)	0.05
Triglycerides (mg/dl)	100 (42)	110 (44)	0.22	110 (43)	120 (44)	0.28
HBA1C (%)	5.6 (0.34)	5.6 (0.42)	0.56	5.7 (0.38)	5.7 (0.46)	0.83
BMI (kg/m^2)	26 (3.9)	26 (5.0)	0.91	28 (4.0)	26 (4.5)	0.03
Yr smoking	-	38 (16)	-	-	47 (11)	-
Pack years	-	34 (28)	-	-	46 (28)	-

Table 2.1: CLEAR subject characteristics, represented as mean (sd) unless otherwise noted.

Each sample was assigned a position on a randomly generated list and experiments were carried out according to this order. Every individual handling the samples was blinded to the corresponding subject characteristics. Investigators became un-blinded in order to analyze data only once the experiments were complete.

Smoking cessation subjects

These plasma samples were kindly provided by Dr. Richard Bruno from The Ohio State University. These subjects were relatively healthy excepting their smoking status. Subjects were normotensive males and females, with an age range of 18-40 years. They had fasting glucose levels of <100 mg/dl and fasting total cholesterol levels of <200 mg/dl. They had a BMI range of 18.5-30. They had not used dietary supplements for at least 2 months prior to the study. EDTA-plasma was collected from each subject at the beginning of the study and after one week of abstention from smoking. During the abstention period, half of the subjects took a supplement once daily containing 500 mg γ-tocopherol, 62 mg α-tocopherol, 24 mg β-tocopherol, and 6 mg δ-tocopherol and half received a placebo containing 0.07 mg α-tocopherol and 0.18 mg γ-tocopherol. Additionally, half of the subjects quit smoking with no assistance while half received a Nicoderm CQ patch that delivered 20 mg nicotine/day(155). Urinary naphthol, a metabolite of naphthalene, which is a polycyclic aromatic hydrocarbon (PAH) in cigarette smoke(156), was measured in order to assess compliance to cessation. 4 of 60 subjects were dropped from the study due to lack of compliance.

Statistical Analysis

Differences between smokers and nonsmokers were assessed using a two-tailed unpaired t-test. If normality assumptions were violated, Mann-Whitney tests were used. Differences pre- and post- smoking cessation were assessed using a two-tailed paired t-test. P values of less than

0.05 were considered significant. Graphics were generated using the ggplot2 R package(157). Proteomics data was corrected for multiple comparisons using Bonferroni's method. Correlation coefficients were calculated according to Pearson. Data are given as boxplots with the thick line representing the median, the box representing the IQR, and the vertical line as 1.5 x IQR. Power calculations based on preliminary data indicated that n = 30 per group would have 80% power to detect 10% changes in sterol efflux capacity at $\alpha = 0.05$. Sterol efflux assays were performed in duplicate; all other experiments were performed once per subject.

Chapter 3

A Discovery Analysis of the Impact of Cigarette Smoking on HDL

Overview

The goals of this study were to test the hypothesis that cigarette smoking causes oxidation of HDL proteins and alters its protein cargo, leading to loss of function; and to generate hypotheses regarding the impact of smoking HDL protein cargo and particle size. In order to minimize confounding by other cardiovascular risk factors, these subjects lacked CCVD and were nondiabetic. Groups were matched for sex, age, body mass index (BMI), and lipid levels. Matching the groups thusly raised the possibility of observing differences between groups that were truly attributable to smoking. However, given the lack of vascular disease after years of smoking, one caveat is that the smokers in this analysis do not represent the majority of long-term smokers.

HDL Oxidation

3-chlorotyrosine was used to detect MPO-mediated damage since it is a specific product of MPO—its presence implies MPO activity. While chlorotyrosine is an MPO-specific product, MPO also generates nitrotyrosine, which is generated through other pathways as well, so should be viewed as a general marker for oxidative stress. Site-specific chlorination and nitration of all seven tyrosine residues in apoA-I were measured by LC-ESI-MS/MS analysis.

Because cigarette smoke activates neutrophils and MPO is a major product of activated neutrophils, we hypothesized that smoker HDL would incur more MPO-mediated modifications than nonsmoker HDL. Furthermore, the recent observation of a positive correlation between smoking and chlorination at Y-192 underlined this key initial hypothesis(74). Due to previous data indicating that Y192 is the most chlorination-prone tyrosine residue in apoA-I(75), we

anticipated that it would exhibit the most marked uptick in chlorination. Additionally, we measured total HDL chlorotyrosine in this population. While this method is unable to yield information about the location of modification, it is advantageous because it provides an overview of tyrosine chlorination in all HDL proteins.

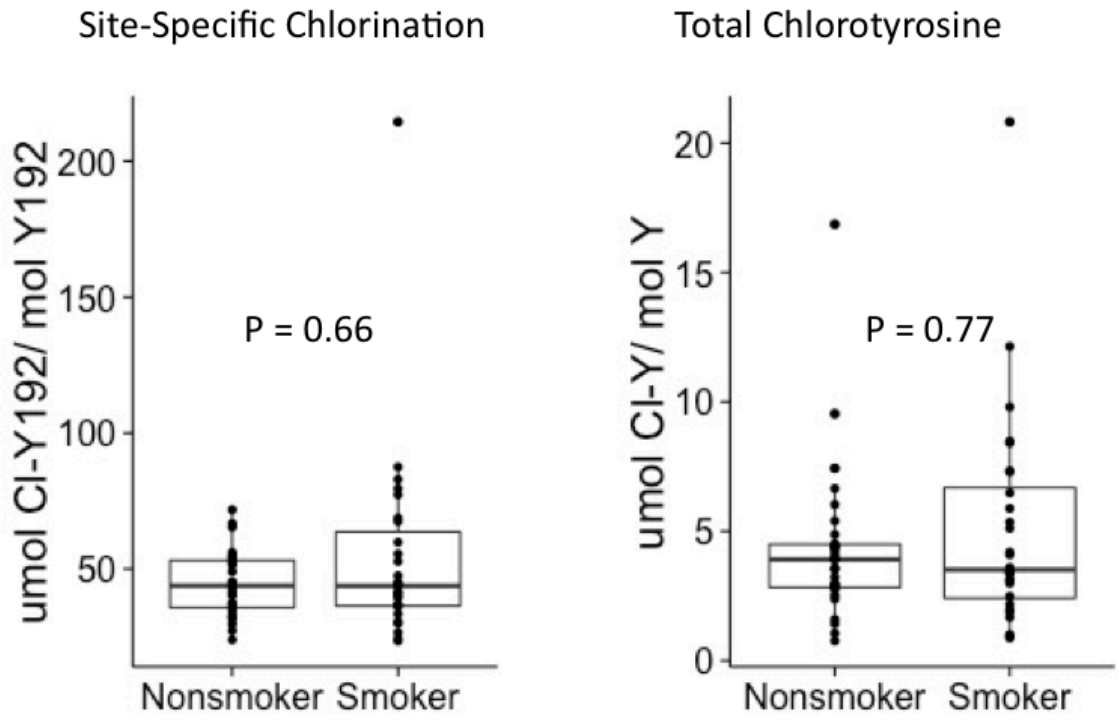

Figure 3.1: Chlorination of Y192 of apoA-1 (left) and total HDL chlorotyrosine (right). (n = 30 per group).

We did not observe a significant difference between chlorination of Y192 of apoA-1 in smokers and nonsmokers in this population (**Figure 3.1**, left). In both groups, the median was 44 μmol/mol, although the mean for smokers was higher (44.8 μmol/mol in nonsmokers vs 54.3 μmol/mol in smokers), skewing the distribution for smokers toward the higher values. No significant difference was observed between total chlorotyrosine in smokers and nonsmokers in this population (**Figure 3.1**, right). Nonsmokers had mean HDL chlorotyrosine levels of 4.3

μmol/mol (median 3.9 μmol/mol); smokers had mean levels of 5.1 μmol/mol (median 3.5 μmol/mol). Once again, the distribution for smokers was more skewed toward higher values.

Taken together, these results indicate that Y192 is over 10 times as prone to chlorination as other tyrosine residues found in HDL. One smoker was a clear outlier in both analyses with Y192 chlorination exceeding 200 μmol/mol and total chlorotyrosine exceeding 20 μmol/mol. This individual was also severely underweight, which suggests that they may have been suffering from a disease.

Site-specific chlorination was observed in 5 out of the 7 tyrosine residues in apoA-I. Of all the tyrosine residues of apoA-I, Y192 was the most susceptible to chlorination and nitration. There were no significant differences between smokers and nonsmokers regarding chlorination or nitration of any of the measured tyrosine residues of apoA-I (**Table 3.1**).

Modification	Residue	Y18	Y29	Y100	Y115	Y166	Y192	Y236
Chloro (μmol/mol)	**Nonsmoker**	20.2	2.8	NA	NA	0.38	44.8	2.6
	Smoker	22.0	1.8	NA	NA	0.53	54.3	2.0
	P	*0.52*	*0.08*	*NA*	*NA*	*0.10*	*0.21*	*0.19*
Nitro (μmol/mol)	**Nonsmoker**	NA	7.5	1.9	10.1	7.45	28.0	5.6
	Smoker	NA	8.2	1.7	6.2	6.08	21.4	6.9
	P	*NA*	*0.74*	*0.28*	*0.65*	*0.33*	*0.40*	*0.40*

Table 3.1: Mean levels of site-specific chlorination and nitration of apoA-I tyrosine residues in smokers and nonsmokers. (n = 30 per group)

Although methionine sulfoxide is not a specific MPO product, oxidation of two of the three methionine residues of apoA-I was also measured as a non-specific marker of oxidative stress. Methionine reacts with HOCl more readily than does tyrosine, meaning that proportionally more methionine than tyrosine residues would be damaged by MPO, and hence would be more likely to have functional ramifications. Methionine residues may also oxidize through improper sample handling; although some of this artifactual oxidation was controlled for

during digestion by addition of excess free methionine, some oxidation may have occurred prior to receipt.

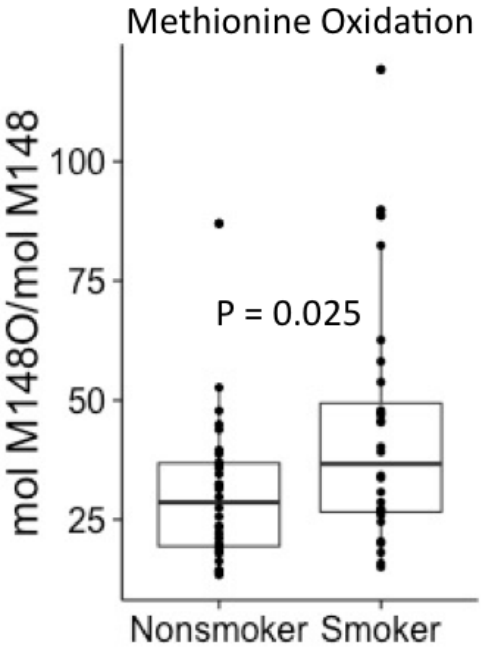

Figure 3.2: Site-specific oxidation of M148 (n = 30 per group).

We observed smokers to have significantly more oxidation at M148 than nonsmokers (**Figure 3.2**; nonsmoker mean = 31 mmol/mol; smoker mean = 43 mmol/mol; P = 0.025). However, site specific oxidation of M112 did not significantly differ between smokers and nonsmokers (nonsmoker mean = 57 mmol/mol; smoker mean = 60 mmol/mol; P = 0.9). Methionine 148 has been observed to be less susceptible to oxidation than the other methionine residues of apoA-I(80). This experiment agreed with this observation; M148 had less oxidation than M112 in smokers and nonsmokers. It is possible that M112 is more prone to artifactual oxidation *ex vivo,* which could mask any potential differences in oxidation that could exist *in vivo*. Previous observations demonstrated that *in vitro* oxidation of M148 using the MPO + Cl system is partially responsible for impairment of apoA-I LCAT activation ability; we hypothesized that in this study, HDL from smokers would activate LCAT less than HDL from

nonsmokers. Because methionine oxidation is not necessarily a result of MPO, these observations provide no definitive indication that the elevation of M148 oxidation in smokers is a result of increased MPO activity.

Since methionine residues are susceptible to artifactual oxidation in storage, we next determined whether there was an association between M148 oxidation and time that sample had been stored. We did not observe a strong association between oxidation at this site and time that the sample had been frozen (**Figure 3.3**; Pearson's R = 0.13). The lack of association suggests that the majority of M148 oxidation occurred prior to sample storage.

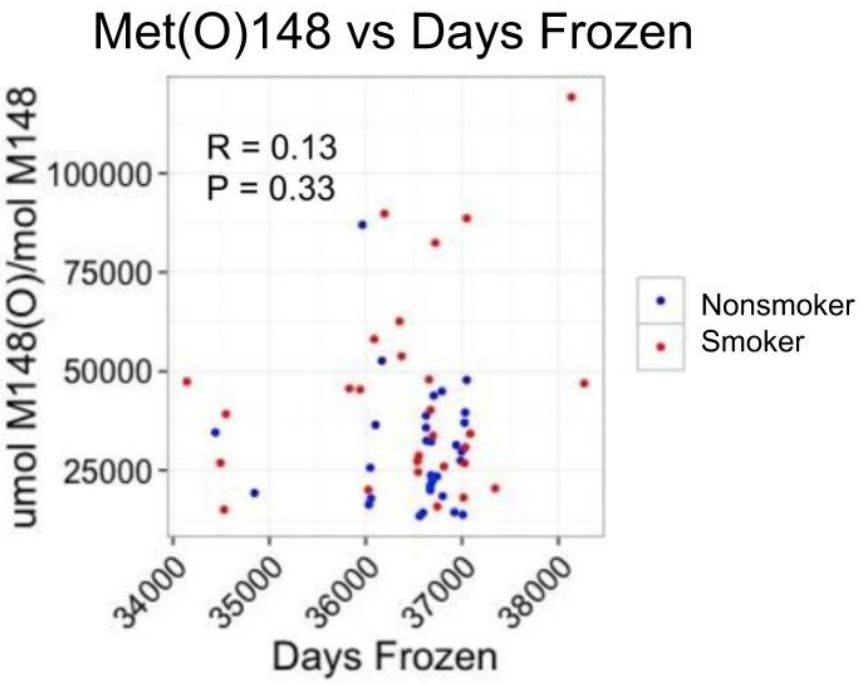

Figure 3.3: Methionine oxidation is not associated with time frozen.

HDL Function

Because oxidation of M148 causes HDL to lose its ability to activate LCAT, we next tested whether the HDL from smokers in this study had reduced ablity to activate LCAT. We did not observe any significant difference in LCAT activation between these two groups (**Figure**

3.4). Both groups had a median of 3.6% cholesterol esterification after 2 hours; although insignificant, the mean was higher in smokers. The percent esterification in the smokers showed a distribution that was more skewed to higher values than nonsmokers, indicating if anything a trend toward increased cholesterol esterification in smokers. Thus, it appears unlikely that oxidation of M148 has any funcitonal bearing on LCAT activation ability. Additionally, we did not observe any correlation between M148 oxidation and LCAT activation in these samples (**Figure 3.4**, right), contrasting our expectation.

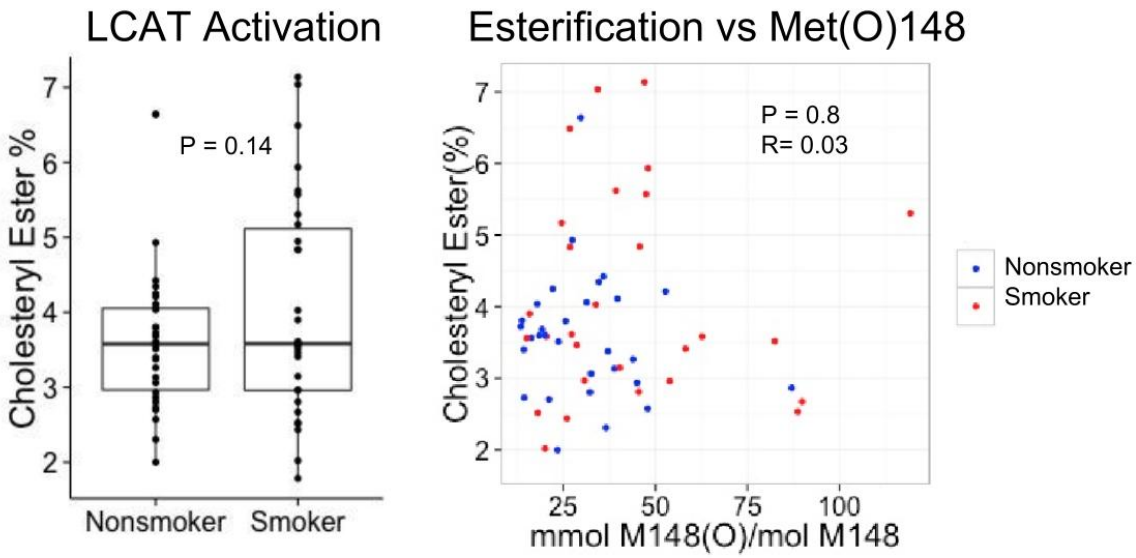

Figure 3.4: LCAT activation (left) and % cholesteryl ester vs site-specific oxidation of M148 (right). (n = 30 per group)

This assay gives LCAT activation by measuring the amount of cholesteryl ester generated by UC-isolated HDL in the presence of recombinant human LCAT and radiolabeled cholesteryl ester. One caveat is that this method does not account for the activity of the endogenous LCAT bound to the isolated HDL. In addition, this method had not been previously used to measure *in vivo* differences in LCAT activation. It is unclear how sensitive this assay is, but possible that while it detects large functional changes brought on by *in vitro* oxidation, it is unable to resolve small differences in LCAT activation ability that arise biologically. Additionally, this assay only

determines the LCAT activation in HDL, but gives no information regarding overall LCAT activity *in vivo*; it is possible that compensatory mechanisms exist to enable individuals with less HDL LCAT activation to sustain normal cholesteryl ester levels.

LCAT activity itself is not an optimal surrogate measure for cardiovascular health or normal lipid homeostasis. Although in some study populations LCAT-deficient individuals are at increased risk for premature atherosclerosis(158; 159), other studies have not observed any atheroprotective benefit of functional LCAT(160). Furthermore, LCAT deficiency was atheroprotective in mice fed an atherogenic diet (161).

We also assayed HDL cholesterol efflux capacity, another aspect of HDL function. For these experiments we used PEG-precipitated serum rather than UC-isolated HDL, as per the method developed by the Rader group(68). We performed the assays in each of two different cell types: J774 murine macrophages and ABCA1-inducible BHK cells. J774 efflux cholesterol through all proposed pathways: the ABCA1, ABCG1, and SR-B1 transporters, as well as passive diffusion. BHK cells do not have innate cholesterol efflux mechanisms, but as this cell line expresses ABCA1 under a mifepristone-inducible promoter, these cells efflux through the ABCA1 transporter in the presence of mifepristone.

We did not observe any difference in cholesterol efflux capacity between smokers and nonsmokers; both groups had a mean percent total efflux of 6.2 (**Figure 3.5**, left). Additionally, there was no significant difference in ABCA1 efflux capacity between smokers and nonsmokers (**Figure 3.5**, right). There was a trend toward smokers having increased ABCA1 mediated efflux; the mean percent efflux was 8.6 in nonsmokers and 9.3 in smokers.

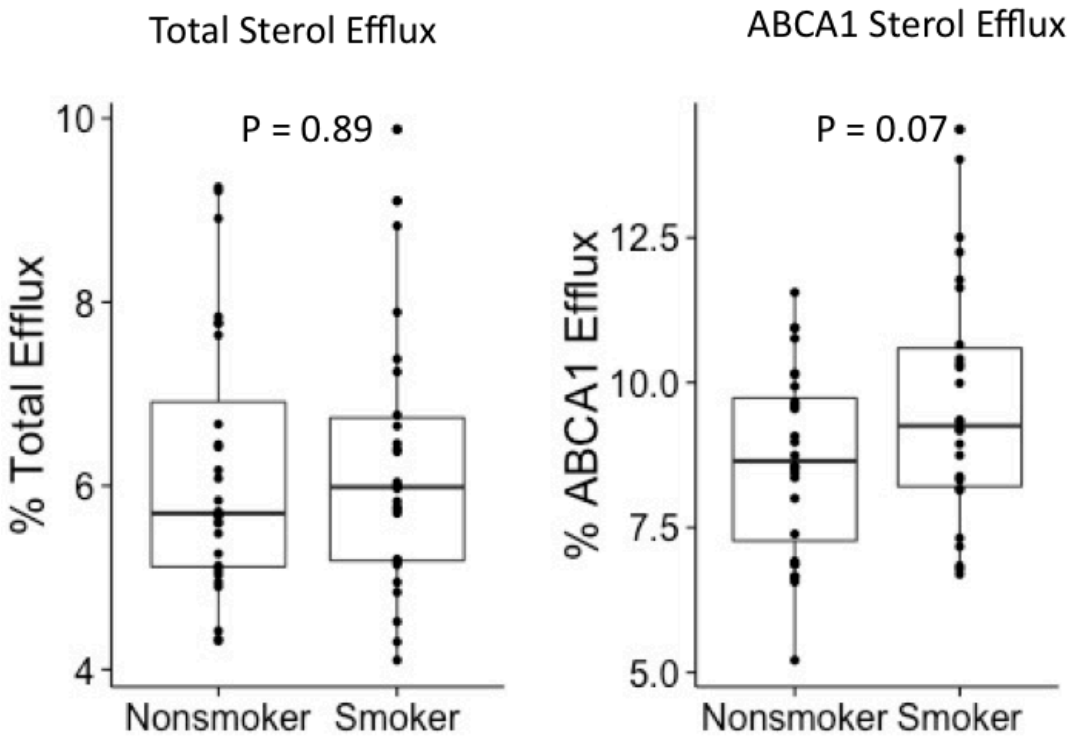

Figure 3.5 Total Sterol Efflux (left) and ABCA1-specific efflux (right). (n = 30 per group)

These results provide no indication that smoking impairs HDL lipid metabolism through its ability to activate LCAT or to efflux cholesterol from cells. However, since the lipid characterisitcs (e.g. HDL-C, LDL-C, triglycerides) did not significantly differ between smokers and nonsmokers, it is possible that these subjects did not have altered lipid metabolism and thus had normal HDL funciton. Therefore it is possible that we would have observed significant differences in HDL function in a set of subjects whose lipid profiles differed between smokers and nonsmokers in a more expected fashion.

HDL Particle Concentration

Because smoking alters lipid metabolism, we determined whether smokers and nonsmokers differed regarding concentration of three different sized HDL particle subpopulations. This technique provides a snapshot of the relative amounts of different sized HDLs present in an individual at a given time, which gives an approximation of the patricle

maturation state. We observed smokers to have significantly more small HDL paticles (diameter = 8.1 nm) than nonsmokers **(Figure 3.6)**. There was no significant difference between smokers and nonsmokers in medium (diameter = 8.9 nm) or large (diameter = 10.5 nm) particle concentrations. There was also no significant difference in total particle concentration.

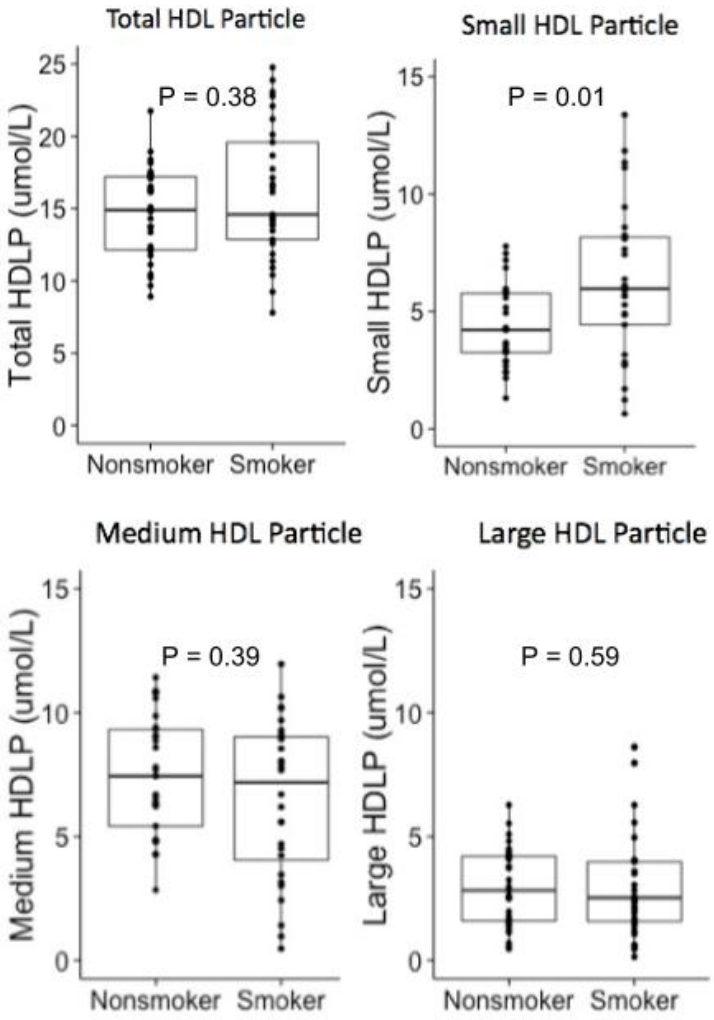

Figure 3.6: Total HDLP (top left), small HDLP (top right), medium HDLP (bottom left), and large HDLP (bottom right). (n = 30 per group) In order to overcome the violated normality assumption of equal variances between groups, P values are reported for Mann Whitney's U.

The HDL particle subpopulation concentrations are a distinct measurement from HDL-cholesterol. The majority of HDL cholesterol is found in the large HDL particles; it is consistent

with the fact that HDL-C and large HDL particle concentration are indistinguishable in these subjects. The observed elevation in small HDL particle concentration in smokers indicates that smoking may somehow stunt HDL particle maturation by rendering some HDL particles unable to grow larger. It is also possible that the increased small particle concentration is the result of an increase in secretion of nascent HDL particles, although this would fail to explain why smokers characteristically have lower HDL-C than nonsmokers.

HDL Proteomics

We also sought to determine the effect of smoking on HDL's protein cargo. This workflow involved an initial shotgun proteomic analysis, which served to identify which proteins comprised the HDL proteome of these samples, and provided a semi-quantitative view of relative protein abundances **(Figure 3.7)**. After such proteins were identified, we then performed a targeted SRM analysis of these proteins to determine any quantitative differences between the groups.

The shotgun proteomics analysis identified several well-established HDL proteins, as well as some less commonly observed on HDL. These less commonly observed proteins such as SFTPB (pulmonary surfactant protein B) and LPLUNC1 (Long PLUNC1) were added to the list of protein targets for the subsequent SRM analysis. We also used the shotgun proteomics data to semi-quantitatively analyze whether any proteins were relatively more or less abundant in smokers. To do this, we calculated the previously described spectral index for each protein(140). Essentially, this figure uses a protein's number of spectral counts in each subject to determine the degree to which the protein level under a certain condition deviates from control levels. It accounts for the total number of spectral counts present, as well as the number of samples in which the protein is present. It assigns each protein a value between -1 and 1, with negative

values indicating greater prevalence in the controls, positive values indicating greater prevalence in the cases, and zero indicating no difference between cases and controls. Translated to a statistical perspective, a P value < 0.01 corresponds with a SPI with an absolute value of ≥ 0.75.

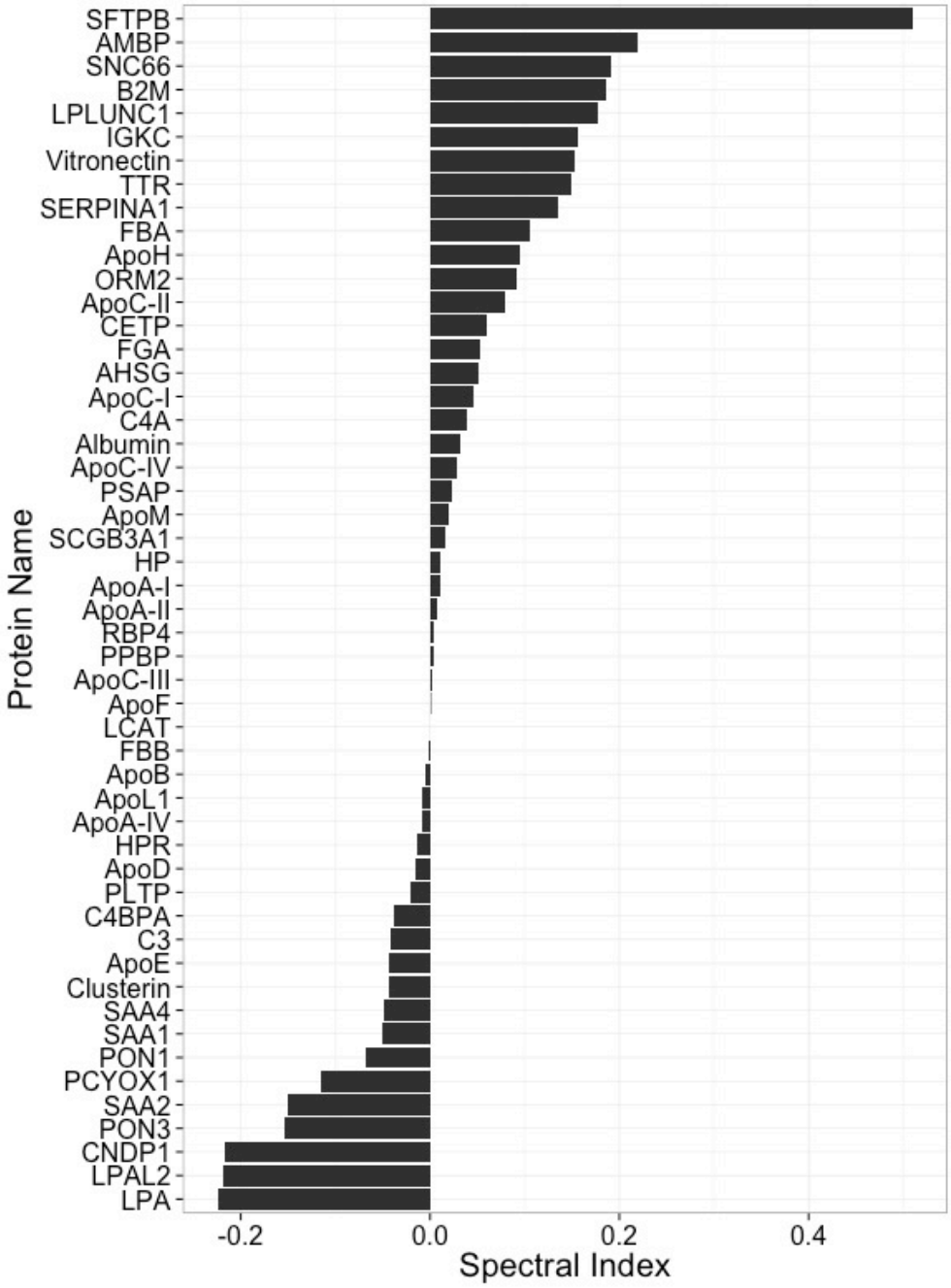

Figure 3.7: Spectral Indices of HDL-associated proteins in smokers and nonsmokers

Although no protein's SPI had an absolute value exceeding 0.75, SFTPB came the closest, with a SPI of 0.51. SFTPB spectra were observed in 26 out of 30 smokers and only 14/30 nonsmokers. Thus, we strongly suspected that smokers would have higher levels of HDL-associated SFTPB than nonsmokers. We chose the two peptides that appeared the most consistently in the shotgun analysis to target in the SRM analysis.

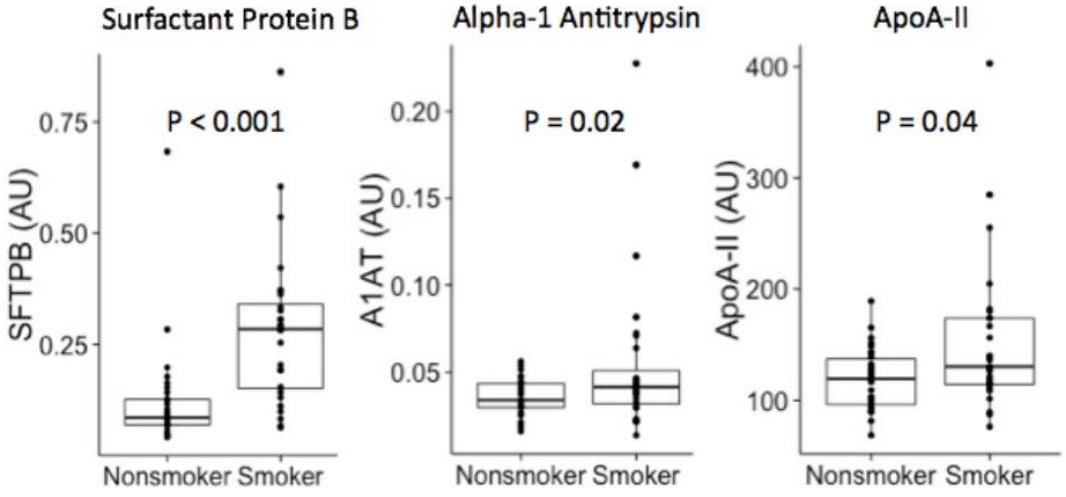

Figure 3.8: Targeted proteomics of Surfactant Protein B (left), Alpha-1 Antitrypsin (middle), and ApoA-II (right). (n = 30 per group; AU = arbitrary units)

SRM analysis confirmed that SFTPB is enriched in smokers (**Figure 3.8**, left). The median SFTPB level in smoker HDL was three times that in nonsmoker HDL; the mean was 2.4 times higher in smokers than in nonsmokers. Furthermore, the 25th percentile level in smokers exceeded the 75th percentile in nonsmokers; over 75% of smokers had higher SFTPB levels than 75% of nonsmokers. The median level in smokers was 3 times that of nonsmokers. The mean level in smokers was 2.4 times higher than the mean level in nonsmokers. ($P < 0.05$ after Bonferroni's correction) This result is not surprising, given that SFTPB is a lipophilic protein and previous studies observed circulating SFTPB to be enriched in smokers and individuals with atherosclerosis(128).

Additionally, we observed smokers to have higher levels of HDL-associated A1AT (encoded by the SERPINA1 gene) than nonsmokers, although this difference was less marked than that of SFTPB (**Figure 3.8**, middle). A1AT is an acute phase protein that is released in response to activated neutrophils; its elevated presence in smokers suggests a regulatory response to increased neutrophil activation or perhaps smoking-induced systemic inflammation. The median level in smokers was 1.2 times that in nonsmokers. The mean level in smokers was 1.5 times that in nonsmokers. This trend appears to be primarily driven by the highest quartile in the smoker group; the bottom three quartiles of smokers have A1AT levels in a range that is similar to that of all quartiles of nonsmokers. This raises interest in determining if the top quartile of smokers differs from the other subjects in any additional ways. This result was not significant after using Bonferroni's method for multiple comparisons correction. However, because the experiment was conducted with the intent to generate hypotheses, this result spurred interest in A1AT in confirmatory analyses.

Although SFTPB had a relatively high spectral index of 0.51, the spectral index of A1AT (SERPINA1) was only 0.14, which was less than or equal to many proteins that showed no significant different in quantitative SRM analysis. Additionally, the spectral index of apoA-II was 0.007, which was indicative of no change, but by SRM apoA-II was significantly higher in smokers than in nonsmokers (**Figure 3.8**, right). It is possible that spectral counting did not identify the change in apoA-II because it barely reaches significance at the 0.05 level (and is not significant following multiple comparison correction). It is also possible that the spectral counting technique is more reliable with lower-abundance proteins; ionization patterns and instrument scan settings could conflate information about protein abundance obtained via spectral counting.

By nature, a hypothesis generating set of experiments tests a large number of hypotheses. This introduces the problem of multiple comparisons: when simultaneously making several statistical inferences, random chance may result in one or more false-positive results. For example, accepting significance at $P = 0.05$ is equivalent to accepting a 5% chance of a false positive result. This means that if 20 inferences are simultaneously made, one false positive result is expected to arise. Therefore, the P-values must be adjusted when making multiple comparisons. Bonferroni's method, which multiplies the P-value by the number of comparisons made, is the most conservative adjustment for multiple comparisons. In a hypothesis generating experiment, it is likely that even true positive results may be masked after adjustment for multiple comparisons. In the above proteomics experiments, the elevation in SFTPB was the only result that remained significant after multiple comparisons adjustment.

Because there are few reports of HDL-associated SFTPB, our next step was to validate this result by immunoblot. We also were interested whether HDL was the primary carrier for circulating SFTPB. We ultracentrifugally separated plasma from two subjects: a nonsmoker with low HDL-associated SFTPB levels and a smoker with high HDL-associated SFTPB levels. We set aside the bottom fraction after the first spin ($d > 1.21$g/ml, non-lipoprotein associated plasma proteins) and the HDL and LDL fractions after the second spin, and determined protein concentration via the Bradford protein assay.

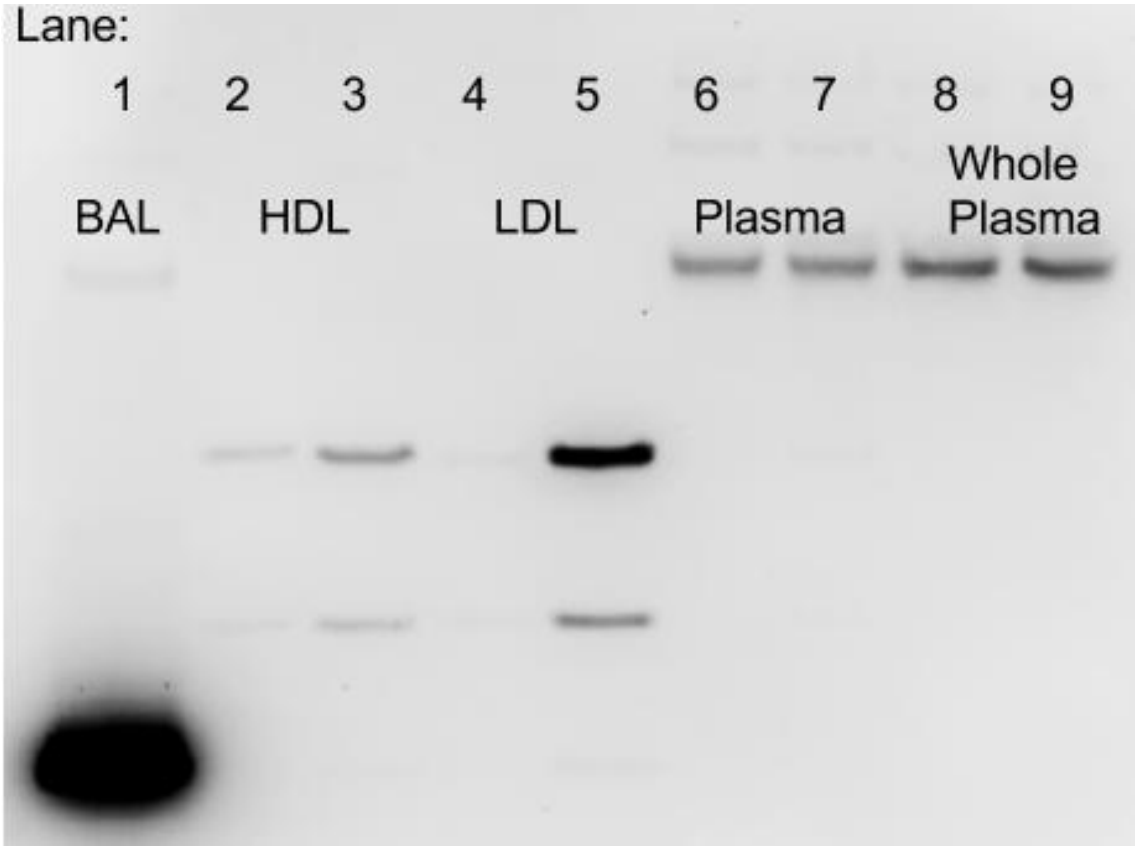

Figure 3.9: SFTPB immunoblot. Lane 1 BAL fluid; lane 2 nonsmoker HDL; lane 3 smoker HDL; lane 4 nonsmoker LDL; lane 5 smoker LDL; lane 6 nonsmoker non-lipoprotein plasma; lane 7 smoker non-lipoprotein plasma; lane 8 nonsmoker whole plasma; lane 9 smoker whole plasma.

We separated 3 μg protein per fraction via SDS-PAGE, and immunoblotted for SFTPB (**Figure 3.9**). BAL from a healthy human was run as a positive control for SFTPB. We observed several different SFTPB processing intermediates: fully mature SFTPB (42 kDa), two processing intermediates (approximately 25 and 16 kDa), and mature SFTPB (8 kDa). These processing intermediates existed at different relative amounts in the various fractions. We only observed fully mature SFTPB in the BAL fluid, suggesting that fully processed SFTPB is absent from the circulation. In both lipoprotein fractions, we observed the intermediate bands. It appeared that the LDL fraction was particularly enriched for SFTPB. In the non-lipoprotein and whole plasma

fractions, we observed the mature SFTPB and some higher molecular weight bands possibly corresponding with dimmers. That we only observed the mature form in whole plasma indicates that the majority of circulating SFTPB exists in a non-lipoprotein associated, unprocessed form. The amount injected per well was based total micrograms protein; the plasma fraction has the highest protein concentration and the LDL fraction has the lowest protein concentration. Per particle, LDL contains less protein than HDL, suggesting that LDL particles are enriched in SFTPB compared to HDL. Because lung surfactant itself is a lipoprotein, it is unclear whether any circulating SFTPB is bound to HDL and LDL particles or whether it is associated with other components of lung surfactant and floats at the same densities as lipoproteins.

The presence of lipoprotein-associated SFTPB raises the question of how the surfactant protein entered the circulation. One possibility is that the pulmonary vasculature becomes more permeable under conditions that stress the lung, such as smoking. Because surfactant proteins are lipophilic, it would not be surprising for them to associate with lipoproteins in the circulation. Type-II alveolar cells have also been proposed to take up HDL particles; perhaps these HDL particles form associations with SFTPB in the alveolar cell, and are subsequently released into the circulation. Because exchange of lipid cargo occurs between HDL and LDL particles, it is possible that SFTPB could be transferred from one lipoprotein subclass to another.

We wondered whether the altered protein cargo of smoker HDL could impact HDL particle maturation, leading to the observed elevation in small HDL particle concentration. We performed simple linear regression with SFTPB, A1AT, or apoA-II as predictors and small HDL particle concentration as the outcome (**Figure 3.10**). We did not observe a significant relationship between HDL SFTPB levels and small HDL particle concentration. While small HDL particle concentration significantly associated with A1AT and apoA-II, each protein

accounted for less than 10% of the variation in small particle concentration. ApoA-II is known to affect HDL particle maturation by inhibiting association phospholipid transfer protein (PLTP), preventing HDL particle growth(162; 163).

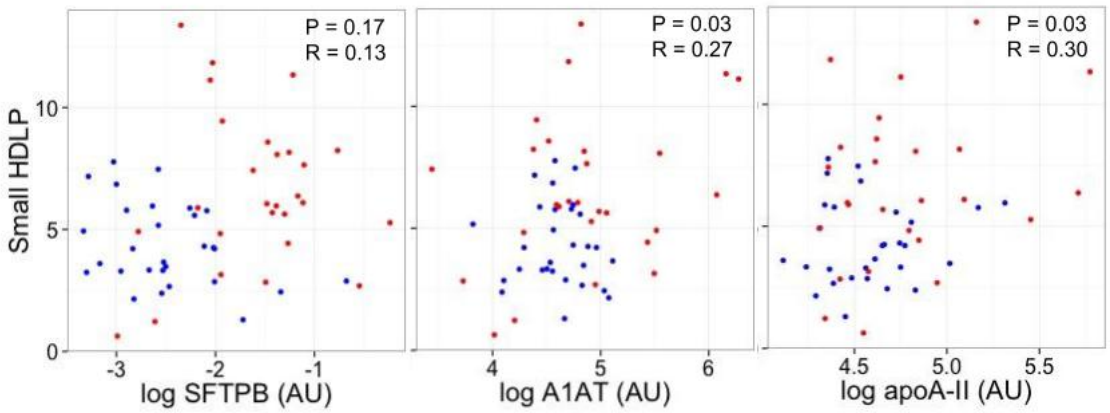

Figure 3.10: Small HDL Particle concentration (μmol/L) vs SFTPB (left), A1AT (middle), and apoA-II (right). (AU = arbitrary units; R = Pearson's R; red points = smoker; blue points = nonsmoker)

Conclusions

This analysis did not provide strong evidence in support of our hypothesis that smoking is associated with elevated HDL protein oxidation and compromised HDL function. Site-specific and total apoA-I chlorotyrosine levels did not significantly differ between smokers and nonsmokers, but smokers had significantly higher Met(O)148 levels than nonsmokers, suggesting that smokers had elevated oxidative stress that was not specific to MPO. Smoking was not associated with impairment of HDL's efflux capacity or LCAT activation ability, although there was evidence for a trend of elevated ABCA-1 specific efflux in smokers. These results do not provide evidence that healthy smokers have less functional HDL than nonsmokers.

This analysis also enabled us to generate hypotheses regarding the effect of smoking on HDL protein cargo and particle subpopulations. We observed elevated small HDL particles, but no change in medium, large, or total HDL particle populations. We also observed elevation of

three proteins in smoker HDL: apoA-II, A1AT, and SFTPB. Although we observed apoA-II and A1AT to weakly associate with small HDL particle concentration, we did not observe SFTPB to associate with HDL function or particle subpopulations.

Chapter 4

Validation Analyses of the Impact of Cigarette Smoking on HDL

Overview

The objective of these experiments was to confirm the hypotheses generated in the previous chapter. We used two different sample sets that were markedly different from one another in order to broadly test the hypotheses. Based on the results from the initial analysis, we determined that our subsequent two analyses would not be adequately powered to detect significant inter-group differences in tyrosine modification or apoA-I LCAT activation ability. Addressing fewer hypotheses also had the advantage of minimizing the multiple comparisons made. Therefore, our measure of HDL function was serum cholesterol efflux in J774 cells (total efflux) and BHK cells (ABCA1-specific efflux). We also measured concentrations of all 3 HDL subpopulation concentrations, as well as that of LDL. The only site-specific oxidation product we measured was Met(O)148 of apoA-I. We measured the levels of apoA-II, A1AT, and SFTPB, all of which were significantly different or trending in the exploratory study.

One group of subjects was from a smoking cessation study in which young healthy smokers with relatively low pack year histories refrained from smoking for one week. We used two samples from every subject that completed the study: plasma collected immediately prior to cessation and plasma collected after one week of cessation. Due to the paired nature, our null hypothesis for each measured variable was that the difference between pre- and post- cessation HDL would be equal to zero.

The other group of subjects was like the initial group of subjects from the exploratory analysis in that it too was a made up of smokers and nonsmokers from the CLEAR cohort.

Unlike the first subjects, however, these subjects had CCVD, as indicated by >15% angiographically measured carotid stenosis. The motivation for using these samples was to attempt to determine whether smoking had the same effect on HDL in subjects with vascular disease as it did on subjects without vascular disease. Because these samples were unpaired, our null hypothesis was that there was no significant difference between the smoker and nonsmoker groups.

Cholesterol Efflux

In the previous analysis, overall cholesterol efflux did not significantly differ between smokers and nonsmokers. However, ABCA1-specific efflux showed a trend of being increased in smokers. In this analysis, smokers with CCVD had significantly higher ABCA1-specific efflux than nonsmokers with CCVD; the mean efflux was 20% in nonsmokers and 21% in smokers. However, there was no significant difference in overall cholesterol efflux (mean for both groups 15%) (**Figure 4.1**). The implication of this observed elevation in ABCA1 efflux in smokers is paradoxical; since smoking is atherogenic, it is unexpected for it to cause an increase in ABCA1-specific efflux. Although this implies that smoking does not impair cholesterol efflux in terms of HDL function, it does not mean that the other components of the pathway (such as the ABCA1 transporter) are fully functional. Thus, it cannot be inferred that the in vivo process of ABCA1-specific cholesterol efflux is elevated in smokers. Since the smokers had significantly lower HDL-C than the nonsmokers, we wondered whether smoker HDL might more readily participate in ABCA1-specific cholesterol efflux due to presumably having less cholesterol initially bound. However, simple linear regression did not suggest any relationship between HDL-C and ABCA1 efflux (**Figure 4.2**).

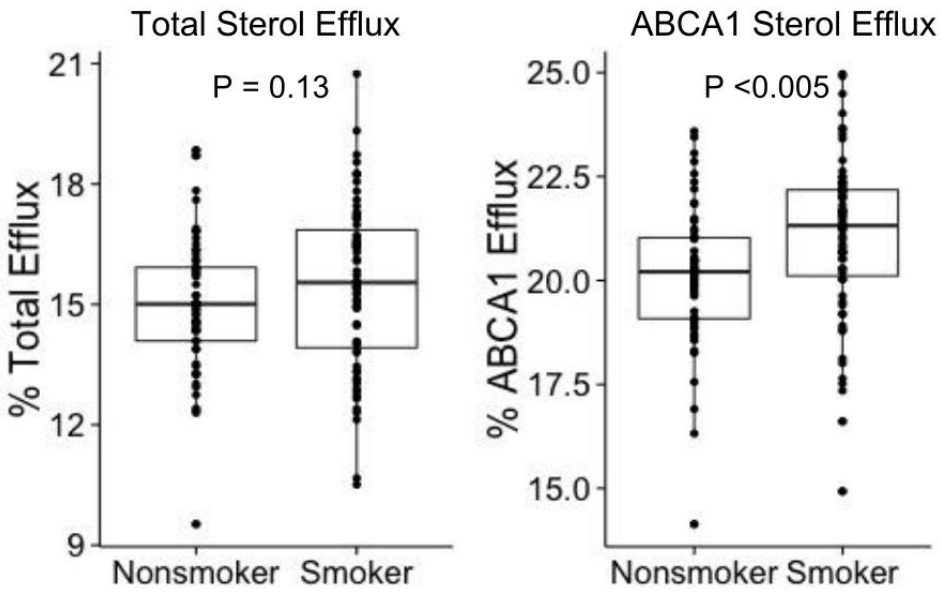

Figure 4.1: Total sterol efflux (left) and ABCA1-specific efflux (right). (nonsmoker n = 58; smoker n = 67)

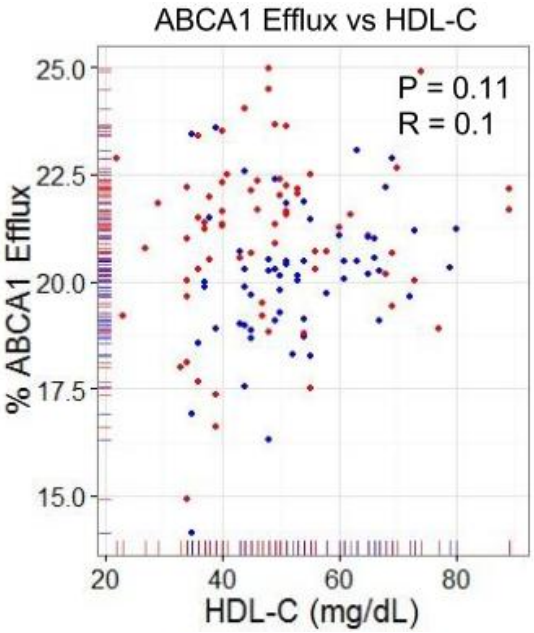

Figure 4.2: ABCA1 Efflux vs HDL-C (R = Pearson's R; red points = smoker; blue points = nonsmoker)

In contrast, we observed no significant change in overall or ABCA1-specific cholesterol efflux after one week of smoking cessation (**Figure 4.3**). Nicotine treatment status and γ-

tocopherol treatment status were not significant predictors for cholesterol efflux capacity. **Table 4.1** provides means and medians for groups under each set of conditions. It is possible that 7 days of smoking abstention was not long enough to witness a significant change in the ABCA1 efflux in the cessation subjects; the half life of an HDL particle is 3 to 4 days, indicating that many of the HDL particles from pre-cessation would still be present after one week.

		γ-tocohperol			Nicotine		
		-	+	P	-	+	P
Total Efflux	mean	0.18	0.14	0.88	0.11	0.22	0.71
	median	*0.32*	*0.16*		*0.32*	*0.16*	
ABCA1 Efflux	mean	-0.30	0.23	0.17	0.23	-0.31	0.16
	median	*-0.31*	*0.26*		*0.51*	*-0.14*	

Table 4.1: Efflux capacity across treatment groups

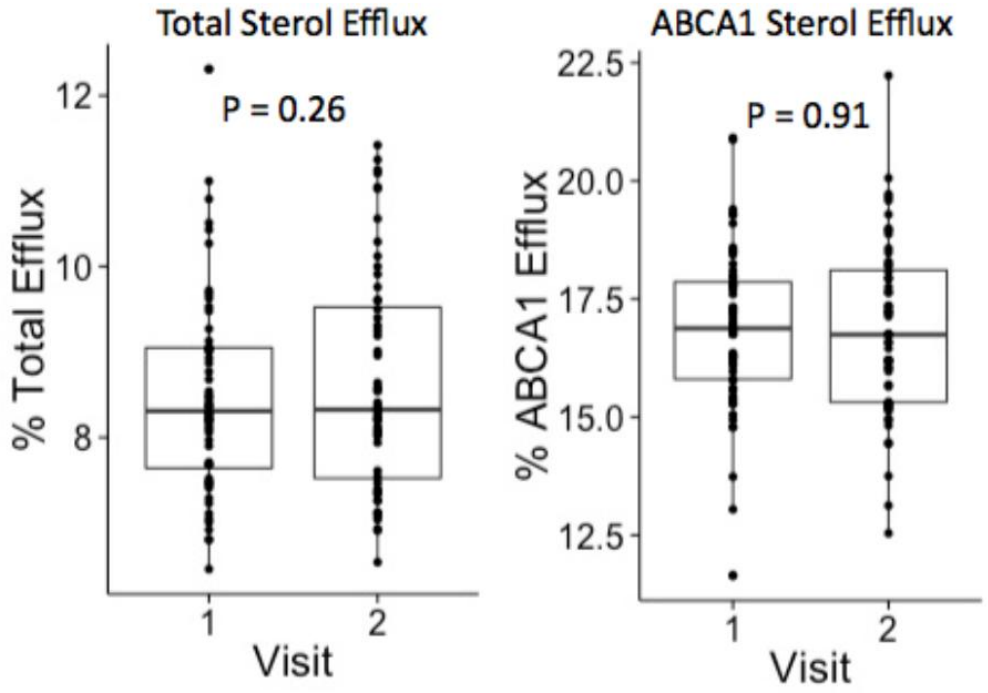

Figure 4.3: Change in total (left) and ABCA1-specific (right) cholesterol efflux capacity after one week of smoking cessation (n = 56 per visit)

HDL Particle Concentration

Our preliminary analysis generated the hypothesis that smokers had a higher mean small HDL particle concentration than nonsmokers. Once again, due to the half-life of HDL particles, the possibility remained that subjects from the smoking cessation study may not have had a long enough abstention interval to observe any marked change in particle concentrations. However, we expected the confirmatory analysis of CLEAR subjects to have sufficient power to detect differences between smokers and nonsmokers.

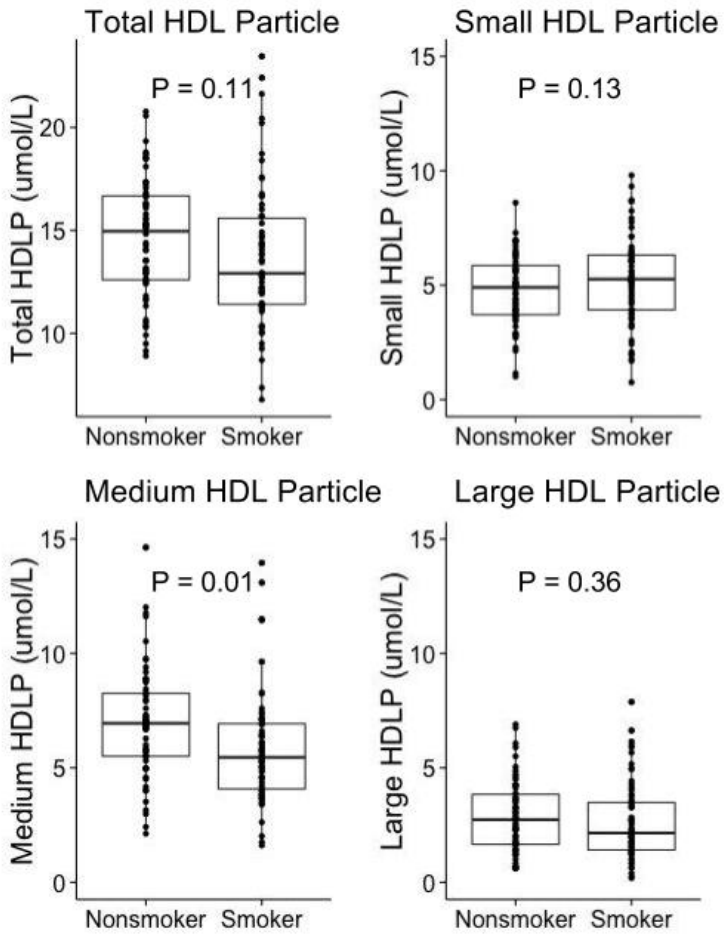

Figure 4.4: Total HDL particle concentration (top left), small HDL particle concentration (top right), medium HDL particle concentration (bottom left), and large HDL particle concentration (bottom right). (nonsmoker n = 58; smoker n = 67)

We did not detect a significantly higher small HDL particle concentration in smokers with CCVD (**Figure 4.4**, top right). However, smokers in this population had a significantly lower medium HDL particle concentration (**Figure 4.4**, bottom left); the mean medium particle concentration was 6.9 μmol/L in nonsmokers, and 5.8 μmol/L in smokers. It is possible that these subjects differed from those in the exploratory study due to the presence of CCVD. Interestingly, CCVD is associated with lower medium HDLP concentration(150), indicating that smoking may augment this effect. In the previous analysis, the medium HDL particle concentration in subjects without CCVD (smokers and nonsmokers) did not significantly differ from that of the nonsmokers with CCVD in this analysis. Large HDL particle concentration (**Figure 4.4**, bottom right) and total HDL particle concentration (**Figure 4.4**, top left) did not significantly differ between groups.

We did not observe any differences in the concentrations of HDL particle subpopulations or total HDL-P after one week of smoking cessation (**Figure 4.5**). This may in part be due to one week being too short a cessation interval for HDL particle subpopulations to markedly change. Additionally, the mean change in LDLP was 0.18 μmol/L, a small but significant increase (**Figure 4.5**, bottom left). This result was unexpected, since LDLP is highly correlated with LDLC; smokers characteristically have higher LDLC levels than nonsmokers and LDLC levels have been previously reported to decrease after smoking cessation(164). Furthermore, the half life of a circulating LDL particle is 5 days—longer than that of an HDL particle. This increase was independent of γ-tocopherol treatment or nicotine replacement therapy. There is a lack of previous studies addressing the short term effect of smoking cessation lipid levels; it is possible that this result is a temporary phenomenon that disappears in the longer term. It is also possible that smoking cessation caused changes in dietary habits, which led to this increase. Lipid panel

values are currently unknown for these subjects; it will be of interest whether LDLP correlates with LDLC.

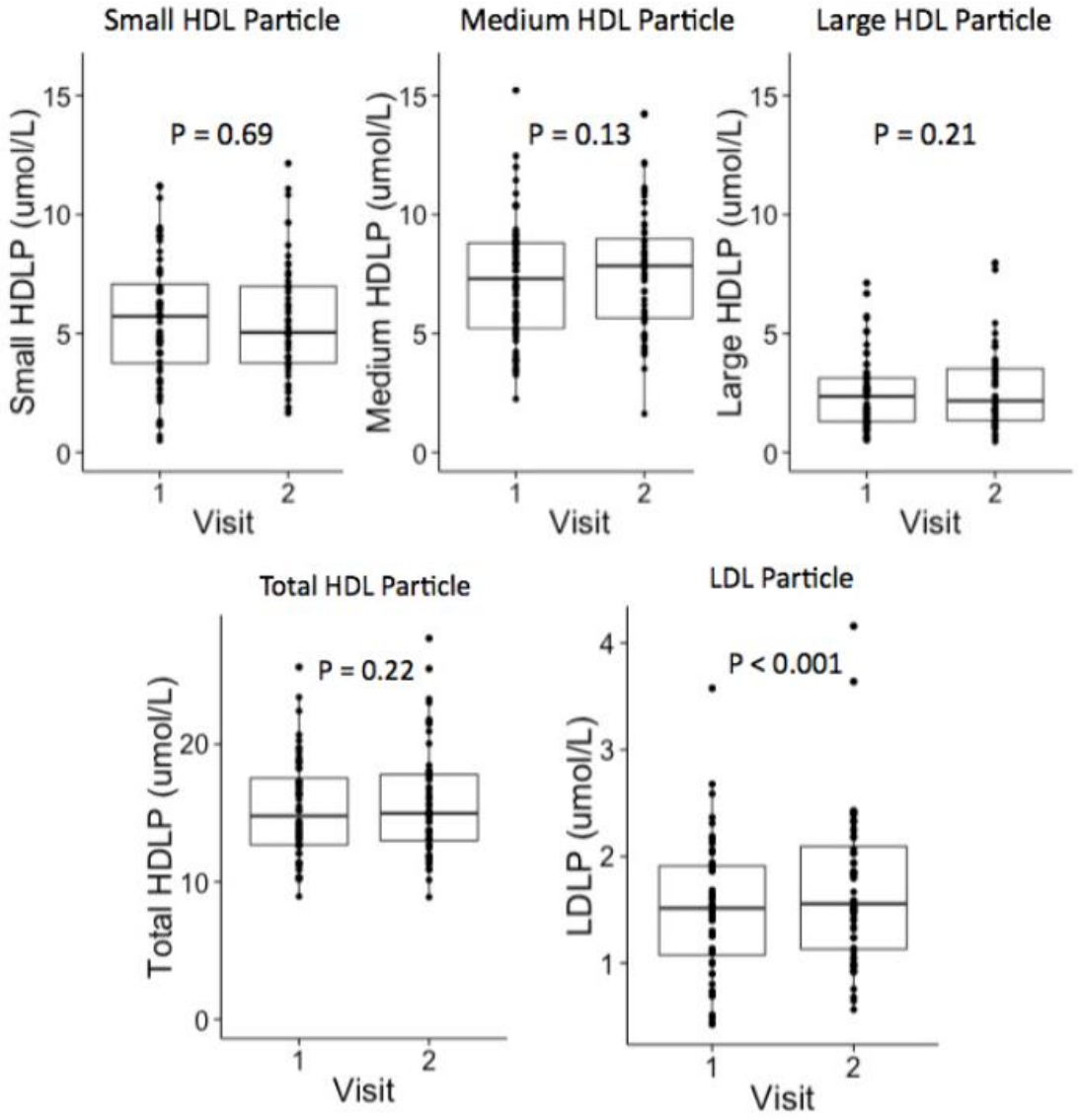

Figure 4.5: Concentration of Small HDL particles (top left), medium HDL particles (top middle), large HDL particles (top right), total HDL particles (bottom left), and LDL particles (bottom right). (n = 56 per visit)

γ-tocopherol treatment status did not associate with significant differences in the net changes of any HDL particle subpopulations. However, we observed the net change in small HDL particle concentration to differ significantly based upon nicotine status; subjects that

underwent nicotine replacement had a more negative net change in small particle concentration than those that did not undergo nicotine replacement (**Figure 4.6**, left; **Table 4.2**). 9 out of 30 non NRT-treated subjects had a net decrease in small HDL particle concentration, while 16 out of 26 NRT-treated subjects had a net decrease in this measure (**Figure 4.6,** right). Additionally, we observed nicotine treated subjects to have a trend of a more positive net increase in medium HDL particles than subjects without nicotine treatment. This suggests that nicotine may be associated with decreased small HDL particle concentration and therefore likely isn't the component of cigarette smoke that contributed to elevated small particle concentration in the initial study.

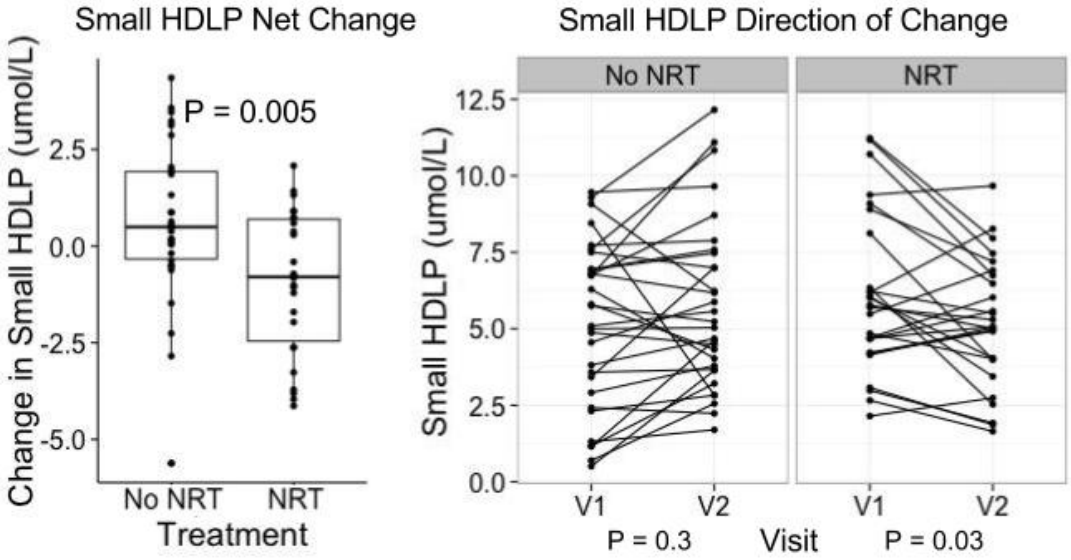

Figure 4.6: Net change in Small HDL particle concentration (left) and direction of change in small HDL particle concentration (right) (NRT = nicotine replacement therapy; NRT n = 26; no NRT n = 30)

		γ-tocohperol			Nicotine		
		-	+	P	-	+	P
Small HDLP	mean	-0.24	0.00	0.67	0.61	-0.94	0.005
	median	*0.19*	*0.16*		*0.50*	*-0.80*	
Medium HDLP	mean	0.51	0.29	0.68	-0.03	0.89	0.08
	median	*0.18*	*0.25*		*-0.11*	*0.50*	
Large HDLP	mean	0.28	0.08	0.47	0.24	0.10	0.63
	median	*0.20*	*-0.03*		*0.07*	*0.16*	
Total HDLP	mean	0.56	0.37	0.81	0.82	0.05	0.31
	median	*0.49*	*0.36*		*0.78*	*-0.09*	
LDLP	mean	0.24	0.11	0.19	0.20	0.15	0.63
	median	*0.25*	*0.12*		*0.25*	*0.14*	

Table 4.2: Particle subpopulations across treatment groups

HDL Proteomics

In the validation proteomics analysis, we only addressed three proteins with differences that were either significant or trending in the exploratory analysis: SFTPB, A1AT, and apoA-II. Targeting fewer proteins enabled us to minimize loss of significance after multiple comparisons adjustment. Once again, we were unsure whether the cessation interval would be sufficiently long to observe changes in the HDL protein cargo. It is likely that not all proteins associate with an HDL particle during the entirety of its existence, which could make it possible to observe changes after shorter time intervals. Proteomics of the CCVD subjects is underway.

Of the three proteins examined, we observed median HDL levels of A1AT after one week of smoking cessation to significantly decrease (**Figure 4.7**, middle). The mean HDL-associated A1AT post-cessation was approximately 85% that of pre-cessation levels. This decrease probably indicates a reduction in acute-phase response, and general neutrophil activation following smoking cessation. In the preliminary study, the mean A1AT level in nonsmokers was approximately 70% of that in smokers; it is exciting to observe that a mere week of smoking cessation was associated with a decrease of approximately half this magnitude.

The median level of HDL-associated SFTPB was lower after one week of cessation (**Figure 4.7**, left); however, the distribution of the net changes showed that the majority of subjects had very little change in their SFTPB levels with an extremely narrow interquartile range, and a minority with clear net negative or positive changes. The net negative changes were greater in magnitude than the net positive changes. This observation may be partially due to the fact that the average baseline SFTPB peak areas for these subjects were close to an order of magnitude lower than the average SFTPB peak areas for the smokers in the exploratory analysis. One possible explanation is that these subjects had shorter smoking histories and were younger and healthier than those in the exploratory analysis. While A1AT may be a marker for acute lung inflammation, SFTPB may be a marker for long-term lung damage.

Due to the trend in the preliminary study toward higher apoA-II levels in smokers, we expected apoA-II levels to drop following cessation. However, the net change in HDL apoA-II levels did not significantly differ from zero (**Figure 4.7**, right). It is possible that one week was not a sufficiently long time of cessation to observe changes in apoA-II levels.

Neither γ-tocopherol treatment nor nicotine replacement therapy was significantly associated with the net change in these proteins. Because the γ-tocopherol treated group was reported to have a larger net decrease in MPO and TNF-α, we hypothesized that this treatment would result in a greater reduction in A1AT(155). That the treatment groups did not significantly differ in net change of A1AT suggests that there are other factors that govern the release of some acute-phase proteins.

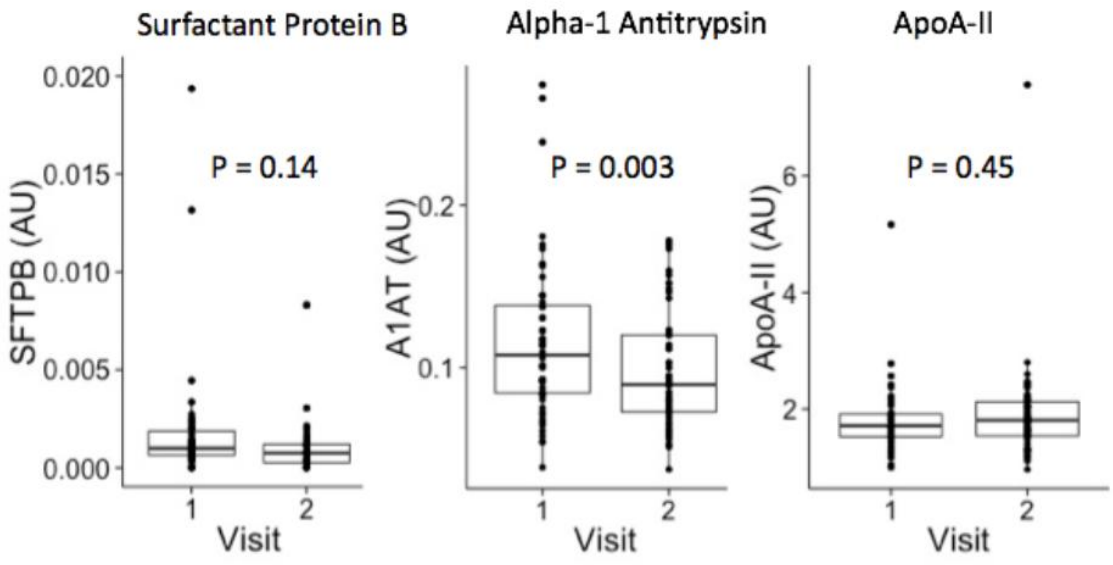

Figure 4.7: HDL-associated SFTPB (left), A1AT (middle), and apoA-II (right). (n = 56 per visit)

M148 Oxidation

We also measured whether there was a change in site-specific oxidation of M148 of apoA-I. In the preliminary study, we observed smokers to have 28% more oxidation at this residue than nonsmokers, leading us to hypothesize that oxidation at this residue would decrease after smoking cessation. We did not observe a significant change in M148 oxidation after smoking cessation. (**Figure 4.8**) Notably, these subjects had overall lower levels of M148 oxidation than those in the exploratory analysis. While in the latter study the median levels of oxidized M148 were 2.9% in nonsmokers and 3.7% in smokers, in this study the median level of oxidation was 2.1%. That the subjects in the confirmatory analysis had lower M148 oxidation than those in the exploratory analysis suggests that increasing age and smoking history may lead to reduction in endogenous defenses against oxidative damage. This absence of observed change after cessation could be due to either the short cessation interval or alternatively to low baseline oxidation levels.

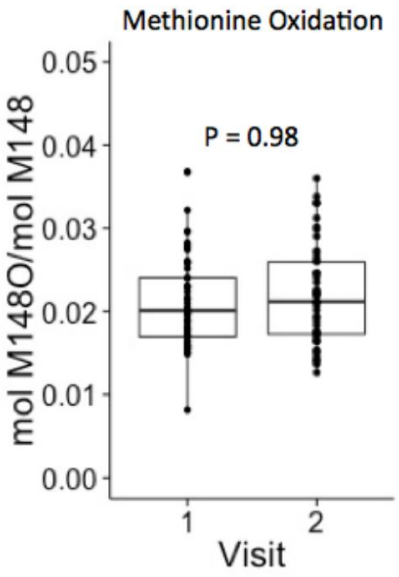

Figure 4.8: The net change in M148 oxidation does not significantly differ from zero.

Conclusions

In these validation analyses, we did not observe higher SFTPB levels in HDL from smokers than in that from nonsmokers, in spite of this being one of the primary hypotheses. We did observe lower A1AT levels in smokers, implicating this protein as a marker for smoking-related inflammation. We did not observe any significant difference between smokers and nonsmokers regarding overall cholesterol efflux, but did observe ABCA1-specific efflux to be significantly higher in smokers. In the discovery analysis, we observed smokers to have a higher small HDL particle concentration than nonsmokers. In the validation analysis, we did not repeat this observation, but observed lower medium HDL particle concentration in smokers and increased total LDL particle concentration following one week of smoking cessation. We also did not confirm that M148 oxidation is significantly higher in smokers.

Chapter 5

Discussion

This discussion will highlight some of the biological implications of these findings. It will compare these findings to those in recent literature and will describe potential future directions worthy of exploration. It will also address some apparent discrepancies in the findings from this work and propose explanations for these observations.

These experiments were initially motivated by the hypothesis that smoking would lead to loss of HDL function as a result of MPO-mediated protein damage. This hypothesis was prompted by a post-hoc analysis of a group of subjects that had stable CAD, ACS, or were healthy, in which the smokers had higher site-specific chlorination at Y-192 of apoA-I, a definitive product of MPO(74). However, in this population, smoking was also correlated with cardiovascular disease, making it possible that this observation was a result of CAD status rather than smoking. If this observed relationship was only a result of smoking being a covariate with CAD status we would expect there to be no difference in Cl-Y192 levels between smokers and nonsmokers of same CAD status. Indeed, this is the result we observed in this analysis: Cl-Y192 levels did not significantly differ between smokers and nonsmokers that lacked CCVD. Therefore, it seems likely that Cl-Y192 levels are a predictor of CVD, but that smoking status does not promote HDL chlorination. We also failed to observe a difference in total HDL chlorotyrosine levels between smokers and nonsmokers, demonstrating no evidence of elevated MPO oxidation products in smokers.

As Y192 of apoA-I exists in a functionally critical hinge domain, chlorination at this site could hinder the protein's ability to function. However, since the proportion of chlorinated Y192 residues is at most approximately 1:10,000, it seems unlikely that relatively few dysfunctional

molecules would result in a marked functional impairment. Although this chlorination reaction occurs at a relatively slow rate in vivo, its presence could be indicative of oxidation of residues with which MPO reacts more readily. Therefore, relatively high Cl-Y192 could be indicative of biologically relevant levels of modifications nonspecific to MPO at other sites on the HDL particle. Another possibility is that these oxidized proteins are cleared more rapidly than their unmodified counterparts, which would make the relative proportion of oxidation at this site appear lower than it really is. Lipid-free apoA-I is rapidly cleared from the circulation, meaning that if modification precludes apoA-I lipidation, modified apoA-I could be cleared more quickly. In order to explore the possibility that smoking alters HDL clearance rate, future studies could compare clearance of labeled HDL particles between smokers and nonsmokers.

An additional possibility is that the pseudohalide thiocyanate (SCN-), a product of inhaled cyanide, could be competing with chloride. Previous studies indicate smokers to have approximately threefold higher circulating thiocyanate levels than nonsmokers(165; 166). Furthermore, circulating thiocyanate levels are negatively associated with HDL-C(167). Cl- is a less favorable MPO substrate than Br- or SCN-, but Cl- is the most abundant circulating halide, causing MPO to react with it in vivo(168-170). At 100 mM Cl- and 100 μM SCN-, approximately 40% of the H_2O_2 consumed forms HOSCN(168). Since smokers have plasma SCN- levels exceeding 100 μM, it is likely that close to half of the H_2O_2 consumed generates HOSCN. However, MPO is not saturated at these concentrations, suggesting that Cl- and SCN- do not compete as its substrate. In future studies it would be prudent to measure levels of circulating SCN- and associated HDL adducts in addition to chlorotyrosine.

Although we observed smokers to have higher oxidation at M148 of apoA-I in the discovery analysis, we did not observe this result in the validation analysis. As the discovery

analysis made many comparisons regarding site-specific modifications, and the P value was not highly significant (0.025), it is possible that this observed difference was a false positive result.

Due to our hypothesis of increased protein modification, we also hypothesized that smokers would have less functional HDL than nonsmokers. Because the ability to efflux cholesterol from cells—particularly macrophages—is a key cardioprotective function of HDL, we measured sterol efflux to determine HDL function. Using Rader's efflux assay we did not observe the sterol efflux capacity of smokers and nonsmokers to differ significantly. One potential flaw with Rader's method for measuring total cholesterol efflux is that it uses a murine macrophage cell line. Human apoA-I shares only 70% sequence homology with murine apoA-I, and the two proteins differ vastly in terms of tertiary structure(40; 171). This assay measures function as interaction of human HDL with murine cells, which does not necessarily translate to its function with human cells. However, it could be argued that since this assay is a robust predictor of CAD status, it is irrelevant whether human HDL interacts with mouse macrophages and human cells similarly.

The ABCA1-specific efflux assay used BHK cells expressing human ABCA1 under mifepristone stimulation. Because these cells do not ordinarily express any of the known cholesterol exporters (including ABCA1 and ABCG1), ABCA1 is the only efflux mechanism when the protein is induced in the cells by mifepristone. By this assay, we observed smoker HDL to promote significantly higher levels of efflux than nonsmoker HDL. This result was unexpected, given that sterol efflux is atheroprotective, while smoking is atherogenic, suggesting that impaired HDL efflux capacity is not playing a role in the accelerated atherosclerosis in smokers. However, reverse cholesterol transport could be impaired independently of this HDL function. For instance, dysfunctional ABCA1 would also result in decreased ABCA1 efflux.

Mulya et al report that after the initial lipidation by ABCA1, maturing HDL particles interact with ABCA1 less readily than those particles that have not previously interacted with ABCA1(18). Therefore, if ABCA1 is less functional (or less prevalent) in smokers, it is possible that proportionally fewer HDL particles in smokers would have previously interacted with ABCA1, and would therefore undergo ABCA1 efflux more readily in the efflux assay. It is also possible that previous interaction with human ABCA1 would not preclude HDL from interaction with murine ABCA1, which would explain the lack of difference in efflux capacities using the J774 cells. It would be difficult to test *in vivo* ABCA1 function in smokers, since cells expressing ABCA1 also undergo other efflux mechanisms. However, it would be possible to measure ABCA1 modifications—since smoking generates reactive carbonyls, these products are possible candidates for protein adducts. It would also be possible to measure ABCA1 expression *in vivo* using qPCR to assess gene transcription and using antibody-based techniques to detect protein expression.

We did not observe any trend toward change in total or ABCA1-specific cholesterol efflux capacity after one week of smoking cessation. However, although there was no universal tendency for efflux capacity to change in a specific direction, in several individuals the magnitude of the change was >1%, a substantial change since the mean total efflux was 8.6% and the mean ABCA1 efflux was 17%. There is little known about inter-individual changes in efflux capacity; it is unclear whether these individual changes in efflux capacity across one week are a normal characteristic of this measure.

In the future, it would be ideal to optimize the LCAT activation assay, since the current assay used in the exploratory analysis has a few major flaws. For example, LCAT is bound to HDL *in vivo,* meaning that endogenous LCAT could also be carrying out the esterification

reaction, and observed differences in cholesteryl ester production could be due to different levels of bound LCAT. In order to account for bound LCAT activity, esterification could be measured in the presence and absence of recombinant LCAT. However, doing this for every sample would double the number of reactions required. Additionally, because the assay involves radiolabeled cholesterol, there are limited automation options available. This technique is acceptable for the small sample size that is typical of in *vitro assays*, but is unsuitable as a high-throughput method for large clinical sample sets. It would be ideal to develop a method involving a fluorescent cholesterol homolog that could serve as a labeled LCAT substrate. Potential problems with such substrates include weak signal, causing a high limit of detection.

For future studies it would also be prudent to develop additional assays of HDL functions, since HDL plays other known physiological roles, such as acting as an antioxidant. This is a complimentary approach to measuring oxidation of apoA-I; high levels of oxidative stress would modify HDL proteins such as apoA-I, which could potentially quench HDL's ability to act as an antioxidant. While the RCT function is thought to primarily involve apoA-I, additional HDL functional assays would present information about the function of other HDL proteins. Assays of additional HDL functions, such as its anti-inflammatory effects on macrophages and endothelial cells, would likewise be a useful complement to HDL protemoics studies, potentially enabling the elucidation of the functional roles of particular HDL-associated proteins(172-174).

Our preliminary proteomics study suggested that smokers have higher HDL-associated SFTPB than nonsmokers. Although the elevation of SFTPB in smokers was highly significant in the discovery analysis, it existed at markedly lower baseline levels in the smoking cessation study, and was undetectable by immunoblot in the CCVD subjects. One possible explanation for

this discrepancy is inter- HDL prep variation; SFTPB could be a contaminant from the denser plasma proteins fraction that is present in trace amounts in some HDL preps. It is also possible that the antibody is cross-reacting with a different lipoprotein-associated protein since this antibody was tested in pulmonary tissue but not plasma and SFTPB shares structural similarities to apolipoproteins. A previous study described elevated circulating levels of SFTPB in smokers, but did not established which plasma fraction contains it(128). It is also possible that SFTPB is unstable and sensitive to storage conditions, which could make it prone to degradation. To date, there is only one publication reporting SFTPB as an HDL-associated protein; it was enriched in subjects with end stage renal disease(48) Although the elevation of SFTPB levels in smokers was highly significant in the exploratory analysis, we remain skeptical of this result since it was not validated in the confirmatory study. It is also possible that this protein is only elevated in smokers in certain populations; additional studies will be required to form conclusions.

The discovery analysis also suggested a trend for higher A1AT and higher apoA-II in smokers. We observed smokers to have elevated A1AT in the validation analysis, but we did not observe elevated apoA-II in the validation analysis. The mean level of HDL-associated A1AT in never smokers was 65% that of the level in current smokers. After a mere week of smoking cessation, the mean level of HDL-associated A1AT decreased by 85%, indicating this protein to be a current indicator of acute-phase response. The elevation of A1AT in smokers is likely a marker for neutrophil activation; evidence exists that neutrophils store A1AT and release it when activated(175). As an inhibitor of proteolysis, there is also evidence that HDL-bound A1AT inhibits vascular ECM degradation and other hallmarks of endothelial dysfunction(176). Thus, it is likely that HDL-bound A1AT is atheroprotective. A1AT has three N-linked glycosylation sites and several different glycan groups have been observed at each site(177). These variable

modifications could impact biological function, as well as stability. However, we did not observe any variably sized A1AT bands by immunoblot to suggest a variety of A1AT glycoforms bound to HDL. This suggests that A1AT secretion likely determines HDL-associated A1AT levels.

The population in the smoking cessation study is markedly different from that in the discovery analysis. For example, the mean age in the former was 21 years; the mean in the latter was 67 years. Some differences in the HDL proteomes of healthy young and elderly subjects have been described; the elderly have lower levels of apoE and higher levels of acute phase proteins such as A1AT(178). That our study populations were extremely different from one another has detrimental and beneficial aspects. It is detrimental in that our inability to validate some observations may be a result of the differences in populations, but could be validated with a more similar population. Conversely, because the populations are extensively different, any results that are consistent in both analyses likely indicate an association with smoking status, rather than with another factor.

All three groups of subjects showed different relationships between lipoprotein particle subpopulations and smoking. In the exploratory analysis, smokers had a higher small HDL particle concentration than nonsmokers; in the smoking cessation study, there was no change in HDL subpopulations, but an increase in LDL particle concentration after cessation, and a possible trend for nicotine treatment to be associated with a reduction in small HDL particles. The LDL result is most likely due to dietary alterations following smoking cessation. The potential association of nicotine treatment and small HDL particles is more difficult to explain; since smoking delivers nicotine, it is surprising that there would be a large net change in subjects undergoing nicotine replacement. This result should be approached cautiously since it was not

part of the initial hypothesis; conclusions could only be drawn if it were validated with another smoking cessation study.

Since the half life of an HDL particle is 3-4 days, it is likely that one week was not a long enough cessation interval to observe significant decreases in HDL particle subpopulation concentrations. However, there exists the possibility that smoking status influences the half life of certain particles. That we observed a significant increase in the LDL particle concentration within this interval indicates an increase in LDL biogenesis. Although previous studies have reported LDL-C and LDL size to remain at the same level following smoking cessation(179), it is possible that there is an increase in LDL particle concentration immediately after quitting, potentially due to metabolic changes. It is also important to make the distinction between LDL particle concentration and LDL-C; it is possible that LDL-C did not change, but subjects had more LDL particles, each of which contained less cholesterol.

In the validation analysis with CCVD subjects, smokers had a lower concentration of medium HDL particles. These seemingly discrepant results could underline potential interactions between HDL particle concentration and disease status. It is interesting that in CCVD subjects, smokers had fewer medium HDL particles than nonsmokers; in a separate study, CCVD status was associated with fewer medium HDL particles(150). This indicates that smoking and CCVD may have additive effects on medium HDL particle concentration.

A longitudinal study design is the ideal strategy to control for inter-individual variation in lipoprotein metabolism. However, a recurring concern with the described smoking cessation study is that the cessation interval wasn't adequately long to detect changes in HDL. It would be most effective for such a study to span several years after smoking cessation. Because intra-individual changes HDL measures remain largely unknown, it would be prudent to include

healthy nonsmoking controls in such a study. In a long enough study, these individuals would also enable adjustment for the effects of aging. It would be ideal to measure not only the effect of smoking cessation but of smoking initiation as well; due to the known hazards of smoking, a study of this nature would be ethically unsound. The obvious drawbacks in longitudinal studies are expense and time. Additionally, a significant proportion of subjects in a long term smoking cessation study would likely be unsuccessful at continued smoking abstention.

These studies did not provide strong evidence that dysfunctional HDL is the mechanistic link between smoking and heart disease. We did not observe evidence that smoking is associated with elevated MPO-induced protein modification, nor that it is associated with impaired sterol efflux capacity. Thus, we found no evidence in favor of our hypothesis that smoking promotes HDL protein oxidation and dysfunction. However, these studies succeeded in discovering HDL proteins that are associated with smoking status. It is possible that these proteins are key to some of the many biological functions of HDL. It is also possible that these proteins are biomarkers for smoking-induced stress, such as pulmonary injury. Future studies will be needed to address these possible roles.

References:

1. Bloch K, Berg BN, Rittenberg D: The Biological Conversion of Cholesterol to Cholic Acid. J Biol Chem 1943:511-517
2. Yeagle PL: Cholesterol and the cell membrane. Biochim Biophys Acta 1985;822:267-287
3. Hanukoglu I: Steroidogenic enzymes: structure, function, and role in regulation of steroid hormone biosynthesis. J Steroid Biochem Mol Biol 1992;43:779-804
4. Bloch K: The biological synthesis of cholesterol. Science 1965;150:19-28
5. Lecerf JM, de Lorgeril M: Dietary cholesterol: from physiology to cardiovascular risk. Br J Nutr 2011;106:6-14
6. Kindel T, Lee DM, Tso P: The mechanism of the formation and secretion of chylomicrons. Atheroscler Suppl 2010;11:11-16
7. Nelson D, Cox M: *Lehninger Principles of Biochemistry*. W. H. Freeman and Company, 2005
8. Olson RE: Discovery of the lipoproteins, their role in fat transport and their significance as risk factors. J Nutr 1998;128:439s-443s
9. Havel RJ: Receptor and non-receptor mediated uptake of chylomicron remnants by the liver. Atherosclerosis 1998;141 Suppl 1:S1-7
10. Gibbons GF, Wiggins D, Brown AM, Hebbachi AM: Synthesis and function of hepatic very-low-density lipoprotein. Biochem Soc Trans 2004;32:59-64
11. Goldstein JL, Brown MS: History of Discovery: The LDL Receptor. Arterioscler Thromb Vasc Biol 2009;29:431-438
12. Hobbs HH, Brown MS, Goldstein JL: Molecular genetics of the LDL receptor gene in familial hypercholesterolemia. Hum Mutat 1992;1:445-466
13. Ishibashi S, Goldstein JL, Brown MS, Herz J, Burns DK: Massive xanthomatosis and atherosclerosis in cholesterol-fed low density lipoprotein receptor-negative mice. J Clin Invest 1994;93:1885-1893
14. MacDougall ED, Kramer F, Polinsky P, Barnhart S, Askari B, Johansson F, Varon R, Rosenfeld ME, Oka K, Chan L, Schwartz SM, Bornfeldt KE: Aggressive very low-density lipoprotein (VLDL) and LDL lowering by gene transfer of the VLDL receptor combined with a low-fat diet regimen induces regression and reduces macrophage content in advanced atherosclerotic lesions in LDL receptor-deficient mice. Am J Pathol 2006;168:2064-2073
15. Navab M, Reddy ST, Van Lenten BJ, Fogelman AM: HDL and cardiovascular disease: atherogenic and atheroprotective mechanisms. Nat Rev Cardiol 2011;8:222-232
16. Ono K: Current concept of reverse cholesterol transport and novel strategy for atheroprotection. J Cardiol 2012;60:339-343
17. Vedhachalam C, Duong PT, Nickel M, Nguyen D, Dhanasekaran P, Saito H, Rothblat GH, Lund-Katz S, Phillips MC: Mechanism of ATP-binding cassette transporter A1-mediated cellular lipid efflux to apolipoprotein A-I and formation of high density lipoprotein particles. J Biol Chem 2007;282:25123-25130
18. Mulya A, Lee JY, Gebre AK, Thomas MJ, Colvin PL, Parks JS: Minimal lipidation of pre-beta HDL by ABCA1 results in reduced ability to interact with ABCA1. Arterioscler Thromb Vasc Biol 2007;27:1828-1836
19. Acton S, Rigotti A, Landschulz KT, Xu S, Hobbs HH, Krieger M: Identification of scavenger receptor SR-BI as a high density lipoprotein receptor. Science 1996;271:518-520

20. Kennedy MA, Barrera GC, Nakamura K, Baldan A, Tarr P, Fishbein MC, Frank J, Francone OL, Edwards PA: ABCG1 has a critical role in mediating cholesterol efflux to HDL and preventing cellular lipid accumulation. Cell Metab 2005;1:121-131
21. Glomset JA: The plasma lecithins:cholesterol acyltransferase reaction. J Lipid Res 1968;9:155-167
22. Fielding CJ, Shore VG, Fielding PE: A protein cofactor of lecithin:cholesterol acyltransferase. Biochem Biophys Res Commun 1972;46:1493-1498
23. Scott BR, McManus DC, Franklin V, McKenzie AG, Neville T, Sparks DL, Marcel YL: The N-terminal globular domain and the first class A amphipathic helix of apolipoprotein A-I are important for lecithin:cholesterol acyltransferase activation and the maturation of high density lipoprotein in vivo. J Biol Chem 2001;276:48716-48724
24. Shih AY, Sligar SG, Schulten K: Maturation of high-density lipoproteins. J R Soc Interface 2009;6:863-871
25. Moore KJ, Sheedy FJ, Fisher EA: Macrophages in atherosclerosis: a dynamic balance. Nat Rev Immunol 2013;13:709-721
26. Lusis AJ: Atherosclerosis. Nature 2000;407:233-241
27. Libby P, Ridker PM, Maseri A: Inflammation and atherosclerosis. Circulation 2002;105:1135-1143
28. Gomez D, Owens GK: Smooth muscle cell phenotypic switching in atherosclerosis. Cardiovasc Res 2012;95:156-164
29. Rudijanto A: The role of vascular smooth muscle cells on the pathogenesis of atherosclerosis. Acta Med Indones 2007;39:86-93
30. Nelken NA, Coughlin SR, Gordon D, Wilcox JN: Monocyte chemoattractant protein-1 in human atheromatous plaques. J Clin Invest 1991;88:1121-1127
31. Yu X, Dluz S, Graves DT, Zhang L, Antoniades HN, Hollander W, Prusty S, Valente AJ, Schwartz CJ, Sonenshein GE: Elevated expression of monocyte chemoattractant protein 1 by vascular smooth muscle cells in hypercholesterolemic primates. Proc Natl Acad Sci U S A 1992;89:6953-6957
32. Feil S, Fehrenbacher B, Lukowski R, Essmann F, Schulze-Osthoff K, Schaller M, Feil R: Transdifferentiation of vascular smooth muscle cells to macrophage-like cells during atherogenesis. Circ Res 2014;115:662-667
33. Badimon JJ, Badimon L, Fuster V: Regression of atherosclerotic lesions by high density lipoprotein plasma fraction in the cholesterol-fed rabbit. J Clin Invest 1990;85:1234-1241
34. Berliner JA, Navab M, Fogelman AM, Frank JS, Demer LL, Edwards PA, Watson AD, Lusis AJ: Atherosclerosis: basic mechanisms. Oxidation, inflammation, and genetics. Circulation 1995;91:2488-2496
35. Havel RJ, Eder HA, Bragdon JH: THE DISTRIBUTION AND CHEMICAL COMPOSITION OF ULTRACENTRIFUGALLY SEPARATED LIPOPROTEINS IN HUMAN SERUM. J Clin Invest 1955;34:1345-1353
36. Kunitake ST, La Sala KJ, Kane JP: Apolipoprotein A-I-containing lipoproteins with pre-beta electrophoretic mobility. J Lipid Res 1985;26:549-555
37. O'Connor PM, Zysow BR, Schoenhaus SA, Ishida BY, Kunitake ST, Naya-Vigne JM, Duchateau PN, Redberg RF, Spencer SJ, Mark S, Mazur M, Heilbron DC, Jaffe RB, Malloy MJ, Kane JP: Prebeta-1 HDL in plasma of normolipidemic individuals: influences of plasma lipoproteins, age, and gender. J Lipid Res 1998;39:670-678

38. Tian L, Li C, Liu Y, Chen Y, Fu M: The value and distribution of high-density lipoprotein subclass in patients with acute coronary syndrome. PLoS One 2014;9:e85114
39. Phillips MC: New insights into the determination of HDL structure by apolipoproteins: Thematic review series: high density lipoprotein structure, function, and metabolism. J Lipid Res 2013;54:2034-2048
40. Bashtovyy D, Jones MK, Anantharamaiah GM, Segrest JP: Sequence conservation of apolipoprotein A-I affords novel insights into HDL structure-function. In *J Lipid Res* United States, 2011, p. 435-450
41. Silva RA, Huang R, Morris J, Fang J, Gracheva EO, Ren G, Kontush A, Jerome WG, Rye KA, Davidson WS: Structure of apolipoprotein A-I in spherical high density lipoproteins of different sizes. Proc Natl Acad Sci U S A 2008;105:12176-12181
42. Segrest JP: Amphipathic helixes and plasma lipoproteins: thermodynamic and geometric considerations. Chem Phys Lipids 1977;18:7-22
43. Li L, Chen J, Mishra VK, Kurtz JA, Cao D, Klon AE, Harvey SC, Anantharamaiah GM, Segrest JP: Double belt structure of discoidal high density lipoproteins: molecular basis for size heterogeneity. J Mol Biol 2004;343:1293-1311
44. Wu Z, Wagner MA, Zheng L, Parks JS, Shy JM, 3rd, Smith JD, Gogonea V, Hazen SL: The refined structure of nascent HDL reveals a key functional domain for particle maturation and dysfunction. Nat Struct Mol Biol 2007;14:861-868
45. Mehrabian M, Qiao JH, Hyman R, Ruddle D, Laughton C, Lusis AJ: Influence of the apoA-II gene locus on HDL levels and fatty streak development in mice. Arterioscler Thromb 1993;13:1-10
46. Vaisar T, Pennathur S, Green PS, Gharib SA, Hoofnagle AN, Cheung MC, Byun J, Vuletic S, Kassim S, Singh P, Chea H, Knopp RH, Brunzell J, Geary R, Chait A, Zhao XQ, Elkon K, Marcovina S, Ridker P, Oram JF, Heinecke JW: Shotgun proteomics implicates protease inhibition and complement activation in the antiinflammatory properties of HDL. J Clin Invest 2007;117:746-756
47. Cheung MC, Vaisar T, Han X, Heinecke JW, Albers JJ: Phospholipid transfer protein in human plasma associates with proteins linked to immunity and inflammation. Biochemistry 2010;49:7314-7322
48. Weichhart T, Kopecky C, Kubicek M, Haidinger M, Doller D, Katholnig K, Suarna C, Eller P, Tolle M, Gerner C, Zlabinger GJ, van der Giet M, Horl WH, Stocker R, Saemann MD: Serum amyloid A in uremic HDL promotes inflammation. J Am Soc Nephrol 2012;23:934-947
49. Wilson PW, Garrison RJ, Castelli WP, Feinleib M, McNamara PM, Kannel WB: Prevalence of coronary heart disease in the Framingham Offspring Study: role of lipoprotein cholesterols. Am J Cardiol 1980;46:649-654
50. Gordon T, Castelli WP, Hjortland MC, Kannel WB, Dawber TR: High density lipoprotein as a protective factor against coronary heart disease. The Framingham Study. Am J Med 1977;62:707-714
51. Castelli WP: Epidemiology of coronary heart disease: the Framingham study. Am J Med 1984;76:4-12
52. Ali KM, Wonnerth A, Huber K, Wojta J: Cardiovascular disease risk reduction by raising HDL cholesterol - current therapies and future opportunities. Br J Pharmacol 2012;167:1177-1194
53. Alberts AW, Chen J, Kuron G, Hunt V, Huff J, Hoffman C, Rothrock J, Lopez M, Joshua H, Harris E, Patchett A, Monaghan R, Currie S, Stapley E, Albers-Schonberg G, Hensens O,

Hirshfield J, Hoogsteen K, Liesch J, Springer J: Mevinolin: a highly potent competitive inhibitor of hydroxymethylglutaryl-coenzyme A reductase and a cholesterol-lowering agent. Proc Natl Acad Sci U S A 1980;77:3957-3961
54. Endo A, Tsujita Y, Kuroda M, Tanzawa K: Inhibition of cholesterol synthesis in vitro and in vivo by ML-236A and ML-236B, competitive inhibitors of 3-hydroxy-3-methylglutaryl-coenzyme A reductase. Eur J Biochem 1977;77:31-36
55. Tobert JA: Lovastatin and beyond: the history of the HMG-CoA reductase inhibitors. Nat Rev Drug Discov 2003;2:517-526
56. Blumenthal RS: Statins: effective antiatherosclerotic therapy. Am Heart J 2000;139:577-583
57. Boekholdt SM, Hovingh GK, Mora S, Arsenault BJ, Amarenco P, Pedersen TR, LaRosa JC, Waters DD, DeMicco DA, Simes RJ, Keech AC, Colquhoun D, Hitman GA, Betteridge DJ, Clearfield MB, Downs JR, Colhoun HM, Gotto AM, Jr., Ridker PM, Grundy SM, Kastelein JJ: Very low levels of atherogenic lipoproteins and the risk for cardiovascular events: a meta-analysis of statin trials. J Am Coll Cardiol 2014;64:485-494
58. Ray KK, Cannon CP, Cairns R, Morrow DA, Ridker PM, Braunwald E: Prognostic utility of apoB/AI, total cholesterol/HDL, non-HDL cholesterol, or hs-CRP as predictors of clinical risk in patients receiving statin therapy after acute coronary syndromes: results from PROVE IT-TIMI 22. Arterioscler Thromb Vasc Biol 2009;29:424-430
59. Boden WE, Probstfield JL, Anderson T, Chaitman BR, Desvignes-Nickens P, Koprowicz K, McBride R, Teo K, Weintraub W: Niacin in patients with low HDL cholesterol levels receiving intensive statin therapy. N Engl J Med 2011;365:2255-2267
60. Nissen SE, Tardif JC, Nicholls SJ, Revkin JH, Shear CL, Duggan WT, Ruzyllo W, Bachinsky WB, Lasala GP, Tuzcu EM: Effect of torcetrapib on the progression of coronary atherosclerosis. N Engl J Med 2007;356:1304-1316
61. Mohammadpour AH, Akhlaghi F: Future of cholesteryl ester transfer protein (CETP) inhibitors: a pharmacological perspective. Clin Pharmacokinet 2013;52:615-626
62. Robins SJ, Collins D, Wittes JT, Papademetriou V, Deedwania PC, Schaefer EJ, McNamara JR, Kashyap ML, Hershman JM, Wexler LF, Rubins HB: Relation of gemfibrozil treatment and lipid levels with major coronary events: VA-HIT: a randomized controlled trial. Jama 2001;285:1585-1591
63. Berge KG, Canner PL: Coronary drug project: experience with niacin. Coronary Drug Project Research Group. Eur J Clin Pharmacol 1991;40 Suppl 1:S49-51
64. Barter PJ, Caulfield M, Eriksson M, Grundy SM, Kastelein JJ, Komajda M, Lopez-Sendon J, Mosca L, Tardif JC, Waters DD, Shear CL, Revkin JH, Buhr KA, Fisher MR, Tall AR, Brewer B: Effects of torcetrapib in patients at high risk for coronary events. In *N Engl J Med* United States, 2007 Massachusetts Medical Society., 2007, p. 2109-2122
65. Barter P: Lessons learned from the Investigation of Lipid Level Management to Understand its Impact in Atherosclerotic Events (ILLUMINATE) trial. In *Am J Cardiol* United States, 2009, p. 10E-15E
66. Tall AR, Yvan-Charvet L, Wang N: The failure of torcetrapib: was it the molecule or the mechanism? In *Arterioscler Thromb Vasc Biol* United States, 2007, p. 257-260
67. Schwartz GG, Olsson AG, Abt M, Ballantyne CM, Barter PJ, Brumm J, Chaitman BR, Holme IM, Kallend D, Leiter LA, Leitersdorf E, McMurray JJ, Mundl H, Nicholls SJ, Shah PK, Tardif JC, Wright RS: Effects of dalcetrapib in patients with a recent acute coronary syndrome. N Engl J Med 2012;367:2089-2099

68. Khera AV, Cuchel M, de la Llera-Moya M, Rodrigues A, Burke MF, Jafri K, French BC, Phillips JA, Mucksavage ML, Wilensky RL, Mohler ER, Rothblat GH, Rader DJ: Cholesterol efflux capacity, high-density lipoprotein function, and atherosclerosis. N Engl J Med 2011;364:127-135
69. Mora S, Glynn RJ, Ridker PM: High-density lipoprotein cholesterol, size, particle number, and residual vascular risk after potent statin therapy. Circulation 2013;128:1189-1197
70. Klebanoff SJ: Myeloperoxidase: friend and foe. In *J Leukoc Biol* United States, 2005, p. 598-625
71. Klebanoff SJ: Myeloperoxidase-Halide-Hydrogen Peroxide Antibacterial System. J Bacteriol 1968;95:2131-2138
72. Pattison DI, Davies MJ: Absolute rate constants for the reaction of hypochlorous acid with protein side chains and peptide bonds. Chem Res Toxicol 2001;14:1453-1464
73. Shao B, Pennathur S, Heinecke JW: Myeloperoxidase targets apolipoprotein A-I, the major high density lipoprotein protein, for site-specific oxidation in human atherosclerotic lesions. J Biol Chem 2012;287:6375-6386
74. Shao B, Tang C, Sinha A, Mayer PS, Davenport GD, Brot N, Oda MN, Zhao XQ, Heinecke JW: Humans with atherosclerosis have impaired ABCA1 cholesterol efflux and enhanced high-density lipoprotein oxidation by myeloperoxidase. Circ Res 2014;114:1733-1742
75. Shao B, Oda MN, Oram JF, Heinecke JW: Myeloperoxidase: An oxidative pathway for generating dysfunctional HDL. Chem Res Toxicol 2010;23:447-454
76. Shao B, Heinecke JW: Using tandem mass spectrometry to quantify site-specific chlorination and nitration of proteins: model system studies with high-density lipoprotein oxidized by myeloperoxidase. Methods Enzymol 2008;440:33-63
77. Bergt C, Fu X, Huq NP, Kao J, Heinecke JW: Lysine Residues Direct the Chlorination of Tyrosines in YXXK Motifs of Apolipoprotein A-I When Hypochlorous Acid Oxidizes High Density Lipoprotein. 2004;
78. Shao B, Oda MN, Bergt C, Fu X, Green PS, Brot N, Oram JF, Heinecke JW: Myeloperoxidase impairs ABCA1-dependent cholesterol efflux through methionine oxidation and site-specific tyrosine chlorination of apolipoprotein A-I. J Biol Chem 2006;281:9001-9004
79. Souza JM, Daikhin E, Yudkoff M, Raman CS, Ischiropoulos H: Factors determining the selectivity of protein tyrosine nitration. Arch Biochem Biophys 1999;371:169-178
80. Shao B, Cavigiolio G, Brot N, Oda MN, Heinecke JW: Methionine oxidation impairs reverse cholesterol transport by apolipoprotein A-I. In *Proc Natl Acad Sci U S A* United States, 2008, p. 12224-12229
81. Organization WWH: Warning About the Dangers of Tobacco. In *WHO REPORT ON THE GLOBAL TOBACCO EPIDEMIC* Geneva, Switzerland, World Health Organization, 2011, p. 164
82. Jha P, Ramasundarahettige C, Landsman V, Rostron B, Thun M, Anderson RN, McAfee T, Peto R: 21st-century hazards of smoking and benefits of cessation in the United States. N Engl J Med 2013;368:341-350
83. Siahpush M, McNeill A, Hammond D, Fong GT: Socioeconomic and country variations in knowledge of health risks of tobacco smoking and toxic constituents of smoke: results from the 2002 International Tobacco Control (ITC) Four Country Survey. Tob Control 2006;15 Suppl 3:iii65-70

84. Wannamethee SG, Lowe GD, Shaper AG, Rumley A, Lennon L, Whincup PH: Associations between cigarette smoking, pipe/cigar smoking, and smoking cessation, and haemostatic and inflammatory markers for cardiovascular disease. Eur Heart J 2005;26:1765-1773
85. Hecht SS: Tobacco smoke carcinogens and lung cancer. J Natl Cancer Inst 1999;91:1194-1210
86. MacNee W, Wiggs B, Belzberg AS, Hogg JC: The effect of cigarette smoking on neutrophil kinetics in human lungs. N Engl J Med 1989;321:924-928
87. Hoonhorst S, Timens W, Koenderman L, Lo Tam Loi AT, Lammers JW, Boezen H, van Oosterhout A, Postma DS, Ten Hacken N: Increased activation of blood neutrophils after cigarette smoking in young individuals susceptible to COPD. Respir Res 2014;15:121
88. Schwartz J, Weiss ST: Cigarette smoking and peripheral blood leukocyte differentials. Ann Epidemiol 1994;4:236-242
89. Trush MA, Seed JL, Kensler TW: Oxidant-dependent metabolic activation of polycyclic aromatic hydrocarbons by phorbol ester-stimulated human polymorphonuclear leukocytes: possible link between inflammation and cancer. Proc Natl Acad Sci U S A 1985;82:5194-5198
90. London SJ, Lehman TA, Taylor JA: Myeloperoxidase genetic polymorphism and lung cancer risk. Cancer Res 1997;57:5001-5003
91. Cullen P, Schulte H, Assmann G: Smoking, lipoproteins and coronary heart disease risk. Data from the Munster Heart Study (PROCAM). Eur Heart J 1998;19:1632-1641
92. Chiolero A, Faeh D, Paccaud F, Cornuz J: Consequences of smoking for body weight, body fat distribution, and insulin resistance. Am J Clin Nutr 2008;87:801-809
93. Facchini FS, Hollenbeck CB, Jeppesen J, Chen YD, Reaven GM: Insulin resistance and cigarette smoking. Lancet 1992;339:1128-1130
94. Pham CT: Neutrophil serine proteases: specific regulators of inflammation. Nat Rev Immunol 2006;6:541-550
95. Korkmaz B, Horwitz MS, Jenne DE, Gauthier F: Neutrophil elastase, proteinase 3, and cathepsin G as therapeutic targets in human diseases. Pharmacol Rev 2010;62:726-759
96. Russell RE, Thorley A, Culpitt SV, Dodd S, Donnelly LE, Demattos C, Fitzgerald M, Barnes PJ: Alveolar macrophage-mediated elastolysis: roles of matrix metalloproteinases, cysteine, and serine proteases. Am J Physiol Lung Cell Mol Physiol 2002;283:L867-873
97. Huntington JA, Read RJ, Carrell RW: Structure of a serpin-protease complex shows inhibition by deformation. Nature 2000;407:923-926
98. Abboud RT, Vimalanathan S: Pathogenesis of COPD. Part I. The role of protease-antiprotease imbalance in emphysema. Int J Tuberc Lung Dis 2008;12:361-367
99. Stockley RA: Neutrophils and protease/antiprotease imbalance. Am J Respir Crit Care Med 1999;160:S49-52
100. Wallaert B, Gressier B, Marquette CH, Gosset P, Remy-Jardin M, Mizon J, Tonnel AB: Inactivation of alpha 1-proteinase inhibitor by alveolar inflammatory cells from smoking patients with or without emphysema. Am Rev Respir Dis 1993;147:1537-1543
101. Hubbard RC, Ogushi F, Fells GA, Cantin AM, Jallat S, Courtney M, Crystal RG: Oxidants spontaneously released by alveolar macrophages of cigarette smokers can inactivate the active site of alpha 1-antitrypsin, rendering it ineffective as an inhibitor of neutrophil elastase. J Clin Invest 1987;80:1289-1295
102. Sohrab S, Petrusca DN, Lockett AD, Schweitzer KS, Rush NI, Gu Y, Kamocki K, Garrison J, Petrache I: Mechanism of alpha-1 antitrypsin endocytosis by lung endothelium. Faseb j 2009;23:3149-3158

103. Eriksson S, Alm R, Astedt B: Organ cultures of human fetal hepatocytes in the study of extra-and intracellular alpha1-antitrypsin. Biochim Biophys Acta 1978;542:496-505
104. Voulgari F, Cummins P, Gardecki TI, Beeching NJ, Stone PC, Stuart J: Serum levels of acute phase and cardiac proteins after myocardial infarction, surgery, and infection. Br Heart J 1982;48:352-356
105. Karlsson H, Leanderson P, Tagesson C, Lindahl M: Lipoproteomics II: mapping of proteins in high-density lipoprotein using two-dimensional gel electrophoresis and mass spectrometry. Proteomics 2005;5:1431-1445
106. Moreno JA, Ortega-Gomez A, Rubio-Navarro A, Louedec L, Ho-Tin-Noe B, Caligiuri G, Nicoletti A, Levoye A, Plantier L, Meilhac O: High Density Lipoproteins potentiate alpha-1 antitrypsin therapy in elastase-induced pulmonary emphysema. Am J Respir Cell Mol Biol 2014;
107. Carrell RW, Lomas DA: Alpha1-antitrypsin deficiency--a model for conformational diseases. N Engl J Med 2002;346:45-53
108. Long GL, Chandra T, Woo SL, Davie EW, Kurachi K: Complete sequence of the cDNA for human alpha 1-antitrypsin and the gene for the S variant. Biochemistry 1984;23:4828-4837
109. Ward HE, Nicholas TE: Alveolar type I and type II cells. Aust N Z J Med 1984;14:731-734
110. Agassandian M, Mallampalli RK: Surfactant phospholipid metabolism. Biochim Biophys Acta 2013;1831:612-625
111. Hass MA, Longmore WJ: Regulation of lung surfactant cholesterol metabolism by serum lipopoteins. Lipids 1980;15:401-406
112. Weaver TE, Na CL, Stahlman M: Biogenesis of lamellar bodies, lysosome-related organelles involved in storage and secretion of pulmonary surfactant. Semin Cell Dev Biol 2002;13:263-270
113. Wright JR: Clearance and recycling of pulmonary surfactant. Am J Physiol 1990;259:L1-12
114. Baldan A, Tarr P, Vales CS, Frank J, Shimotake TK, Hawgood S, Edwards PA: Deletion of the transmembrane transporter ABCG1 results in progressive pulmonary lipidosis. J Biol Chem 2006;281:29401-29410
115. Baldan A, Gomes AV, Ping P, Edwards PA: Loss of ABCG1 results in chronic pulmonary inflammation. J Immunol 2008;180:3560-3568
116. Out R, Hoekstra M, Meurs I, de Vos P, Kuiper J, Van Eck M, Van Berkel TJ: Total body ABCG1 expression protects against early atherosclerotic lesion development in mice. Arterioscler Thromb Vasc Biol 2007;27:594-599
117. Wojcik AJ, Skaflen MD, Srinivasan S, Hedrick CC: A critical role for ABCG1 in macrophage inflammation and lung homeostasis. J Immunol 2008;180:4273-4282
118. Pikaar JC, Voorhout WF, van Golde LM, Verhoef J, Van Strijp JA, van Iwaarden JF: Opsonic activities of surfactant proteins A and D in phagocytosis of gram-negative bacteria by alveolar macrophages. J Infect Dis 1995;172:481-489
119. LeVine AM, Whitsett JA, Gwozdz JA, Richardson TR, Fisher JH, Burhans MS, Korfhagen TR: Distinct effects of surfactant protein A or D deficiency during bacterial infection on the lung. J Immunol 2000;165:3934-3940
120. Suzuki Y, Fujita Y, Kogishi K: Reconstitution of tubular myelin from synthetic lipids and proteins associated with pig pulmonary surfactant. Am Rev Respir Dis 1989;140:75-81
121. Hawgood S, Derrick M, Poulain F: Structure and properties of surfactant protein B. Biochim Biophys Acta 1998;1408:150-160
122. Stahlman MT, Gray MP, Falconieri MW, Whitsett JA, Weaver TE: Lamellar body formation in normal and surfactant protein B-deficient fetal mice. Lab Invest 2000;80:395-403

123. Ryan MA, Qi X, Serrano AG, Ikegami M, Perez-Gil J, Johansson J, Weaver TE: Mapping and analysis of the lytic and fusogenic domains of surfactant protein B. Biochemistry 2005;44:861-872
124. Vorbroker DK, Profitt SA, Nogee LM, Whitsett JA: Aberrant processing of surfactant protein C in hereditary SP-B deficiency. Am J Physiol 1995;268:L647-656
125. Ueno T, Linder S, Na CL, Rice WR, Johansson J, Weaver TE: Processing of pulmonary surfactant protein B by napsin and cathepsin H. J Biol Chem 2004;279:16178-16184
126. Hermans C, Bernard A: Lung epithelium-specific proteins: characteristics and potential applications as markers. Am J Respir Crit Care Med 1999;159:646-678
127. Doyle IR, Bersten AD, Nicholas TE: Surfactant proteins-A and -B are elevated in plasma of patients with acute respiratory failure. Am J Respir Crit Care Med 1997;156:1217-1229
128. Nguyen AB, Rohatgi A, Garcia CK, Ayers CR, Das SR, Lakoski SG, Berry JD, Khera A, McGuire DK, de Lemos JA: Interactions between smoking, pulmonary surfactant protein B, and atherosclerosis in the general population: the Dallas Heart Study. Arterioscler Thromb Vasc Biol 2011;31:2136-2143
129. Rustow B, Haupt R, Stevens PA, Kunze D: Type II pneumocytes secrete vitamin E together with surfactant lipids. Am J Physiol 1993;265:L133-139
130. Kolleck I, Wissel H, Guthmann F, Schlame M, Sinha P, Rustow B: HDL-holoparticle uptake by alveolar type II cells: effect of vitamin E status. Am J Respir Cell Mol Biol 2002;27:57-63
131. Tolle A, Kolleck I, Schlame M, Wauer R, Stevens PA, Rustow B: Effect of hyperoxia on the composition of the alveolar surfactant and the turnover of surfactant phospholipids, cholesterol, plasmalogens and vitamin E. Biochim Biophys Acta 1997;1346:198-204
132. Mehrani H, Ghanei M, Aslani J, Golmanesh L: Bronchoalveolar lavage fluid proteomic patterns of sulfur mustard-exposed patients. Proteomics Clin Appl 2009;3:1191-1200
133. de Torre C, Ying SX, Munson PJ, Meduri GU, Suffredini AF: Proteomic analysis of inflammatory biomarkers in bronchoalveolar lavage. Proteomics 2006;6:3949-3957
134. Forey BA, Fry JS, Lee PN, Thornton AJ, Coombs KJ: The effect of quitting smoking on HDL-cholesterol - a review based on within-subject changes. Biomark Res 2013;1:26
135. Craig WY, Palomaki GE, Haddow JE: Cigarette smoking and serum lipid and lipoprotein concentrations: an analysis of published data. Bmj 1989;298:784-788
136. Scigelova M, Makarov A: Orbitrap mass analyzer--overview and applications in proteomics. Proteomics 2006;6 Suppl 2:16-21
137. Johnson RS, Martin SA, Biemann K, Stults JT, Watson JT: Novel fragmentation process of peptides by collision-induced decomposition in a tandem mass spectrometer: differentiation of leucine and isoleucine. Anal Chem 1987;59:2621-2625
138. Hunt DF, Yates JR, 3rd, Shabanowitz J, Winston S, Hauer CR: Protein sequencing by tandem mass spectrometry. Proc Natl Acad Sci U S A 1986;83:6233-6237
139. Deutsch EW: The PeptideAtlas Project. Methods Mol Biol 2010;604:285-296
140. Fu X, Gharib SA, Green PS, Aitken ML, Frazer DA, Park DR, Vaisar T, Heinecke JW: Spectral index for assessment of differential protein expression in shotgun proteomics. J Proteome Res 2008;7:845-854
141. Eng JK, McCormack AL, Yates JR: An approach to correlate tandem mass spectral data of peptides with amino acid sequences in a protein database. J Am Soc Mass Spectrom 1994;5:976-989

142. Pedrioli PG: Trans-proteomic pipeline: a pipeline for proteomic analysis. Methods Mol Biol 2010;604:213-238
143. Rauch A, Bellew M, Eng J, Fitzgibbon M, Holzman T, Hussey P, Igra M, Maclean B, Lin CW, Detter A, Fang R, Faca V, Gafken P, Zhang H, Whiteaker J, States D, Hanash S, Paulovich A, McIntosh MW: Computational Proteomics Analysis System (CPAS): an extensible, open-source analytic system for evaluating and publishing proteomic data and high throughput biological experiments. J Proteome Res 2006;5:112-121
144. Ma K, Vitek O, Nesvizhskii AI: A statistical model-building perspective to identification of MS/MS spectra with PeptideProphet. BMC Bioinformatics 2012;13 Suppl 16:S1
145. MacLean B, Tomazela DM, Shulman N, Chambers M, Finney GL, Frewen B, Kern R, Tabb DL, Liebler DC, MacCoss MJ: Skyline: an open source document editor for creating and analyzing targeted proteomics experiments. Bioinformatics 2010;26:966-968
146. Wessel D, Flugge UI: A method for the quantitative recovery of protein in dilute solution in the presence of detergents and lipids. Anal Biochem 1984;138:141-143
147. Demacker PN, Vos-Janssen HE, Hijmans AG, van't Laar A, Jansen AP: Measurement of high-density lipoprotein cholesterol in serum: comparison of six isolation methods combined with enzymic cholesterol analysis. Clin Chem 1980;26:1780-1786
148. Vaughan AM, Oram JF: ABCA1 redistributes membrane cholesterol independent of apolipoprotein interactions. J Lipid Res 2003;44:1373-1380
149. Cavigiolio G, Shao B, Geier EG, Ren G, Heinecke JW, Oda MN: The interplay between size, morphology, stability, and functionality of high-density lipoprotein subclasses. Biochemistry 2008;47:4770-4779
150. Hutchins PM, Ronsein GE, Monette JS, Pamir N, Wimberger J, He Y, Anantharamaiah GM, Kim DS, Ranchalis JE, Jarvik GP, Vaisar T, Heinecke JW: Quantification of HDL Particle Concentration by Calibrated Ion Mobility Analysis. Clin Chem 2014;
151. Wojdyr M: Fityk: a general-purpose peak fitting program. *J Appl Cryst* 2010;43:1126-1128
152. Jarvik GP, Rozek LS, Brophy VH, Hatsukami TS, Richter RJ, Schellenberg GD, Furlong CE: Paraoxonase (PON1) phenotype is a better predictor of vascular disease than is PON1(192) or PON1(55) genotype. Arterioscler Thromb Vasc Biol 2000;20:2441-2447
153. Jarvik GP, Hatsukami TS, Carlson C, Richter RJ, Jampsa R, Brophy VH, Margolin S, Rieder M, Nickerson D, Schellenberg GD, Heagerty PJ, Furlong CE: Paraoxonase activity, but not haplotype utilizing the linkage disequilibrium structure, predicts vascular disease. In *Arterioscler Thromb Vasc Biol* United States, 2003, p. 1465-1471
154. Leffondre K, Abrahamowicz M, Siemiatycki J, Rachet B: Modeling smoking history: a comparison of different approaches. Am J Epidemiol 2002;156:813-823
155. Mah E, Pei R, Guo Y, Ballard KD, Barker T, Rogers VE, Parker BA, Taylor AW, Traber MG, Volek JS, Bruno RS: gamma-Tocopherol-rich supplementation additively improves vascular endothelial function during smoking cessation. Free Radic Biol Med 2013;65:1291-1299
156. Yang M, Koga M, Katoh T, Kawamoto T: A study for the proper application of urinary naphthols, new biomarkers for airborne polycyclic aromatic hydrocarbons. Arch Environ Contam Toxicol 1999;36:99-108
157. Wickham H: *ggplot2: elegant graphics for data analysis*. Springer New York, 2009
158. Hovingh GK, Hutten BA, Holleboom AG, Petersen W, Rol P, Stalenhoef A, Zwinderman AH, de Groot E, Kastelein JJ, Kuivenhoven JA: Compromised LCAT function is associated with increased atherosclerosis. Circulation 2005;112:879-884

159. Ayyobi AF, McGladdery SH, Chan S, John Mancini GB, Hill JS, Frohlich JJ: Lecithin: cholesterol acyltransferase (LCAT) deficiency and risk of vascular disease: 25 year follow-up. Atherosclerosis 2004;177:361-366
160. Calabresi L, Baldassarre D, Castelnuovo S, Conca P, Bocchi L, Candini C, Frigerio B, Amato M, Sirtori CR, Alessandrini P, Arca M, Boscutti G, Cattin L, Gesualdo L, Sampietro T, Vaudo G, Veglia F, Calandra S, Franceschini G: Functional lecithin: cholesterol acyltransferase is not required for efficient atheroprotection in humans. Circulation 2009;120:628-635
161. Lambert G, Sakai N, Vaisman BL, Neufeld EB, Marteyn B, Chan CC, Paigen B, Lupia E, Thomas A, Striker LJ, Blanchette-Mackie J, Csako G, Brady JN, Costello R, Striker GE, Remaley AT, Brewer HB, Jr., Santamarina-Fojo S: Analysis of glomerulosclerosis and atherosclerosis in lecithin cholesterol acyltransferase-deficient mice. J Biol Chem 2001;276:15090-15098
162. Huuskonen J, Olkkonen VM, Jauhiainen M, Ehnholm C: The impact of phospholipid transfer protein (PLTP) on HDL metabolism. Atherosclerosis 2001;155:269-281
163. Pussinen PJ, Jauhiainen M, Ehnholm C: ApoA-II/apoA-I molar ratio in the HDL particle influences phospholipid transfer protein-mediated HDL interconversion. J Lipid Res 1997;38:12-21
164. Allen SS, Hatsukami D, Gorsline J, Christen A, Rennard S, Heatley S, Fortmann S, Hughes J, Glover E, Repsher L, Lichtenstein E, Rolf CN: Cholesterol changes in smoking cessation using the transdermal nicotine system. Transdermal Nicotine Study Group. Prev Med 1994;23:190-196
165. Morgan PE, Pattison DI, Talib J, Summers FA, Harmer JA, Celermajer DS, Hawkins CL, Davies MJ: High plasma thiocyanate levels in smokers are a key determinant of thiol oxidation induced by myeloperoxidase. Free Radic Biol Med 2011;51:1815-1822
166. Vogt TM, Selvin S, Widdowson G, Hulley SB: Expired air carbon monoxide and serum thiocyanate as objective measures of cigarette exposure. Am J Public Health 1977;67:545-549
167. Hulley S, Ashman P, Kuller L, Lasser N, Sherwin R: HDL-cholesterol levels in the Multiple Risk Factor Intervention Trial (MRFIT) by the MRFIT Research Group 1,2. Lipids 1979;14:119-123
168. van Dalen CJ, Whitehouse MW, Winterbourn CC, Kettle AJ: Thiocyanate and chloride as competing substrates for myeloperoxidase. Biochem J 1997;327 (Pt 2):487-492
169. Furtmuller PG, Burner U, Obinger C: Reaction of myeloperoxidase compound I with chloride, bromide, iodide, and thiocyanate. Biochemistry 1998;37:17923-17930
170. Domigan NM, Charlton TS, Duncan MW, Winterbourn CC, Kettle AJ: Chlorination of tyrosyl residues in peptides by myeloperoxidase and human neutrophils. J Biol Chem 1995;270:16542-16548
171. Tanaka M, Koyama M, Dhanasekaran P, Nguyen D, Nickel M, Lund-Katz S, Saito H, Phillips MC: Influence of tertiary structure domain properties on the functionality of apolipoprotein A-I. Biochemistry 2008;47:2172-2180
172. Kratzer A, Giral H, Landmesser U: High-density lipoproteins as modulators of endothelial cell functions: alterations in patients with coronary artery disease. Cardiovasc Res 2014;103:350-361
173. Navab M, Yu R, Gharavi N, Huang W, Ezra N, Lotfizadeh A, Anantharamaiah GM, Alipour N, Van Lenten BJ, Reddy ST, Marelli D: High-density lipoprotein: antioxidant and anti-inflammatory properties. Curr Atheroscler Rep 2007;9:244-248

174. Podrez EA: Anti-oxidant properties of high-density lipoprotein and atherosclerosis. Clin Exp Pharmacol Physiol 2010;37:719-725
175. Paakko P, Kirby M, du Bois RM, Gillissen A, Ferrans VJ, Crystal RG: Activated neutrophils secrete stored alpha 1-antitrypsin. Am J Respir Crit Care Med 1996;154:1829-1833
176. Ortiz-Munoz G, Houard X, Martin-Ventura JL, Ishida BY, Loyau S, Rossignol P, Moreno JA, Kane JP, Chalkley RJ, Burlingame AL, Michel JB, Meilhac O: HDL antielastase activity prevents smooth muscle cell anoikis, a potential new antiatherogenic property. In *FASEB J*, 2009, p. 3129-3139
177. McCarthy C, Saldova R, Wormald MR, Rudd PM, McElvaney NG, Reeves EP: The role and importance of glycosylation of acute phase proteins with focus on alpha-1 antitrypsin in acute and chronic inflammatory conditions. J Proteome Res 2014;13:3131-3143
178. Holzer M, Trieb M, Konya V, Wadsack C, Heinemann A, Marsche G: Aging affects high-density lipoprotein composition and function. Biochim Biophys Acta 2013;1831:1442-1448
179. Gepner AD, Piper ME, Johnson HM, Fiore MC, Baker TB, Stein JH: Effects of smoking and smoking cessation on lipids and lipoproteins: outcomes from a randomized clinical trial. Am Heart J 2011;161:145-151

Appendix: Transitions Used For Exploratory Proteomics Analysis

precursor m/z	product m/z	peptide	protein	ion	charge	Modification
618.35	736.42	DLATVYVDVLK	apoA-I	y6	2+	n/a
618.35	835.49	DLATVYVDVLK	apoA-I	y7	2+	n/a
618.35	936.54	DLATVYVDVLK	apoA-I	y8	2+	n/a
618.35	1007.58	DLATVYVDVLK	apoA-I	y9	2+	n/a
618.35	762.4	DLATVYVDVLK	apoA-I	b7	2+	n/a
618.35	877.43	DLATVYVDVLK	apoA-I	b8	2+	n/a
624.33	743.4	DLATVYVDVLK	15N apoA-I	y6	2+	n/a
624.33	843.47	DLATVYVDVLK	15N apoA-I	y7	2+	n/a
624.33	945.51	DLATVYVDVLK	15N apoA-I	y8	2+	n/a
624.33	1017.55	DLATVYVDVLK	15N apoA-I	y9	2+	n/a
624.33	769.38	DLATVYVDVLK	15N apoA-I	b7	2+	n/a
624.33	885.41	DLATVYVDVLK	15N apoA-I	b8	2+	n/a
635.35	770.42	DLATVYVDVLK	apoA-I	y6	2+	Y+34
635.35	869.49	DLATVYVDVLK	apoA-I	y7	2+	Y+34
635.35	970.54	DLATVYVDVLK	apoA-I	y8	2+	Y+34
635.35	1041.58	DLATVYVDVLK	apoA-I	y9	2+	Y+34
635.35	796.36	DLATVYVDVLK	apoA-I	b7	2+	Y+34
635.35	911.39	DLATVYVDVLK	apoA-I	b8	2+	Y+34
640.85	781.42	DLATVYVDVLK	apoA-I	y6	2+	Y+45
640.85	880.49	DLATVYVDVLK	apoA-I	y7	2+	Y+45
640.85	981.54	DLATVYVDVLK	apoA-I	y8	2+	Y+45
640.85	1052.58	DLATVYVDVLK	apoA-I	y9	2+	Y+45
640.85	807.39	DLATVYVDVLK	apoA-I	b7	2+	Y+45
640.85	922.42	DLATVYVDVLK	apoA-I	b8	2+	Y+45
641.31	777.36	DLATVYVDVLK	15N apoA-I	y6	2+	Y+34
641.31	877.43	DLATVYVDVLK	15N apoA-I	y7	2+	Y+34
641.31	979.47	DLATVYVDVLK	15N apoA-I	y8	2+	Y+34
641.31	1051.51	DLATVYVDVLK	15N apoA-I	y9	2+	Y+34
641.31	803.34	DLATVYVDVLK	15N apoA-I	b7	2+	Y+34
641.31	919.37	DLATVYVDVLK	15N apoA-I	b8	2+	Y+34
646.82	788.39	DLATVYVDVLK	15N apoA-I	y6	2+	Y+45
646.82	888.45	DLATVYVDVLK	15N apoA-I	y7	2+	Y+45
646.82	990.5	DLATVYVDVLK	15N apoA-I	y8	2+	Y+45
646.82	1062.53	DLATVYVDVLK	15N apoA-I	y9	2+	Y+45
646.82	814.37	DLATVYVDVLK	15N apoA-I	b7	2+	Y+45
646.82	930.39	DLATVYVDVLK	15N apoA-I	b8	2+	Y+45
700.84	661.35	DYVSQFEGSALGK	apoA-I	y7	2+	n/a
700.84	808.42	DYVSQFEGSALGK	apoA-I	y8	2+	n/a
700.84	1023.51	DYVSQFEGSALGK	apoA-I	y10	2+	n/a
700.84	1122.58	DYVSQFEGSALGK	apoA-I	y11	2+	n/a
708.32	669.33	DYVSQFEGSALGK	15N apoA-I	y7	2+	n/a
708.32	817.39	DYVSQFEGSALGK	15N apoA-I	y8	2+	n/a
708.32	1035.48	DYVSQFEGSALGK	15N apoA-I	y10	2+	n/a

708.32	1135.54	DYVSQFEGSALGK	15N apoA-I	y11	2+	n/a
717.84	661.35	DYVSQFEGSALGK	apoA-I	y7	2+	Y+34
717.84	808.42	DYVSQFEGSALGK	apoA-I	y8	2+	Y+34
717.84	1023.51	DYVSQFEGSALGK	apoA-I	y10	2+	Y+34
717.84	1122.58	DYVSQFEGSALGK	apoA-I	y11	2+	Y+34
725.3	669.33	DYVSQFEGSALGK	15N apoA-I	y7	2+	Y+34
725.3	817.39	DYVSQFEGSALGK	15N apoA-I	y8	2+	Y+34
725.3	1035.48	DYVSQFEGSALGK	15N apoA-I	y10	2+	Y+34
725.3	1135.54	DYVSQFEGSALGK	15N apoA-I	y11	2+	Y+34
723.34	661.35	DYVSQFEGSALGK	apoA-I	y7	2+	Y+45
723.34	808.42	DYVSQFEGSALGK	apoA-I	y8	2+	Y+45
723.34	1023.51	DYVSQFEGSALGK	apoA-I	y10	2+	Y+45
723.34	1122.58	DYVSQFEGSALGK	apoA-I	y11	2+	Y+45
730.81	669.33	DYVSQFEGSALGK	15N apoA-I	y7	2+	Y+45
730.81	817.39	DYVSQFEGSALGK	15N apoA-I	y8	2+	Y+45
730.81	1035.48	DYVSQFEGSALGK	15N apoA-I	y10	2+	Y+45
730.81	1135.54	DYVSQFEGSALGK	15N apoA-I	y11	2+	Y+45
626.81	513.25	VQPYLDDFQK	apoA-I	y8 (2+)	2+	n/a
626.81	765.38	VQPYLDDFQK	apoA-I	y6	2+	n/a
626.81	928.44	VQPYLDDFQK	apoA-I	y7	2+	n/a
626.81	1025.49	VQPYLDDFQK	apoA-I	y8	2+	n/a
633.29	518.24	VQPYLDDFQK	15N apoA-I	y8 (2+)	2+	n/a
633.29	773.35	VQPYLDDFQK	15N apoA-I	y6	2+	n/a
633.29	937.41	VQPYLDDFQK	15N apoA-I	y7	2+	n/a
633.29	1035.46	VQPYLDDFQK	15N apoA-I	y8	2+	n/a
643.81	530.25	VQPYLDDFQK	apoA-I	y8 (2+)	2+	Y+34
643.81	765.38	VQPYLDDFQK	apoA-I	y6	2+	Y+34
643.81	962.44	VQPYLDDFQK	apoA-I	y7	2+	Y+34
643.81	1059.49	VQPYLDDFQK	apoA-I	y8	2+	Y+34
650.28	535.22	VQPYLDDFQK	15N apoA-I	y8 (2+)	2+	Y+34
650.28	773.35	VQPYLDDFQK	15N apoA-I	y6	2+	Y+34
650.28	971.38	VQPYLDDFQK	15N apoA-I	y7	2+	Y+34
650.28	1069.43	VQPYLDDFQK	15N apoA-I	y8	2+	Y+34
649.31	535.75	VQPYLDDFQK	apoA-I	y8 (2+)	2+	Y+45
649.31	765.38	VQPYLDDFQK	apoA-I	y6	2+	Y+45
649.31	973.44	VQPYLDDFQK	apoA-I	y7	2+	Y+45
649.31	1070.49	VQPYLDDFQK	apoA-I	y8	2+	Y+45
655.79	540.73	VQPYLDDFQK	15N apoA-I	y8 (2+)	2+	Y+45
655.79	773.35	VQPYLDDFQK	15N apoA-I	y6	2+	Y+45
655.79	982.4	VQPYLDDFQK	15N apoA-I	y7	2+	Y+45
655.79	1080.45	VQPYLDDFQK	15N apoA-I	y8	2+	Y+45
651.33	239.11	THLAPYSDELR	apoA-I	b2	2+	n/a
651.33	352.2	THLAPYSDELR	apoA-I	b3	2+	n/a
651.33	423.24	THLAPYSDELR	apoA-I	b4	2+	n/a
651.33	879.42	THLAPYSDELR	apoA-I	y7	2+	n/a
651.33	950.46	THLAPYSDELR	apoA-I	y8	2+	n/a
651.33	1063.54	THLAPYSDELR	apoA-I	y9	2+	n/a
659.3	243.1	THLAPYSDELR	15N apoA-I	b2	2+	n/a
659.3	357.18	THLAPYSDELR	15N apoA-I	b3	2+	n/a

659.3	429.22	THLAPYSDELR	15N apoA-I	b4	2+	n/a
659.3	889.39	THLAPYSDELR	15N apoA-I	y7	2+	n/a
659.3	961.43	THLAPYSDELR	15N apoA-I	y8	2+	n/a
659.3	1075.51	THLAPYSDELR	15N apoA-I	y9	2+	n/a
668.31	239.11	THLAPYSDELR	apoA-I	b2	2+	Y+34
668.31	352.2	THLAPYSDELR	apoA-I	b3	2+	Y+34
668.31	423.24	THLAPYSDELR	apoA-I	b4	2+	Y+34
668.31	913.38	THLAPYSDELR	apoA-I	y7	2+	Y+34
668.31	984.42	THLAPYSDELR	apoA-I	y8	2+	Y+34
668.31	1097.5	THLAPYSDELR	apoA-I	y9	2+	Y+34
676.28	243.1	THLAPYSDELR	15N apoA-I	b2	2+	Y+34
676.28	357.18	THLAPYSDELR	15N apoA-I	b3	2+	Y+34
676.28	429.22	THLAPYSDELR	15N apoA-I	b4	2+	Y+34
676.28	923.35	THLAPYSDELR	15N apoA-I	y7	2+	Y+34
676.28	995.39	THLAPYSDELR	15N apoA-I	y8	2+	Y+34
676.28	1109.47	THLAPYSDELR	15N apoA-I	y9	2+	Y+34
673.82	239.11	THLAPYSDELR	apoA-I	b2	2+	Y+45
673.82	352.2	THLAPYSDELR	apoA-I	b3	2+	Y+45
673.82	423.24	THLAPYSDELR	apoA-I	b4	2+	Y+45
673.82	924.41	THLAPYSDELR	apoA-I	y7	2+	Y+45
673.82	995.44	THLAPYSDELR	apoA-I	y8	2+	Y+45
673.82	1108.53	THLAPYSDELR	apoA-I	y9	2+	Y+45
681.8	243.1	THLAPYSDELR	15N apoA-I	b2	2+	Y+45
681.8	357.18	THLAPYSDELR	15N apoA-I	b3	2+	Y+45
681.8	429.22	THLAPYSDELR	15N apoA-I	b4	2+	Y+45
681.8	934.38	THLAPYSDELR	15N apoA-I	y7	2+	Y+45
681.8	1006.41	THLAPYSDELR	15N apoA-I	y8	2+	Y+45
681.8	1120.49	THLAPYSDELR	15N apoA-I	y9	2+	Y+45
416.22	185.13	LAEYHAK	apoA-I	b2	2+	n/a
416.22	218.15	LAEYHAK	apoA-I	y2	2+	n/a
416.22	355.21	LAEYHAK	apoA-I	y3	2+	n/a
416.22	518.27	LAEYHAK	apoA-I	y4	2+	n/a
416.22	647.31	LAEYHAK	apoA-I	y5	2+	n/a
416.22	718.35	LAEYHAK	apoA-I	y6	2+	n/a
421.22	187.13	LAEYHAK	15N apoA-I	b2	2+	n/a
421.22	221.15	LAEYHAK	15N apoA-I	y2	2+	n/a
421.22	361.21	LAEYHAK	15N apoA-I	y3	2+	n/a
421.22	525.27	LAEYHAK	15N apoA-I	y4	2+	n/a
421.22	655.31	LAEYHAK	15N apoA-I	y5	2+	n/a
421.22	727.35	LAEYHAK	15N apoA-I	y6	2+	n/a
433.22	185.13	LAEYHAK	apoA-I	b2	2+	Y+34
433.22	218.15	LAEYHAK	apoA-I	y2	2+	Y+34
433.22	355.21	LAEYHAK	apoA-I	y3	2+	Y+34
433.22	552.27	LAEYHAK	apoA-I	y4	2+	Y+34
433.22	681.31	LAEYHAK	apoA-I	y5	2+	Y+34
433.22	752.35	LAEYHAK	apoA-I	y6	2+	Y+34
438.22	187.13	LAEYHAK	15N apoA-I	b2	2+	Y+34
438.22	221.15	LAEYHAK	15N apoA-I	y2	2+	Y+34
438.22	361.21	LAEYHAK	15N apoA-I	y3	2+	Y+34

438.22	559.27	LAEYHAK	15N apoA-I	y4	2+	Y+34
438.22	689.31	LAEYHAK	15N apoA-I	y5	2+	Y+34
438.22	761.35	LAEYHAK	15N apoA-I	y6	2+	Y+34
438.72	185.13	LAEYHAK	apoA-I	b2	2+	Y+45
438.72	218.15	LAEYHAK	apoA-I	y2	2+	Y+45
438.72	355.21	LAEYHAK	apoA-I	y3	2+	Y+45
438.72	563.27	LAEYHAK	apoA-I	y4	2+	Y+45
438.72	692.31	LAEYHAK	apoA-I	y5	2+	Y+45
438.72	763.35	LAEYHAK	apoA-I	y6	2+	Y+45
443.72	187.13	LAEYHAK	15N apoA-I	b2	2+	Y+45
443.72	221.15	LAEYHAK	15N apoA-I	y2	2+	Y+45
443.72	361.21	LAEYHAK	15N apoA-I	y3	2+	Y+45
443.72	570.27	LAEYHAK	15N apoA-I	y4	2+	Y+45
443.72	700.31	LAEYHAK	15N apoA-I	y5	2+	Y+45
443.72	772.35	LAEYHAK	15N apoA-I	y6	2+	Y+45
693.86	782.39	VSFLSALEEYTK	apoA-I	y6	2+	n/a
693.86	853.43	VSFLSALEEYTK	apoA-I	y7	2+	n/a
693.86	940.46	VSFLSALEEYTK	apoA-I	y8	2+	n/a
693.86	1053.55	VSFLSALEEYTK	apoA-I	y9	2+	n/a
700.34	789.37	VSFLSALEEYTK	15N apoA-I	y6	2+	n/a
700.34	861.41	VSFLSALEEYTK	15N apoA-I	y7	2+	n/a
700.34	949.44	VSFLSALEEYTK	15N apoA-I	y8	2+	n/a
700.34	1063.52	VSFLSALEEYTK	15N apoA-I	y9	2+	n/a
710.84	816.35	VSFLSALEEYTK	apoA-I	y6	2+	Y+34
710.84	887.39	VSFLSALEEYTK	apoA-I	y7	2+	Y+34
710.84	974.42	VSFLSALEEYTK	apoA-I	y8	2+	Y+34
710.84	1087.51	VSFLSALEEYTK	apoA-I	y9	2+	Y+34
717.32	823.33	VSFLSALEEYTK	15N apoA-I	y6	2+	Y+34
717.32	895.37	VSFLSALEEYTK	15N apoA-I	y7	2+	Y+34
717.32	983.4	VSFLSALEEYTK	15N apoA-I	y8	2+	Y+34
717.32	1097.48	VSFLSALEEYTK	15N apoA-I	y9	2+	Y+34
716.35	827.38	VSFLSALEEYTK	apoA-I	y6	2+	Y+45
716.35	898.42	VSFLSALEEYTK	apoA-I	y7	2+	Y+45
716.35	985.45	VSFLSALEEYTK	apoA-I	y8	2+	Y+45
716.35	1098.53	VSFLSALEEYTK	apoA-I	y9	2+	Y+45
722.83	834.36	VSFLSALEEYTK	15N apoA-I	y6	2+	Y+45
722.83	906.39	VSFLSALEEYTK	15N apoA-I	y7	2+	Y+45
722.83	994.42	VSFLSALEEYTK	15N apoA-I	y8	2+	Y+45
722.83	1108.5	VSFLSALEEYTK	15N apoA-I	y9	2+	Y+45
642.29	580.31	WQEEMELYR	apoA-I	y4	2+	n/a
642.29	711.35	WQEEMELYR	apoA-I	y5	2+	n/a
642.29	840.39	WQEEMELYR	apoA-I	y6	2+	n/a
642.29	969.43	WQEEMELYR	apoA-I	y7	2+	n/a
649.27	587.29	WQEEMELYR	15N apoA-I	y4	2+	n/a
649.27	719.33	WQEEMELYR	15N apoA-I	y5	2+	n/a
649.27	849.37	WQEEMELYR	15N apoA-I	y6	2+	n/a
649.27	979.41	WQEEMELYR	15N apoA-I	y7	2+	n/a
650.29	580.31	WQEEMELYR	apoA-I	y4	2+	W+16, M+16
650.29	711.35	WQEEMELYR	apoA-I	y5	2+	W+16

650.29	727.34	WQEEMELYR	apoA-I	y5	2+	M+16
650.29	840.39	WQEEMELYR	apoA-I	y6	2+	W+16
650.29	856.39	WQEEMELYR	apoA-I	y6	2+	M+16
650.29	969.43	WQEEMELYR	apoA-I	y7	2+	W+16
650.29	985.43	WQEEMELYR	apoa-I	y7	2+	M+16
657.29	587.29	WQEEMELYR	15N apoA-I	y4	2+	W+16, M+16
657.29	719.33	WQEEMELYR	15N apoA-I	y5	2+	W+16
657.29	735.32	WQEEMELYR	15N apoA-I	y5	2+	M+16
657.29	849.37	WQEEMELYR	15N apoA-I	y6	2+	W+16
657.29	865.36	WQEEMELYR	15N apoA-I	y6	2+	M+16
657.29	979.41	WQEEMELYR	15N apoA-I	y7	2+	W+16
657.29	995.4	WQEEMELYR	15N apoA-I	y7	2+	M+16
664.78	625.29	WQEEMELYR	apoA-I	y4	2+	Y+45
664.78	756.33	WQEEMELYR	apoA-I	y5	2+	Y+45
664.78	885.38	WQEEMELYR	apoA-I	y6	2+	Y+45
664.78	1014.42	WQEEMELYR	apoA-I	y7	2+	Y+45
671.76	632.27	WQEEMELYR	15N apoA-I	y4	2+	Y+45
671.76	764.31	WQEEMELYR	15N apoA-I	y5	2+	Y+45
671.76	894.35	WQEEMELYR	15N apoA-I	y6	2+	Y+45
671.76	1024.39	WQEEMELYR	15N apoA-I	y7	2+	Y+45
516.26	416.21	LSPLGEEMR	apoA-I	y7 (2+)	2+	n/a
516.26	621.27	LSPLGEEMR	apoA-I	y5	2+	n/a
516.26	734.35	LSPLGEEMR	apoA-I	y6	2+	n/a
516.26	831.4	LSPLGEEMR	apoA-I	y7	2+	n/a
522.25	421.19	LSPLGEEMR	15N apoA-I	y7 (2+)	2+	n/a
522.25	629.24	LSPLGEEMR	15N apoA-I	y5	2+	n/a
522.25	743.32	LSPLGEEMR	15N apoA-I	y6	2+	n/a
522.25	841.37	LSPLGEEMR	15N apoA-I	y7	2+	n/a
524.26	424.2	LSPLGEEMR	apoA-I	y7 (2+)	2+	M+16
524.26	637.26	LSPLGEEMR	apoA-I	y5	2+	M+16
524.26	750.35	LSPLGEEMR	apoA-I	y6	2+	M+16
524.26	847.4	LSPLGEEMR	apoA-I	y7	2+	M+16
530.24	429.19	LSPLGEEMR	15N apoA-I	y7 (2+)	2+	M+16
530.24	645.24	LSPLGEEMR	15N apoA-I	y5	2+	M+16
530.24	759.32	LSPLGEEMR	15N apoA-I	y6	2+	M+16
530.24	857.37	LSPLGEEMR	15N apoA-I	y7	2+	M+16
960.48	1474.79	GECVPGEQEPEPILIPR	AMBP	y13	2+	n/a
960.48	737.9	GECVPGEQEPEPILIPR	AMBP	y13 (2+)	2+	n/a
960.48	934.57	GECVPGEQEPEPILIPR	AMBP	y8	2+	n/a
960.48	1063.61	GECVPGEQEPEPILIPR	AMBP	y9	2+	n/a
855.14	1132.58	WYNLAIGSTCPWLK	AMBP	y10	2+	n/a
855.14	543.33	WYNLAIGSTCPWLK	AMBP	y4	2+	n/a
855.14	948.46	WYNLAIGSTCPWLK	AMBP	y8	2+	n/a
855.14	1061.54	WYNLAIGSTCPWLK	AMBP	y9	2+	n/a
1175.55	1436.67	EPCVESLVSQYFQTVTDYGK	apoA-II	y12	2+	n/a
1175.55	583.27	EPCVESLVSQYFQTVTDYGK	apoA-II	y5	2+	n/a
1175.55	783.39	EPCVESLVSQYFQTVTDYGK	apoA-II	y7	2+	n/a
486.75	659.37	SPELQAEAK	apoA-II	y6	2+	n/a

486.75	788.41	SPELQAEAK	apoA-II	y7	2+	n/a
486.75	443.24	SPELQAEAK	apoA-II	y8 (2+)	2+	n/a
488.26	617.33	ISASAEELR	apoA-IV	y5	2+	n/a
488.26	704.36	ISASAEELR	apoA-IV	y6	2+	n/a
488.26	775.39	ISASAEELR	apoA-IV	y7	2+	n/a
704.36	631.34	LGEVNTYAGDLQK	apoA-IV	y6	2+	n/a
704.36	794.4	LGEVNTYAGDLQK	apoA-IV	y7	2+	n/a
704.36	1009.49	LGEVNTYAGDLQK	apoA-IV	y9	2+	n/a
817.92	537.27	SELTQQLNALFQDK	apoA-IV	y4	2+	n/a
817.92	835.43	SELTQQLNALFQDK	apoA-IV	y7	2+	n/a
817.92	948.51	SELTQQLNALFQDK	apoA-IV	y8	2+	n/a
601.28	523.29	EWFSETFQK	apoC-I	y4	2+	n/a
601.28	652.33	EWFSETFQK	apoC-I	y5	2+	n/a
601.28	739.36	EWFSETFQK	apoC-I	y6	2+	n/a
601.28	886.43	EWFSETFQK	apoC-I	y7	2+	n/a
643.8	620.3	ESLSSYWESAK	apoC-II	y5	2+	n/a
643.8	870.4	ESLSSYWESAK	apoC-II	y7	2+	n/a
643.8	957.43	ESLSSYWESAK	apoC-II	y8	2+	n/a
518.27	265.12	TYLPAVDEK	apoC-II	b2	2+	n/a
518.27	658.34	TYLPAVDEK	apoC-II	y6	2+	n/a
518.27	771.42	TYLPAVDEK	apoC-II	y7	2+	n/a
858.93	1144.55	DALSSVQESQVAQQAR	apoC-III	y10	2+	n/a
858.93	502.27	DALSSVQESQVAQQAR	apoC-III	y4	2+	n/a
858.93	887.47	DALSSVQESQVAQQAR	apoC-III	y8	2+	n/a
598.8	753.38	GWVTDGFSSLK	apoC-III	y7	2+	n/a
598.8	854.43	GWVTDGFSSLK	apoC-III	y8	2+	n/a
598.8	953.49	GWVTDGFSSLK	apoC-III	y9	2+	n/a
850.39	607.32	DGWQWFWSPSTFR	apoC-IV	y5	2+	n/a
850.39	694.35	DGWQWFWSPSTFR	apoC-IV	y6	2+	n/a
850.39	880.43	DGWQWFWSPSTFR	apoC-IV	y7	2+	n/a
850.39	1027.5	DGWQWFWSPSTFR	apoC-IV	y8	2+	n/a
536.8	289.16	ELLETVVNR	apoC-IV	y2	2+	n/a
536.8	388.23	ELLETVVNR	apoC-IV	y3	2+	n/a
536.8	588.35	ELLETVVNR	apoC-IV	y5	2+	n/a
536.8	717.39	ELLETVVNR	apoC-IV	y6	2+	n/a
646.8	518.24	MTVTDQVNCPK	apoD	y4	2+	n/a
646.8	860.39	MTVTDQVNCPK	apoD	y7	2+	n/a
646.8	961.44	MTVTDQVNCPK	apoD	y8	2+	n/a
712.38	439.23	NPNLPPETVDSLK	apoD	b4	2+	n/a
712.38	985.52	NPNLPPETVDSLK	apoD	y9	2+	n/a
712.38	493.26	NPNLPPETVDSLK	apoD	y9 (2+)	2+	n/a
824.4	1163.57	GEVQAMLGQSTEELR	apoE	y10	2+	n/a
824.4	919.45	GEVQAMLGQSTEELR	apoE	y8	2+	n/a
824.4	1032.53	GEVQAMLGQSTEELR	apoE	y9	2+	n/a
810.9	1152.53	VQAAVGTSAAPVPSDNH	apoE	y12	2+	n/a
810.9	569.23	VQAAVGTSAAPVPSDNH	apoE	y5	2+	n/a
810.9	765.35	VQAAVGTSAAPVPSDNH	apoE	y7	2+	n/a
849.43	726.41	SGVQQLIQYYQDQK	apoF	b7	2+	n/a
849.43	681.32	SGVQQLIQYYQDQK	apoF	y5	2+	n/a

849.43	972.44	SGVQQLIQYYQDQK	apoF	y7	2+	n/a
849.43	1085.53	SGVQQLIQYYQDQK	apoF	y8	2+	n/a
668.82	479.21	SYDLDPGAGSLEI	apoF	b4	2+	n/a
668.82	594.24	SYDLDPGAGSLEI	apoF	b5	2+	n/a
668.82	743.39	SYDLDPGAGSLEI	apoF	y8	2+	n/a
668.82	858.42	SYDLDPGAGSLEI	apoF	y9	2+	n/a
796	1324.53	ATFGCHDGYSLDGPEEIECT K	apoH	b12	3+	n/a
796	662.77	ATFGCHDGYSLDGPEEIECT K	apoH	b12 (2+)	3+	n/a
796	1005.46	ATFGCHDGYSLDGPEEIECT K	apoH	y8	3+	n/a
796	1062.48	ATFGCHDGYSLDGPEEIECT K	apoH	y9	3+	n/a
886.99	1352.79	FICPLTGLWPINTLK	apoH	y12	2+	n/a
886.99	685.42	FICPLTGLWPINTLK	apoH	y6	2+	n/a
886.99	871.5	FICPLTGLWPINTLK	apoH	y7	2+	n/a
886.99	1041.61	FICPLTGLWPINTLK	apoH	y9	2+	n/a
1244.13	1136.61	EFLGENISNFLSLAGNTYQLT R	apoL-I	y10	2+	n/a
1244.13	1223.64	EFLGENISNFLSLAGNTYQLT R	apoL-I	y11	2+	n/a
1244.13	952.48	EFLGENISNFLSLAGNTYQLT R	apoL-I	y8	2+	n/a
1244.13	1023.52	EFLGENISNFLSLAGNTYQLT R	apoL-I	y9	2+	n/a
815.9	1091.5	VTEPISAESGEQVER	apoL-I	y10	2+	n/a
815.9	1301.63	VTEPISAESGEQVER	apoL-I	y12	2+	n/a
815.9	651.32	VTEPISAESGEQVER	apoL-I	y12 (2+)	2+	n/a
815.9	933.43	VTEPISAESGEQVER	apoL-I	y8	2+	n/a
589.74	845.35	NQEACELSNN	apoM	b7	2+	n/a
589.74	334.14	NQEACELSNN	apoM	y3	2+	n/a
589.74	447.22	NQEACELSNN	apoM	y4	2+	n/a
795.9	648.33	WIYHLTEGSTDLR	apoM	y6	2+	n/a
795.9	878.42	WIYHLTEGSTDLR	apoM	y8	2+	n/a
795.9	991.51	WIYHLTEGSTDLR	apoM	y9	2+	n/a
852.3	989.98	SNFLNCYVSGFHPSDIEVDLL K	B2M	y17 (2+)	2+	n/a
852.3	1047	SNFLNCYVSGFHPSDIEVDLL K	B2M	y18 (2+)	2+	n/a
852.3	1103.55	SNFLNCYVSGFHPSDIEVDLL K	B2M	y19 (2+)	2+	n/a
852.3	1177.08	SNFLNCYVSGFHPSDIEVDLL K	B2M	y20 (2+)	2+	n/a
574.78	696.36	VEHSDLSFSK	B2M	y6	2+	n/a
574.78	783.39	VEHSDLSFSK	B2M	y7	2+	n/a
574.78	920.45	VEHSDLSFSK	B2M	y8	2+	n/a
574.78	460.73	VEHSDLSFSK	B2M	y8 (2+)	2+	n/a
531.75	763.34	ADIGCTPGSGK	C3	y8	2+	n/a
531.75	438.72	ADIGCTPGSGK	C3	y9 (2+)	2+	n/a
531.75	445.24	ADIGCTPGSGK	C3	y5	2+	n/a
531.75	546.29	ADIGCTPGSGK	C3	y9	2+	n/a

939.99	687.86	EYVLPSFEVIVEPTEK	C3	y12 (2+)	2+	n/a
939.99	744.4	EYVLPSFEVIVEPTEK	C3	y13 (2+)	2+	n/a
939.99	815.45	EYVLPSFEVIVEPTEK	C3	y7	2+	n/a
939.99	1374.72	EYVLPSFEVIVEPTEK	C3	y12	2+	n/a
998.42	1263.52	WTPYQGCEALCCPEPK	C4BPA	y10	2+	n/a
998.42	1320.54	WTPYQGCEALCCPEPK	C4BPA	y11	2+	n/a
998.42	1448.6	WTPYQGCEALCCPEPK	C4BPA	y12	2+	n/a
998.42	854.86	WTPYQGCEALCCPEPK	C4BPA	y14 (2+)	2+	n/a
735.91	416.26	LSLEIEQLELQR	C4BPA	y3	2+	n/a
735.91	545.3	LSLEIEQLELQR	C4BPA	y4	2+	n/a
735.91	915.49	LSLEIEQLELQR	C4BPA	y7	2+	n/a
735.91	1028.57	LSLEIEQLELQR	C4BPA	y8	2+	n/a
937.5	1296.75	LFDSDPITVTVPVEVSR	Clusterin	y12	2+	n/a
937.5	686.38	LFDSDPITVTVPVEVSR	Clusterin	y6	2+	n/a
937.5	785.45	LFDSDPITVTVPVEVSR	Clusterin	y7	2+	n/a
937.5	886.5	LFDSDPITVTVPVEVSR	Clusterin	y8	2+	n/a
772.06	1300.6	VTTVASHTSDSDVPSGVTEVVVK	Clusterin	b13	3+	n/a
772.06	1014.58	VTTVASHTSDSDVPSGVTEVVVK	Clusterin	y10	3+	n/a
772.06	507.8	VTTVASHTSDSDVPSGVTEVVVK	Clusterin	y10 (2+)	3+	n/a
772.06	830.5	VTTVASHTSDSDVPSGVTEVVVK	Clusterin	y8	3+	n/a
815.42	1203.68	DSHSLTTNIMEILR	FGA	y10	2+	n/a
815.42	1290.71	DSHSLTTNIMEILR	FGA	y11	2+	n/a
815.42	989.54	DSHSLTTNIMEILR	FGA	y8	2+	n/a
815.42	1090.59	DSHSLTTNIMEILR	FGA	y9	2+	n/a
760.87	652.3	GLIDEVNQDFTNR	FGA	y5	2+	n/a
760.87	780.36	GLIDEVNQDFTNR	FGA	y6	2+	n/a
760.87	894.41	GLIDEVNQDFTNR	FGA	y7	2+	n/a
760.87	993.47	GLIDEVNQDFTNR	FGA	y8	2+	n/a
884.9	1197.56	DNENVVNEYSSELEK	FGB	y10	2+	n/a
884.9	855.41	DNENVVNEYSSELEK	FGB	y7	2+	n/a
884.9	984.45	DNENVVNEYSSELEK	FGB	y8	2+	n/a
884.9	1098.49	DNENVVNEYSSELEK	FGB	y9	2+	n/a
893.4	589.78	NYCGLPGEYWLGNDK	FGB	y10 (2+)	2+	n/a
893.4	608.25	NYCGLPGEYWLGNDK	FGB	b5	2+	n/a
893.4	1178.55	NYCGLPGEYWLGNDK	FGB	y10	2+	n/a
893.4	1348.65	NYCGLPGEYWLGNDK	FGB	y12	2+	n/a
645.87	1062.62	DIAPTLTLYVGK	HP	y10	2+	n/a
645.87	531.81	DIAPTLTLYVGK	HP	y10 (2+)	2+	n/a
645.87	991.58	DIAPTLTLYVGK	HP	y9	2+	n/a
645.87	496.29	DIAPTLTLYVGK	HP	y9 (2+)	2+	n/a
673.3	857.44	SCAVAEYGVYVK	HP	y7	2+	n/a
673.3	928.48	SCAVAEYGVYVK	HP	y8	2+	n/a
673.3	1027.55	SCAVAEYGVYVK	HP	y9	2+	n/a

673.3	1098.58	SCAVAEYGVYVK	HP	y10	2+	n/a
448.24	499.3	NPANPVQR	HPR	y4	2+	n/a
448.24	613.34	NPANPVQR	HPR	y5	2+	n/a
448.24	684.38	NPANPVQR	HPR	y6	2+	n/a
448.24	391.22	NPANPVQR	HPR	y7 (2+)	2+	n/a
772.36	1125.5	VGYVSGWGQSDNFK	HPR	y10	2+	n/a
772.36	610.28	VGYVSGWGQSDNFK	HPR	y5	2+	n/a
772.36	795.36	VGYVSGWGQSDNFK	HPR	y7	2+	n/a
772.36	1038.46	VGYVSGWGQSDNFK	HPR	y9	2+	n/a
1060.49	1078.46	TYIYDHGFPYTDPVGVLYED GDDTVATR	LCAT	y10	3+	n/a
1060.49	1241.53	TYIYDHGFPYTDPVGVLYED GDDTVATR	LCAT	y11	3+	n/a
1060.49	1354.61	TYIYDHGFPYTDPVGVLYED GDDTVATR	LCAT	y12	3+	n/a
1060.49	949.42	TYIYDHGFPYTDPVGVLYED GDDTVATR	LCAT	y9	3+	n/a
646.31	712.35	TYSVEYLDSSK	LCAT	y6	2+	n/a
646.31	841.39	TYSVEYLDSSK	LCAT	y7	2+	n/a
646.31	940.46	TYSVEYLDSSK	LCAT	y8	2+	n/a
646.31	1027.49	TYSVEYLDSSK	LCAT	y9	2+	n/a
749.34	639.31	NPDAVAAPYCYTR	LPA	b7	2+	n/a
749.34	859.38	NPDAVAAPYCYTR	LPA	y6	2+	n/a
749.34	930.41	NPDAVAAPYCYTR	LPA	y7	2+	n/a
749.34	1001.45	NPDAVAAPYCYTR	LPA	y8	2+	n/a
521.76	333.18	GTYSTTVTGR	LPA	y3	2+	n/a
521.76	432.26	GTYSTTVTGR	LPA	y4	2+	n/a
521.76	533.3	GTYSTTVTGR	LPA	y5	2+	n/a
521.76	634.35	GTYSTTVTGR	LPA	y6	2+	n/a
662.34	735.39	ALGFEAAESSLTK	Lplunc1	y7	2+	n/a
662.34	806.43	ALGFEAAESSLTK	Lplunc1	y8	2+	n/a
662.34	935.47	ALGFEAAESSLTK	Lplunc1	y9	2+	n/a
662.34	1139.56	ALGFEAAESSLTK	Lplunc1	y11	2+	n/a
998.54	701.35	DALVLTPASLWKPSSPVSQ	Lplunc1	y7	2+	n/a
998.54	829.44	DALVLTPASLWKPSSPVSQ	Lplunc1	y8	2+	n/a
998.54	1015.52	DALVLTPASLWKPSSPVSQ	Lplunc1	y9	2+	n/a
998.54	1383.73	DALVLTPASLWKPSSPVSQ	Lplunc1	y13	2+	n/a
1056.99	1246.59	EQLGEFYEALDCLCIPR	ORM2	y10	2+	n/a
1056.99	933.43	EQLGEFYEALDCLCIPR	ORM2	y7	2+	n/a
1056.99	1046.51	EQLGEFYEALDCLCIPR	ORM2	y8	2+	n/a
1056.99	1117.55	EQLGEFYEALDCLCIPR	ORM2	y9	2+	n/a
580.8	480.26	WFYIASAFR	ORM2	y4	2+	n/a
580.8	551.29	WFYIASAFR	ORM2	y5	2+	n/a
580.8	664.38	WFYIASAFR	ORM2	y6	2+	n/a
580.8	827.44	WFYIASAFR	ORM2	y7	2+	n/a
883.99	1058.53	IAIIGAGIGGTSAAYYLR	PCYOX1	y10	2+	n/a
883.99	451.27	IAIIGAGIGGTSAAYYLR	PCYOX1	y3	2+	n/a
883.99	614.33	IAIIGAGIGGTSAAYYLR	PCYOX1	y4	2+	n/a
883.99	1001.51	IAIIGAGIGGTSAAYYLR	PCYOX1	y9	2+	n/a
588.33	546.32	LVCSGLLQASK	PCYOX1	y5	2+	n/a

588.33	716.43	LVCSGLLQASK	PCYOX1	y7	2+	n/a
588.33	803.46	LVCSGLLQASK	PCYOX1	y8	2+	n/a
588.33	963.49	LVCSGLLQASK	PCYOX1	y9	2+	n/a
526.62	432.28	AGPHCPTAQLIATLK	PF4V1	y4	3+	n/a
526.62	545.37	AGPHCPTAQLIATLK	PF4V1	y5	3+	n/a
526.62	658.45	AGPHCPTAQLIATLK	PF4V1	y6	3+	n/a
526.62	786.51	AGPHCPTAQLIATLK	PF4V1	y7	3+	n/a
519.27	615.35	GAFFPLTER	PLTP	y5	2+	n/a
519.27	762.41	GAFFPLTER	PLTP	y6	2+	n/a
519.27	909.48	GAFFPLTER	PLTP	y7	2+	n/a
519.27	455.25	GAFFPLTER	PLTP	y7 (2+)	2+	n/a
388.22	375.24	TGLELSR	PLTP	y3	2+	n/a
388.22	504.28	TGLELSR	PLTP	y4	2+	n/a
388.22	617.36	TGLELSR	PLTP	y5	2+	n/a
388.22	674.38	TGLELSR	PLTP	y6	2+	n/a
819.93	1282.68	EVQPVELPNCNLVK	PON1	y11	2+	n/a
819.93	844.43	EVQPVELPNCNLVK	PON1	y7	2+	n/a
819.93	957.52	EVQPVELPNCNLVK	PON1	y8	2+	n/a
607.85	1016.6	PTVLELGITGSK	PON1	y10	2+	n/a
607.85	804.45	PTVLELGITGSK	PON1	y8	2+	n/a
607.85	917.53	PTVLELGITGSK	PON1	y9	2+	n/a
745.38	1218.58	IFLMDLNEQNPR	PON3	b10	2+	n/a
745.38	643.32	IFLMDLNEQNPR	PON3	y5	2+	n/a
745.38	985.47	IFLMDLNEQNPR	PON3	y8	2+	n/a
745.38	1116.51	IFLMDLNEQNPR	PON3	y9	2+	n/a
906.96	959.45	LLNYNPEDPPGSEVLR	PON3	b8	2+	n/a
906.96	1195.6	LLNYNPEDPPGSEVLR	PON3	y11	2+	n/a
906.96	1309.64	LLNYNPEDPPGSEVLR	PON3	y12	2+	n/a
906.96	854.47	LLNYNPEDPPGSEVLR	PON3	y8	2+	n/a
575.62	1074.49	GKEESLDSDLYAELR	PPBP	b10	3+	n/a
575.62	417.25	GKEESLDSDLYAELR	PPBP	y3	3+	n/a
575.62	488.28	GKEESLDSDLYAELR	PPBP	y4	3+	n/a
575.62	651.35	GKEESLDSDLYAELR	PPBP	y5	3+	n/a
528.76	555.29	ICLDPDAPR	PPBP	y5	2+	n/a
528.76	670.32	ICLDPDAPR	PPBP	y6	2+	n/a
528.76	783.4	ICLDPDAPR	PPBP	y7	2+	n/a
528.76	472.22	ICLDPDAPR	PPBP	y8 (2+)	2+	n/a
498.74	406.19	EANYIGSDK	SAA1	y4	2+	n/a
498.74	519.28	EANYIGSDK	SAA1	y5	2+	n/a
498.74	682.34	EANYIGSDK	SAA1	y6	2+	n/a
498.74	796.38	EANYIGSDK	SAA1	y7	2+	n/a
775.87	418.2	SFFSFLGEAFDGAR	SAA1	y4	2+	n/a
775.87	565.27	SFFSFLGEAFDGAR	SAA1	y5	2+	n/a
775.87	822.37	SFFSFLGEAFDGAR	SAA1	y8	2+	n/a
775.87	935.46	SFFSFLGEAFDGAR	SAA1	y9	2+	n/a
1089.49	1117.5	FFGHGAEDSLADQAANEWGR	SAA2	y10	2+	n/a
1089.49	1317.62	FFGHGAEDSLADQAANEWGR	SAA2	y12	2+	n/a
1089.49	931.44	FFGHGAEDSLADQAANEWGR	SAA2	y8	2+	n/a

1089.49	1046.46	FFGHGAEDSLADQAANEWGR	SAA2	y9	2+	n/a
728.86	1089.53	GPGGVWAAEAISDAR	SAA2	y10	2+	n/a
728.86	632.34	GPGGVWAAEAISDAR	SAA2	y6	2+	n/a
728.86	832.42	GPGGVWAAEAISDAR	SAA2	y8	2+	n/a
728.86	903.45	GPGGVWAAEAISDAR	SAA2	y9	2+	n/a
924.93	1200.55	AYWDIMISNHQNSNR	SAA4	y10	2+	n/a
924.93	956.43	AYWDIMISNHQNSNR	SAA4	y8	2+	n/a
924.93	1069.51	AYWDIMISNHQNSNR	SAA4	y9	2+	n/a
465.26	516.26	FRPDGLPK	SAA4	b4	2+	n/a
465.26	686.36	FRPDGLPK	SAA4	b6	2+	n/a
465.26	244.17	FRPDGLPK	SAA4	y2	2+	n/a
699.87	769.46	CVAELGPQAVGAVK	SCGB3A1	y8	2+	n/a
699.87	826.48	CVAELGPQAVGAVK	SCGB3A1	y9	2+	n/a
699.87	939.56	CVAELGPQAVGAVK	SCGB3A1	y10	2+	n/a
699.87	1068.6	CVAELGPQAVGAVK	SCGB3A1	y11	2+	n/a
673.39	611.33	LLLSSLGIPVNHLIEGSQK	SCGB3A1	y11 (2+)	3+	n/a
673.39	696.39	LLLSSLGIPVNHLIEGSQK	SCGB3A1	y13 (2+)	3+	n/a
673.39	752.93	LLLSSLGIPVNHLIEGSQK	SCGB3A1	y14 (2+)	3+	n/a
673.39	896.5	LLLSSLGIPVNHLIEGSQK	SCGB3A1	y17 (2+)	3+	n/a
508.31	418.25	SVLGQLGITK	SERPINA1	y4	2+	n/a
508.31	716.43	SVLGQLGITK	SERPINA1	y7	2+	n/a
508.31	829.51	SVLGQLGITK	SERPINA1	y8	2+	n/a
508.31	415.26	SVLGQLGITK	SERPINA1	y8 (2+)	2+	n/a
917.46	1030.54	VFSNGADLSGVTEEAPLK	SERPINA1	y10	2+	n/a
917.46	1258.65	VFSNGADLSGVTEEAPLK	SERPINA1	y12	2+	n/a
917.46	1386.71	VFSNGADLSGVTEEAPLK	SERPINA1	y14	2+	n/a
917.46	943.51	VFSNGADLSGVTEEAPLK	SERPINA1	y9	2+	n/a
871.46	1163.53	VVPLVAGGICQCLAER	SFTPB	y10	2+	n/a
871.46	1234.57	VVPLVAGGICQCLAER	SFTPB	y11	2+	n/a
871.46	772.39	VVPLVAGGICQCLAER	SFTPB	y14 (2+)	2+	n/a
871.46	936.4	VVPLVAGGICQCLAER	SFTPB	y7	2+	n/a
681.9	1112.7	YSVILLDTLLGR	SFTPB	y10	2+	n/a
681.9	674.38	YSVILLDTLLGR	SFTPB	y6	2+	n/a
681.9	787.47	YSVILLDTLLGR	SFTPB	y7	2+	n/a
681.9	900.55	YSVILLDTLLGR	SFTPB	y8	2+	n/a
697.81	474.18	AADDTWEPFASGK	TTR	b5	2+	n/a
697.81	606.32	AADDTWEPFASGK	TTR	y6	2+	n/a
697.81	735.37	AADDTWEPFASGK	TTR	y7	2+	n/a
697.81	921.45	AADDTWEPFASGK	TTR	y8	2+	n/a
456.26	611.86	GSPAINVAVHVFR	TTR	y11 (2+)	3+	n/a
456.26	408.24	GSPAINVAVHVFR	TTR	y11 (3+)	3+	n/a
456.26	558.31	GSPAINVAVHVFR	TTR	y4	3+	n/a
456.26	941.53	GSPAINVAVHVFR	TTR	y8	3+	n/a
823.91	1076.54	DVWGIEGPIDAAFTR	Vitronectin	y10	2+	n/a

823.91	1246.64	DVWGIEGPIDAAFTR	Vitronectin	y12	2+	n/a
823.91	890.47	DVWGIEGPIDAAFTR	Vitronectin	y8	2+	n/a
823.91	947.49	DVWGIEGPIDAAFTR	Vitronectin	y9	2+	n/a
835.41	1107.54	SIAQYWLGCPAPGHL	Vitronectin	y10	2+	n/a
835.41	423.24	SIAQYWLGCPAPGHL	Vitronectin	y4	2+	n/a
835.41	591.32	SIAQYWLGCPAPGHL	Vitronectin	y6	2+	n/a
835.41	808.38	SIAQYWLGCPAPGHL	Vitronectin	y8	2+	n/a